Transport properties of the QGP within the Dynamical Quasi-Particle Model

Olga Soloveva* , Pierre Moreau, Elena Bratkovskaya

Frontiers in Nuclear and Hadronic Physics 2020

GGI Florence

28 February 2020

*soloveva@fias.uni-frankfurt.de

Motivation

- Explore the **QCD phase diagram** at finite temperature and chemical potential through heavy-ion collisions

Probes of the QGP at finite (T, μ_B)

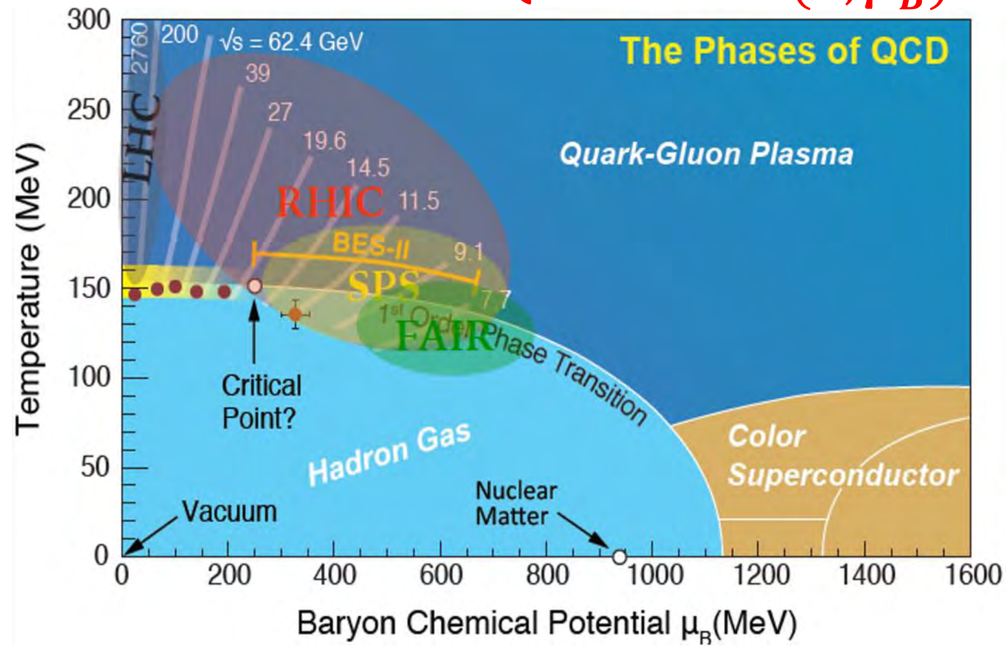

- Available information:
  - Experimental data at SPS, BES at RHIC
  - Lattice QCD calculations

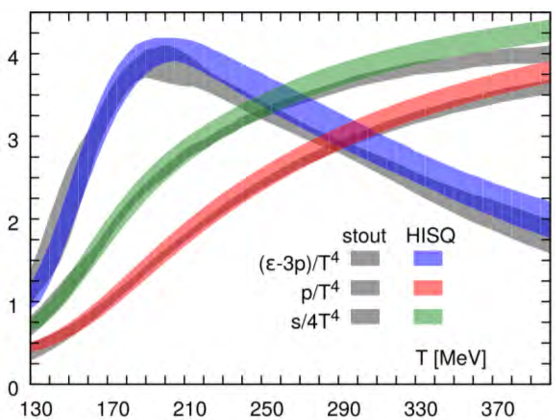

EoS

Lattice results from: Phys.Rev. D90 (2014) 094503; PoS CPOD2017 (2018) 032

- ❖ **How to learn about degrees-of-freedom of QGP ?**

➔ **HIC simulations – transport models**

! Transport models need an input for the partonic phase: cross-sections, masses,..

Transport coefficients of QGP

Hydrodynamical model

$$\Delta T^{\mu\nu} = \boxed{\eta}\left(D^{\mu}u^{\nu} + D^{\nu}u^{\mu} + \frac{2}{3}\Delta^{\mu\nu}\partial_{\rho}u^{\rho}\right) - \boxed{\zeta}\Delta^{\mu\nu}\partial_{\rho}u^{\rho}$$

input for hydro simulations

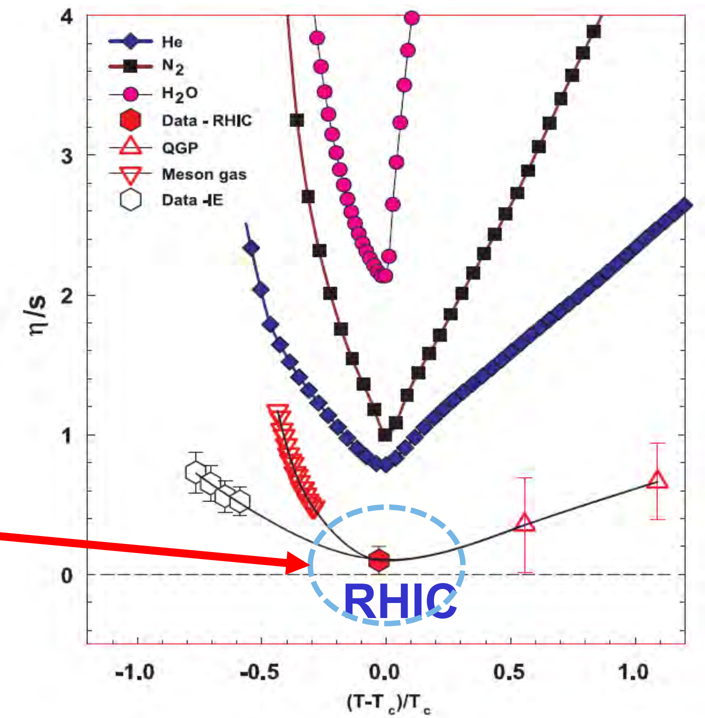

R.A. Lacey, A. Taranenko, PoS CFRNC 2006 (2006) 021

Shear viscosity to entropy density ratio is extremely small

QGP is the most ideal liquid!

Model predictions:

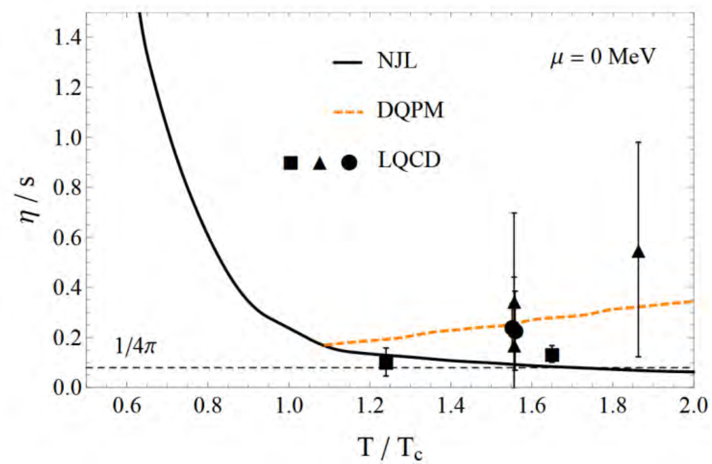

! Different models using the same EoS can have completely different transport coefficients!

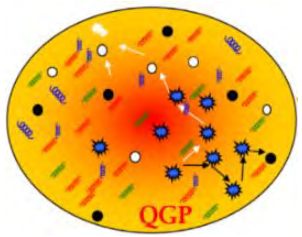

QGP in equilibrium:

Dynamical QuasiParticle Model (DQPM)

DQPM: consider the effects of the nonperturbative nature of the strongly interacting quark-gluon plasma (sQGP) constituents (vs. pQCD models)

Dynamical QuasiParticle Model (DQPM)

- The QGP phase is described in terms of interacting quasiparticles: quarks and gluons with Lorentzian spectral functions:

$$\rho_j(\omega,\mathbf{p}) = \frac{\gamma_j}{\tilde{E}_j}\left(\frac{1}{(\omega-\tilde{E}_j)^2+\gamma_j^2} - \frac{1}{(\omega+\tilde{E}_j)^2+\gamma_j^2}\right)$$
$$\equiv \frac{4\omega\gamma_j}{\left(\omega^2-\mathbf{p}^2-M_j^2\right)^2+4\gamma_j^2\omega^2}$$

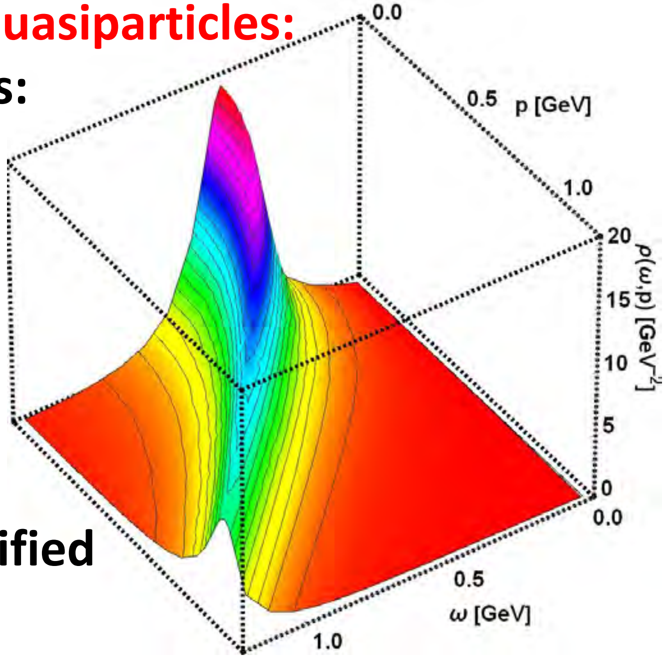

- Resummed properties of the quasiparticles are specified by scalar complex self-energies:

gluon propagator: $\Delta^{-1} = P^2 - \Pi$ &	quark propagator $S_q^{-1} = P^2 - \Sigma_q$
gluon self-energy: $\Pi = M_g^2 - i2g_g\omega$ &	quark self-energy: $\Sigma_q = M_q^2 - i2g_q\omega$

- Real part of the self-energy: thermal mass (M_g, M_q)
- Imaginary part of the self-energy: interaction width of partons (γ_g, γ_q)

Peshier, Cassing, PRL 94 (2005) 172301; Cassing, NPA 791 (2007) 365: NPA 793 (2007)

Parton properties

- Modeling of the quark/gluon masses and widths (inspired by HTL calculations)

$$M^2_{q(\bar{q})}(T,\mu_B) = \frac{N_c^2-1}{8N_c}\boxed{g^2(T,\mu_B)}\left(T^2+\frac{\mu_q^2}{\pi^2}\right)$$

$$\gamma_{q,g}(T,\mu_B) = \frac{c_{A,F}}{3}\frac{\boxed{g^2(T,\mu_B)}T}{8\pi}\ln\left(\frac{2c}{\boxed{g^2(T,\mu_B)}}+1\right)$$

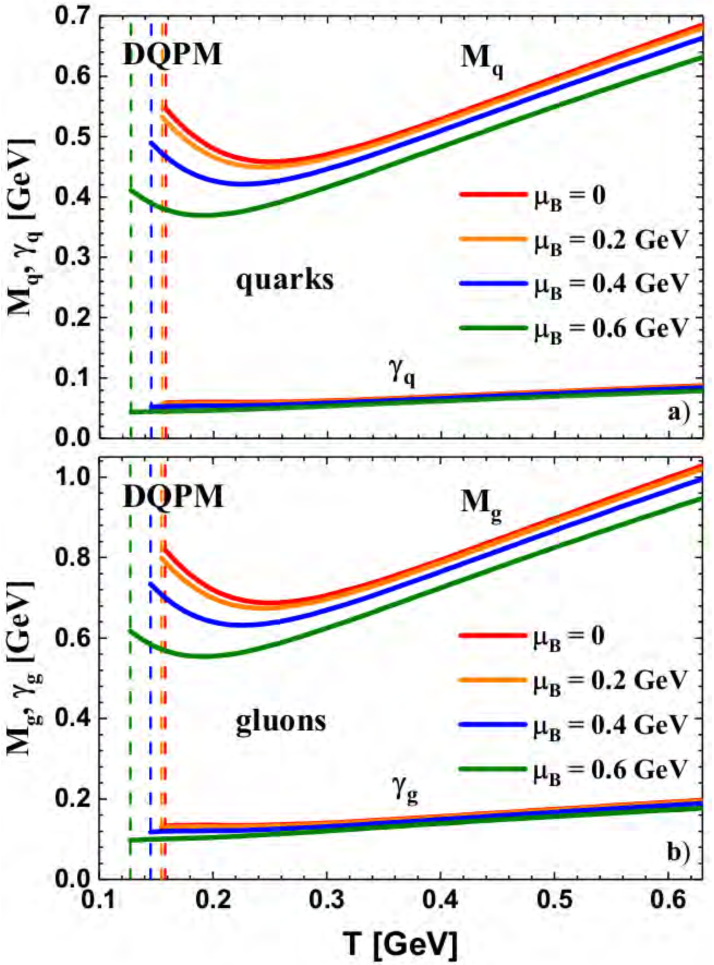

- **Only one parameter (c = 14.4) + (T, μ_B)-dependent coupling constant to determine from lattice results**

- **Entropy and baryon density in the quasiparticle limit (G. Baym 1998, Blaizot et al. 2001)**

$$s^{DQPM}(\Pi,\Delta,S_q,\Sigma), n_B^{DQPM}(\Pi,\Delta,S_q,\Sigma)$$

Peshier, Cassing, PRL 94 (2005) 172301; Cassing, NPA 791 (2007) 365: NPA 793 (2007)

DQPM coupling constant

- **Input: entropy density as a f(T , $\mu_B = 0$)**

$$g^2(s/s_{SB}) = d\left((s/s_{SB})^e - 1\right)^f$$

$$s_{SB}^{QCD} = 19/9\pi^2 T^3$$

$$s^{DQPM}(\Pi, \Delta, S_q, \Sigma) = s^{lattice}$$

fit S from QP to S from lQCD → fix the model parameters

Fit to the lattice data:

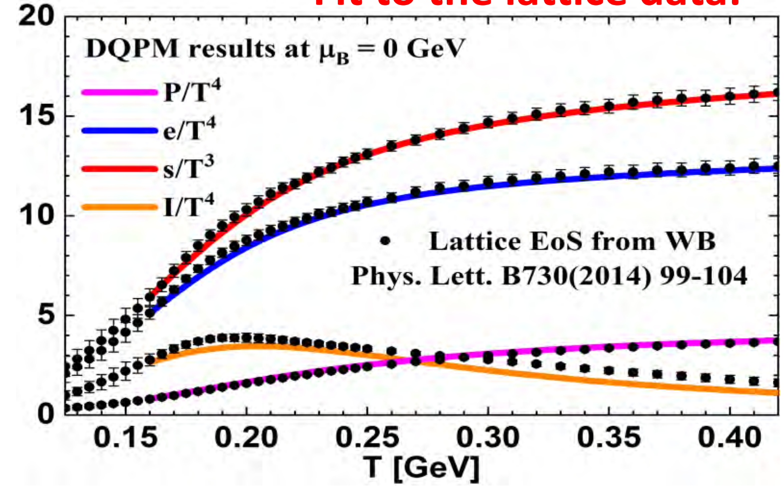

- **Scaling hypothesis at finite $\mu_B \approx 3\mu_q$**

$$g^2(T/T_c, \mu_B) = g^2\left(\frac{T^*}{T_c(\mu_B)}, \mu_B = 0\right)$$

with the effective temperature

$$T^* = \sqrt{T^2 + \mu_q^2/\pi^2}$$

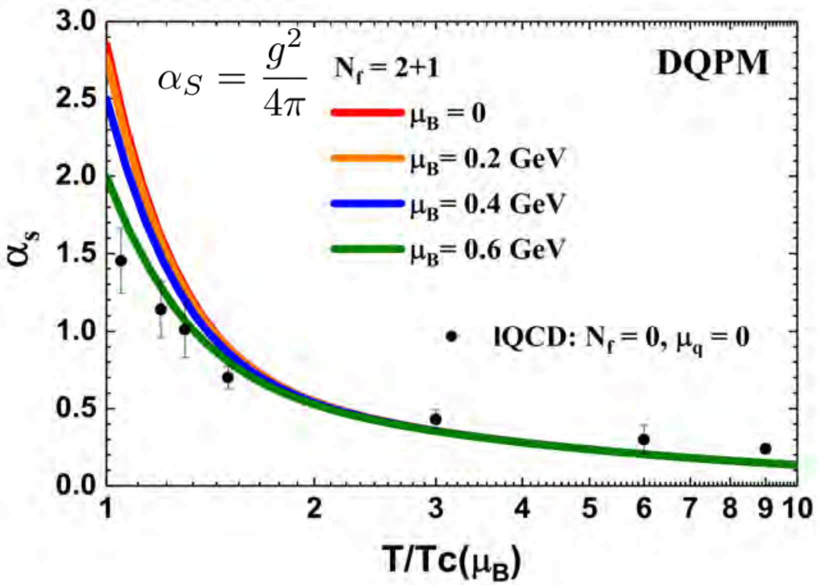

DQPM : Thermodynamics

- **Entropy and baryon density**

in the quasiparticle limit (G. Baym 1998, Blaizot et al. 2001):

$$s^{dqp} = - \int \frac{d\omega}{2\pi} \frac{d^3p}{(2\pi)^3} \left[d_g \frac{\partial n_B}{\partial T} \left(\mathrm{Im}(\ln -\Delta^{-1}) + \mathrm{Im}\,\Pi\, \mathrm{Re}\,\Delta \right) + \sum_{q=u,d,s} d_q \frac{\partial n_F(\omega-\mu_q)}{\partial T} \left(\mathrm{Im}(\ln -S_q^{-1}) + \mathrm{Im}\,\Sigma_q\, \mathrm{Re}\,S_q \right) + \sum_{\bar q=\bar u,\bar d,\bar s} d_{\bar q} \frac{\partial n_F(\omega+\mu_q)}{\partial T} \left(\mathrm{Im}(\ln -S_{\bar q}^{-1}) + \mathrm{Im}\,\Sigma_{\bar q}\, \mathrm{Re}\,S_{\bar q} \right) \right]$$

$$n^{dqp} = - \int \frac{d\omega}{2\pi} \frac{d^3p}{(2\pi)^3} \left[\sum_{q=u,d,s} d_q \frac{\partial n_F(\omega-\mu_q)}{\partial \mu_q} \left(\mathrm{Im}(\ln -S_q^{-1}) + \mathrm{Im}\,\Sigma_q\, \mathrm{Re}\,S_q \right) + \sum_{\bar q=\bar u,\bar d,\bar s} d_{\bar q} \frac{\partial n_F(\omega+\mu_q)}{\partial \mu_q} \left(\mathrm{Im}(\ln -S_{\bar q}^{-1}) + \mathrm{Im}\,\Sigma_{\bar q}\, \mathrm{Re}\,S_{\bar q} \right) \right]$$

Input:
lattice EoS
$\mu_B = 0$

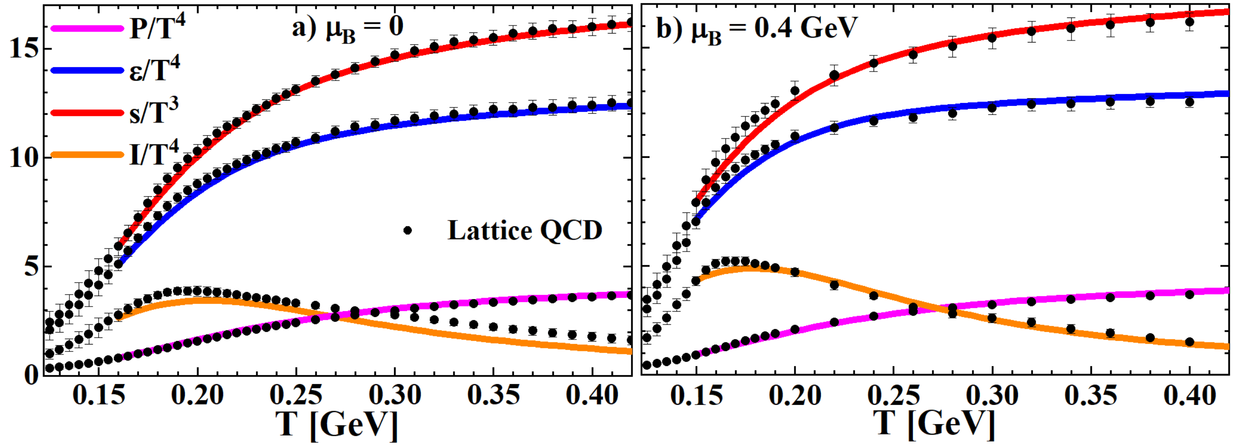

Output:
DQPM EoS
$\mu_B > 0$

DQPM : Thermodynamics

- Masses, widths, coupling are fixed → spectral function

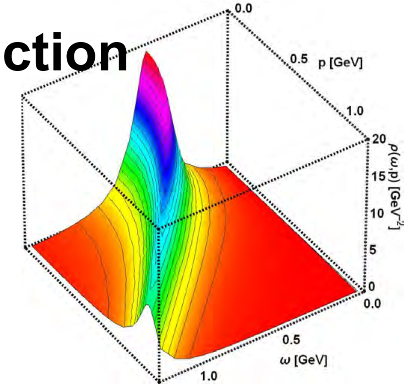

- Entropy and baryon density in the QP limit

$$s^{DQPM}(\Pi, \Delta, S_q, \Sigma), n_B^{DQPM}(\Pi, \Delta, S_q, \Sigma)$$

$$P(T, \mu_B) = P(T_0, 0)$$

$$+ \int_{T_0}^{T} s(T', 0)\, dT' + \int_0^{\mu_B} n_B(T, \mu'_B)\, d\mu'_B$$

$$\epsilon = Ts - P + \mu_B n_B$$

Input:
lattice EoS
$\mu_B = 0$

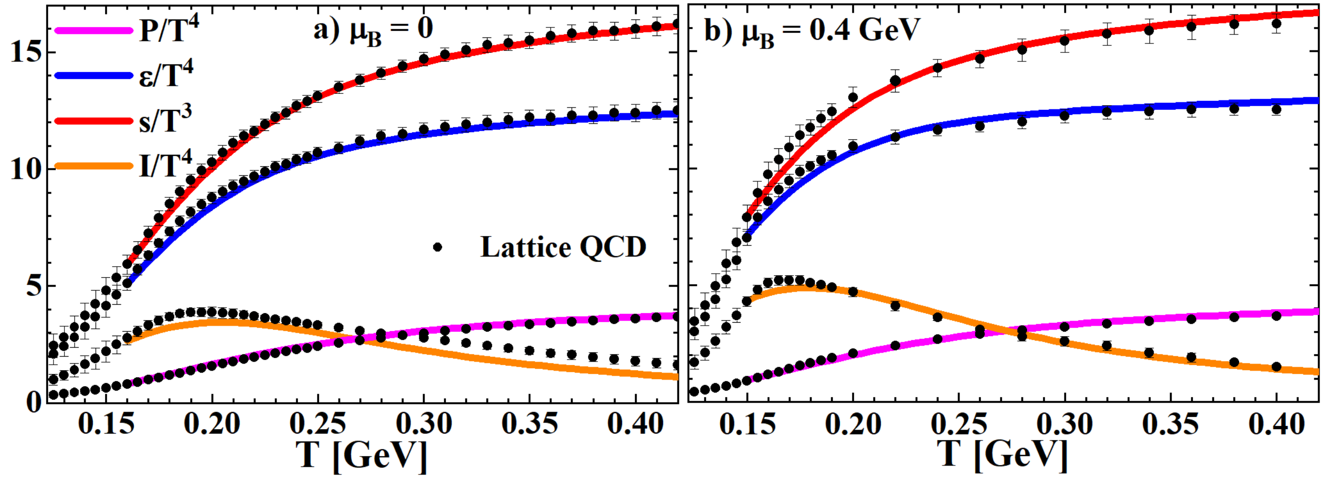

Output:
DQPM EoS
$\mu_B > 0$

Relaxation Time Approximation

- **Boltzmann equation** $f_a = f_a^{\rm eq}\left(1+\phi_a\right)$

$$\frac{df_a^{eq}}{dt} = \mathcal{C}_a = -\frac{f_a^{eq}\phi_a}{\tau_a}$$

RTA: system equilibrates within the relax time τ, Express collisional Integral via τ and fa

- **Relaxation times:**

$$\frac{1+d_a f_a^{\rm eq}}{\tau_a(E_a^*)} = \sum_{bcd} \frac{1}{1+\delta_{ab}} \int d\Gamma_b^*\, d\Gamma_c^*\, d\Gamma_d^*\, W(a,b|c,d)\, f_b^{\rm eq}\left(1+d_c f_c^{\rm eq}\right)\left(1+d_d f_d^{\rm eq}\right) \text{ + (cd), (bc)}$$

$$T^{\mu\nu} = -Pg^{\mu\nu} + wu^\mu u^\nu + \Delta T^{\mu\nu} \qquad J_B^\mu = n_B u^\mu + \Delta J_B^\mu$$

$$\Delta T^{\mu\nu} = \eta\left(D^\mu u^\nu + D^\nu u^\mu + \tfrac{2}{3}\Delta^{\mu\nu}\partial_\rho u^\rho\right) - \zeta \Delta^{\mu\nu}\partial_\rho u^\rho$$

$$\Delta J_B^\mu = \lambda \left(\frac{n_B T}{w}\right)^2 D^\mu \left(\frac{\mu_B}{T}\right)$$

hydrodynamics

Energy-momentum tensor and baryon diffusion current can be expressed using fa :
$T^{\mu\nu}(f_a, m_{q,g}),\, J_B^\mu(f_a, m_{q,g})$

Obtain the transport coefficients using conservation laws, and fa:

$$\begin{cases} \partial_\mu J_B^\mu = 0 \\ \partial_\mu T^{\mu\nu} = 0 \end{cases} \Longrightarrow \eta^{\rm RTA}(T,\mu_B) = \frac{1}{15T}\sum_{i=q,\bar{q},g}\int \frac{d^3p}{(2\pi)^3}\frac{\mathbf{p}^4}{E_i^2}\tau_i(\mathbf{p},T,\mu_B)\, d_i(1\pm f_i)f_i$$

Relaxation times

$$\boxed{1)\tau_i(\mathbf{p}, T, \mu_B) = \frac{1}{\Gamma_i(\mathbf{p}, T, \mu_B)}}$$

$$2)\tau_i(T, \mu_B) = \frac{1}{2\gamma_i(T, \mu_B)},$$

- **on-shell interaction rates**

$$\Gamma_i^{\text{on}}(\mathbf{p}_i, T, \mu_q) = \frac{1}{2E_i} \sum_{j=q,\bar{q},g} \int \frac{d^3p_j}{(2\pi)^3 2E_j}\; d_j\; f_j(E_j, T, \mu_q)$$

$$\int \frac{d^3p_3}{(2\pi)^3 2E_3} \int \frac{d^3p_4}{(2\pi)^3 2E_4} (1 \pm f_3)(1 \pm f_4)$$

$$\boxed{|\bar{\mathcal{M}}|^2(p_i, p_j, p_3, p_4)}\, (2\pi)^4 \delta^{(4)}\,(p_i + p_j - p_3 - p_4)$$

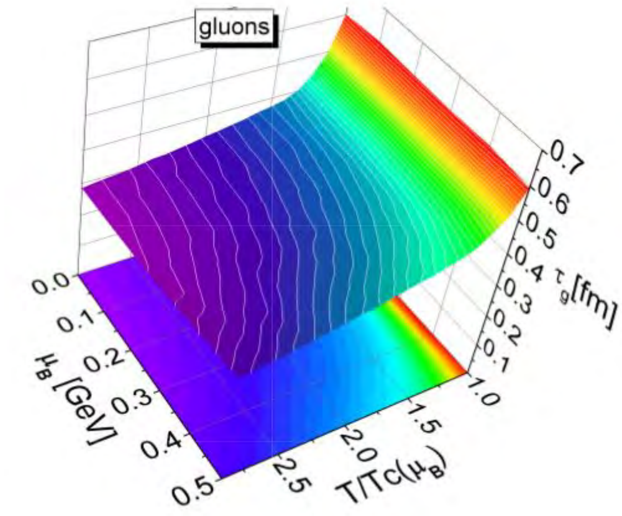

a)

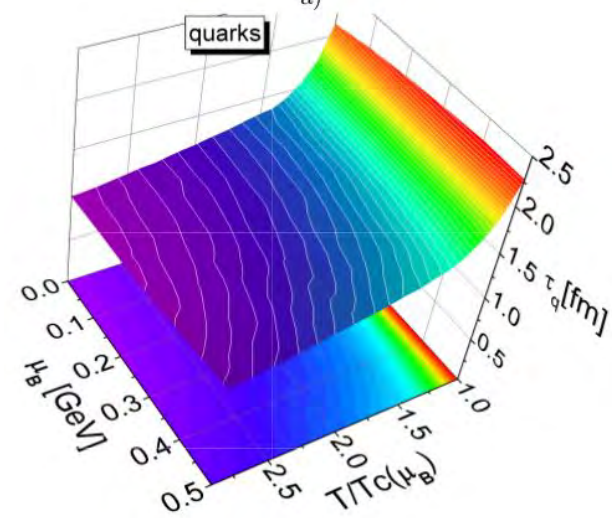

b)

Partonic interactions: matrix elements

DQPM partonic cross sections → leading order diagrams

- **Propagators** for massive bosons and fermions:

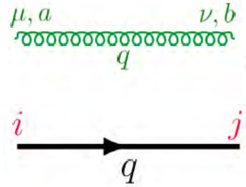

$$= -i\delta_{ab}\frac{g^{\mu\nu} - q^\mu q^\nu / M_g^2}{q^2 - M_g^2 + 2i\gamma_g q_0}$$

$$= i\delta_{ij}\frac{\not{q} + M_q}{q^2 - M_q^2 + 2i\gamma_q q_0}$$

qq' → qq' scattering

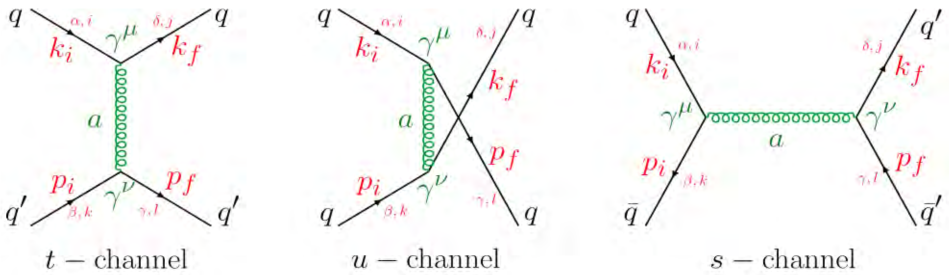

gq → gq scattering

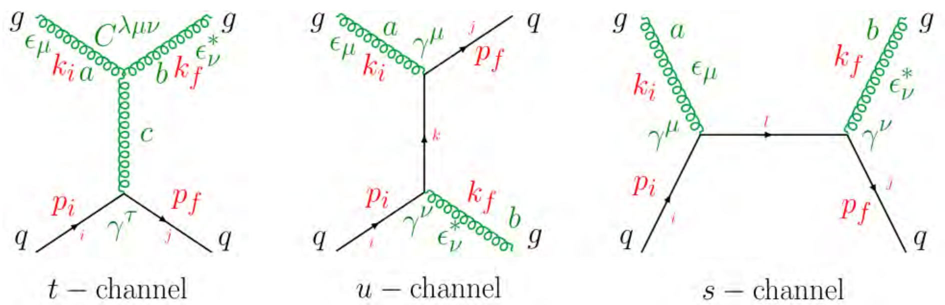

gg → gg scattering

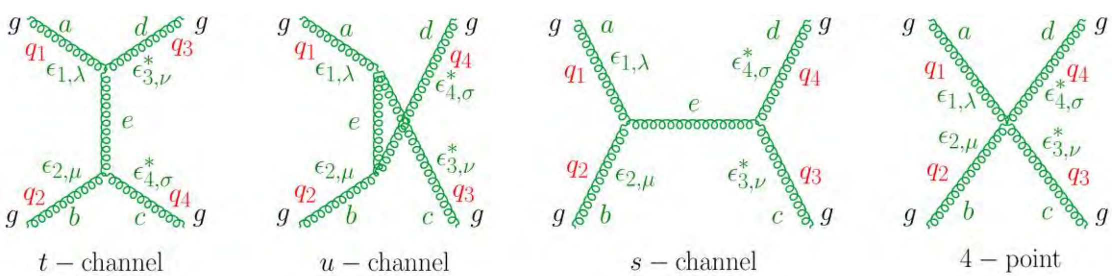

Total cross sections

- **On-shell:**

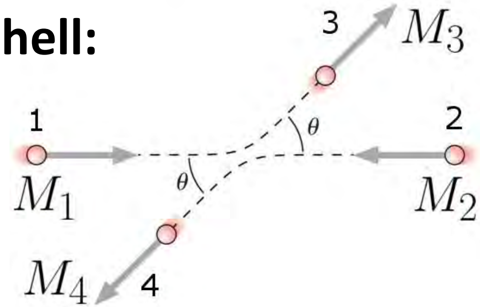

Initial masses: pole masses
Final masses: pole masses

- **Off-shell:**

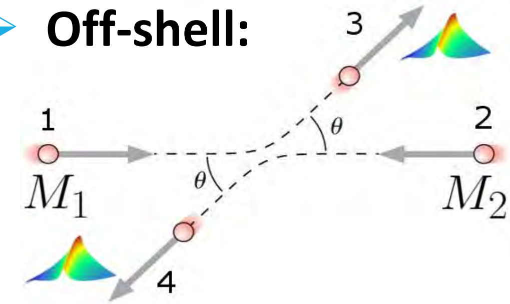

Initial masses: pole masses
Final masses: integrated over spectral functions

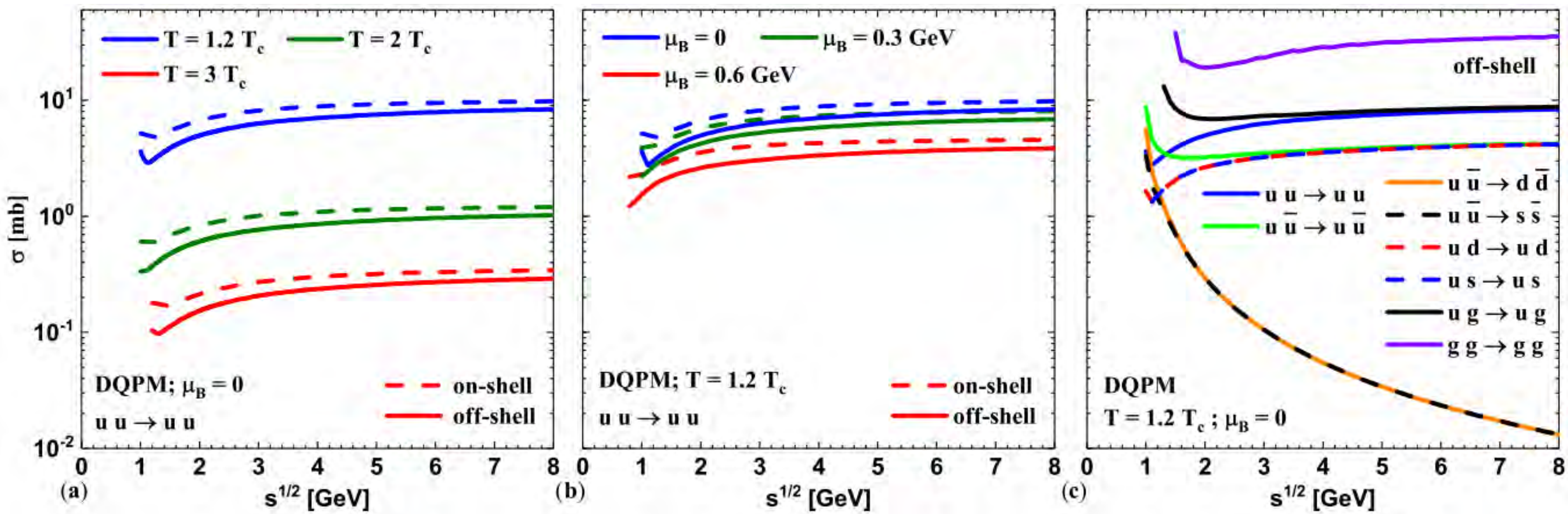

Transport coefficients: shear viscosity

- **Relaxation Time Approximation**

$$1)\,\tau_i(\mathbf{p},T,\mu_B) = \frac{1}{\Gamma_i(\mathbf{p},T,\mu_B)}$$

$$2)\,\tau_i(T,\mu_B) = \frac{1}{2\gamma_i(T,\mu_B)},$$

$$\eta^{\mathrm{RTA}}(T,\mu_B) = \frac{1}{15T}\sum_{i=q,\bar{q},g}\int \frac{d^3p}{(2\pi)^3}\frac{\mathbf{p}^4}{E_i^2}\boxed{\tau_i(\mathbf{p},T,\mu_B)}\,d_i(1\pm f_i)f_i$$

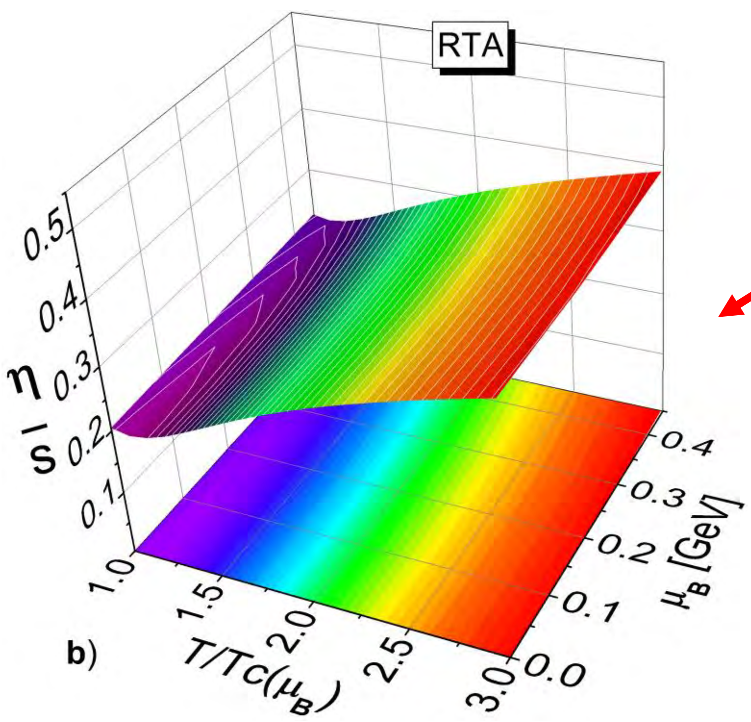

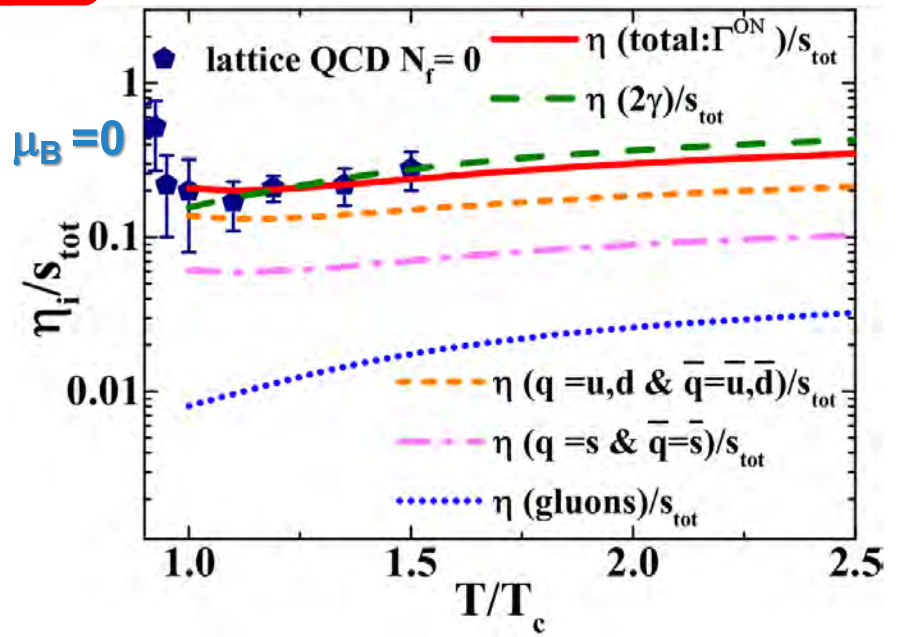

- Main contribution comes from light quarks and anti-quarks

Lattice: N. Astrakhantsev, V. Braguta, A. Kotov JHEP 1704 (2017) 101

Transport coefficients: bulk viscosity

- **Relaxation Time Approximation**

Relaxation times

$$\zeta^{\mathrm{RTA}}(T,\mu_B) = \frac{1}{9T} \sum_{i=q,\bar{q},g} \int \frac{d^3p}{(2\pi)^3} \boxed{\tau_i(\mathbf{p},T,\mu_B)}$$

From DQPM parametrization

$$\frac{d_i(1 \pm f_i)f_i}{E_i^2} \left(\mathbf{p}^2 - 3c_s^2 \left(E_i^2 - T^2 \frac{dm_i^2}{dT^2} \right) \right)^2$$

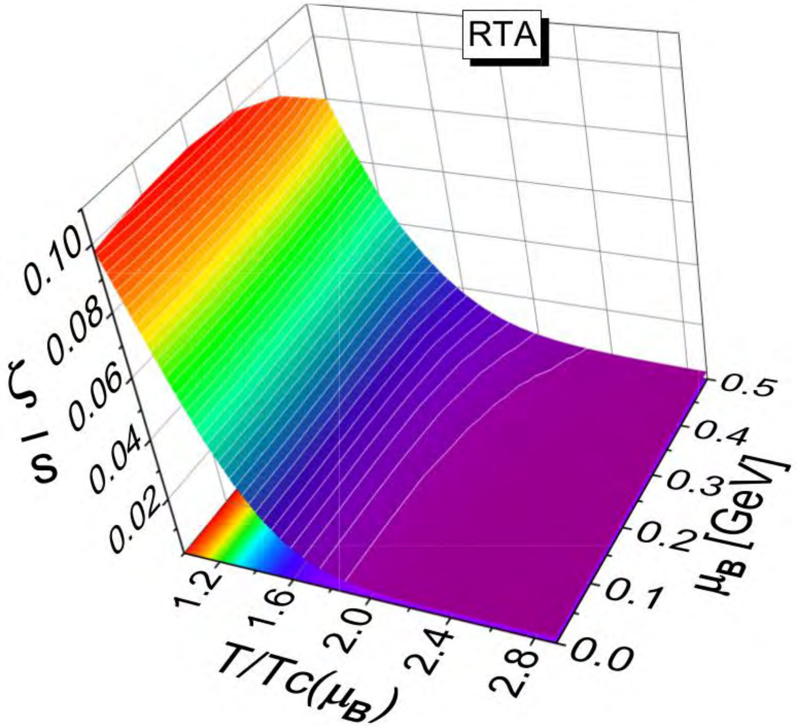

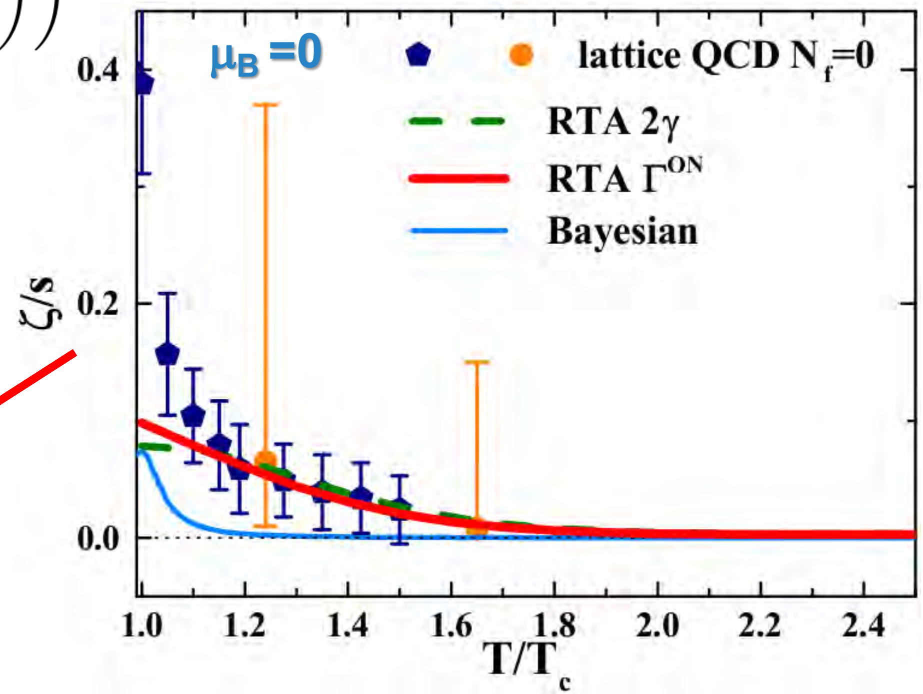

Lattice: Phys.Rev. D98 (2018) no.5, 054515

Transport coefficients: electric conductivity

- **Relaxation Time Approximation**

$$\sigma_0^{\mathrm{RTA}}(T,\mu_B) = \frac{e^2}{3T}\sum_{i=q,\bar{q}} q_i^2 \int \frac{d^3p}{(2\pi)^3}\frac{\mathbf{p}^2}{E_i^2}\boxed{\tau_i(\mathbf{p},T,\mu_B)}\, d_i(1-f_i)f_i$$

Relaxation times

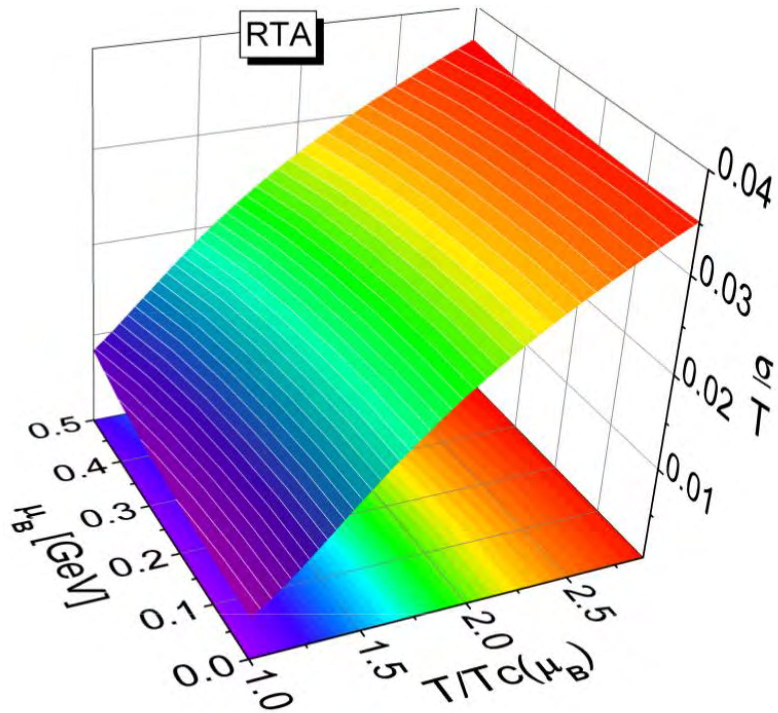

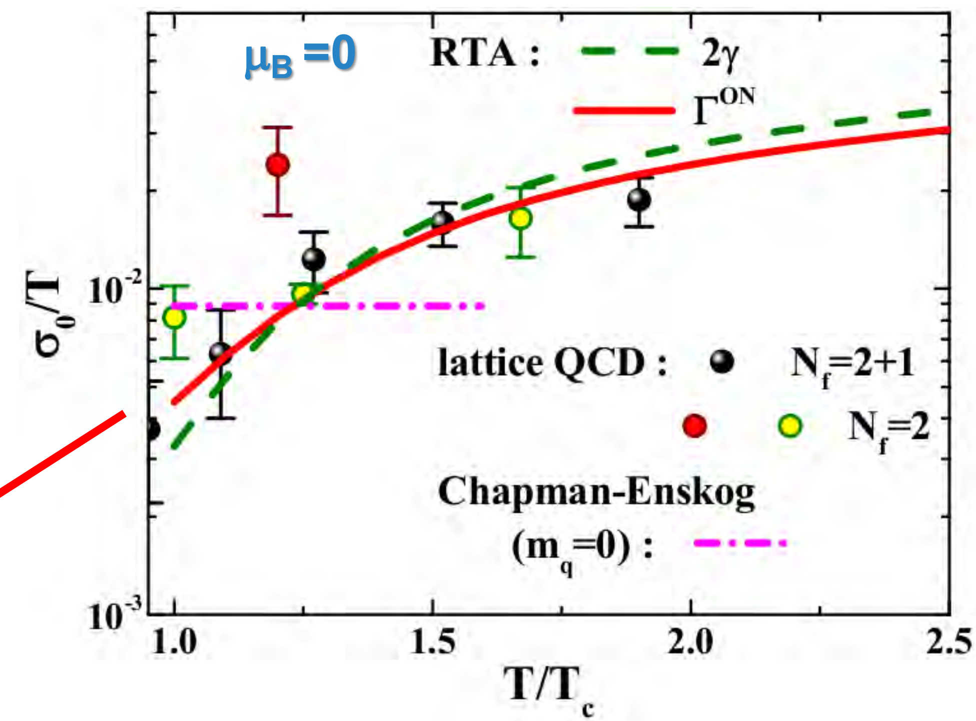

Transport coefficients: baryon diffusion coefficient

- **Relaxation Time Approximation**

DQPM EoS

$$\kappa_B^{\mathrm{RTA}}(T,\mu_B) = \frac{1}{3}\sum_{i=q,\bar{q}}\int \frac{d^3p}{(2\pi)^3}\mathbf{p}^4 \boxed{\tau_i(\mathbf{p},T,\mu_B)} \frac{d_i(1\pm f_i)f_i}{E_i^2}\left(b_a - \frac{n_B E_i}{\epsilon + p}\right)^2$$

Relaxation times

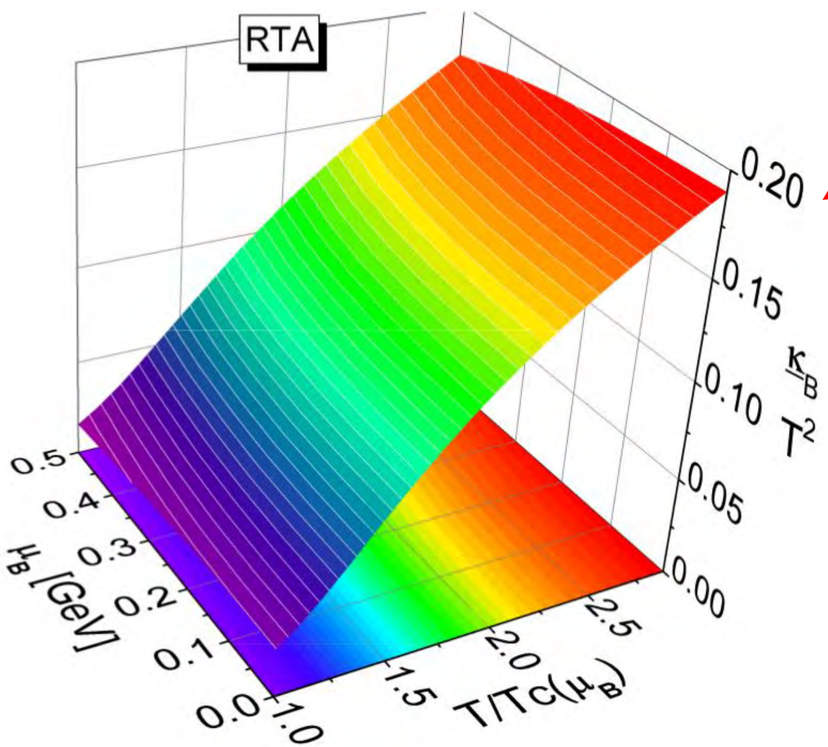

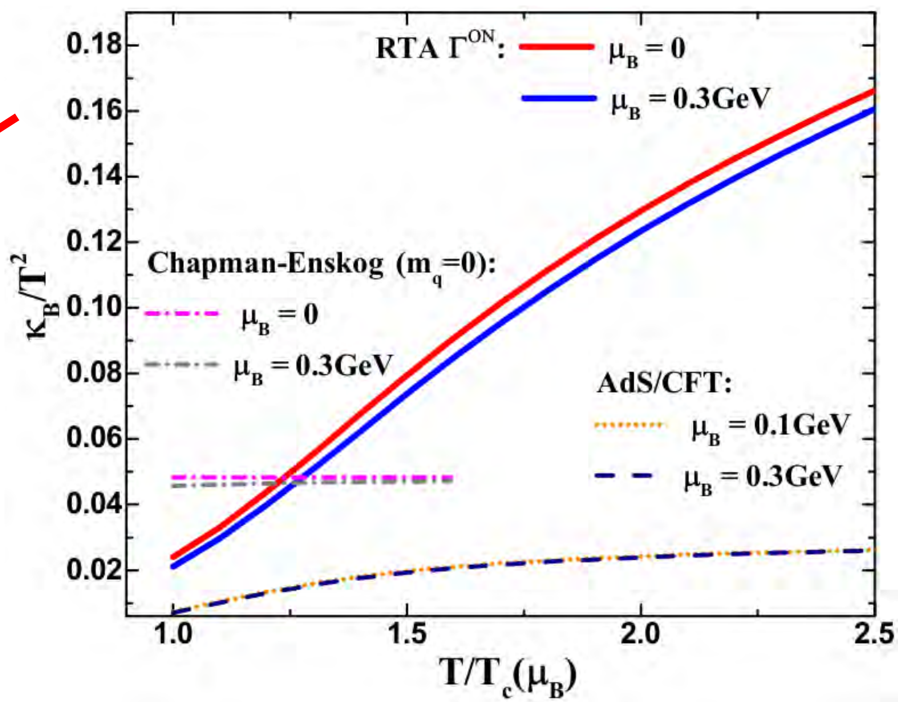

Summary / Outlook

- Transport coefficient at finite T and μ_B have been found using the (T, μ_B)-dependent cross sections(for cross-sections see[2])
- At μ_B= 0 good agreement with the Bayesian analysis estimations and gluodynamic lattice calculations of transport coefficients
- Very weak μ_B dependence is found [1,2]

[1] O Soloveva, Pierre Moreau, Elena Bratkovskaya, arXiv:1911.08547 [nucl-th].
[2] P. Moreau, O. Soloveva, L. Oliva, T. Song, W. Cassing, E. Bratkovskaya, arXiv:1903.10157, PRC 100 (19) no. 1, 014911
[3] O. Soloveva, P. Moreau, L. Oliva, V. Voronyuk, V. Kireyeu, T. Song, E. Bratkovskaya, arXiv:2001.05395

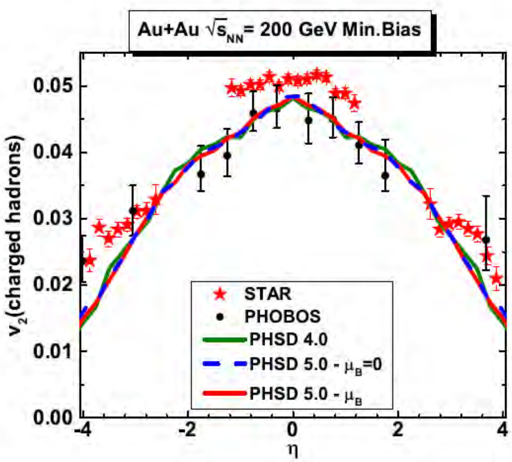

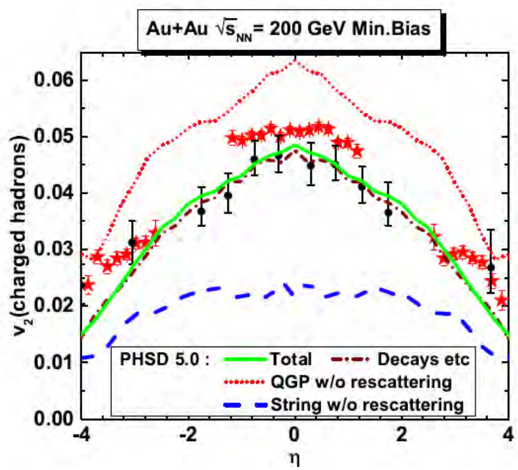

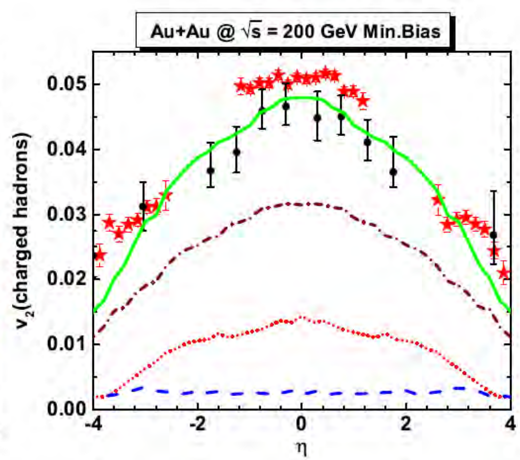

Summary / Outlook

- **Outlook:**
  - **More precise EoS finite/large μ_B**
  - **Possible 1st order phase transition at large μ_B, comparison w PNJL model**

Thank you for your attention!

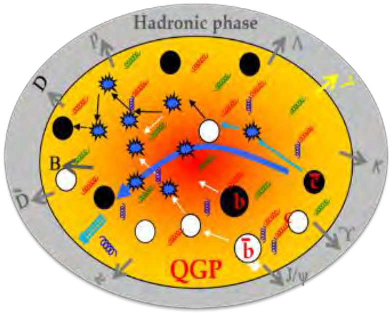

QGP out-of equilibrium ←→ HIC

Parton-Hadron-String-Dynamics (PHSD)

- **Transport theory: off-shell transport equations in phase-space representation based on Kadanoff-Baym equations for the partonic and hadronic phase**

Stages of a collision in the PHSD

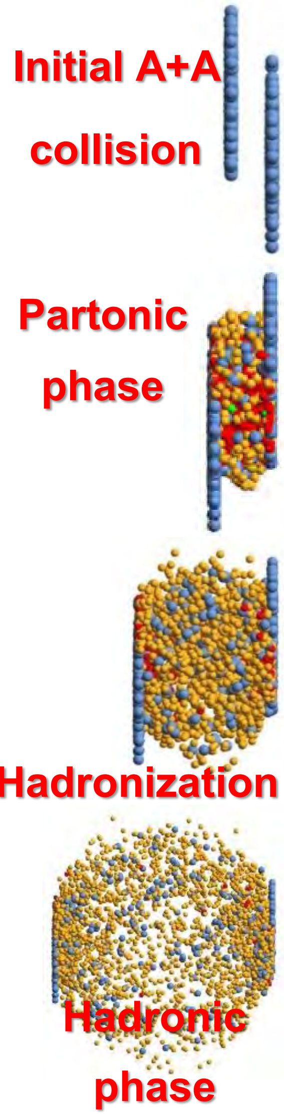

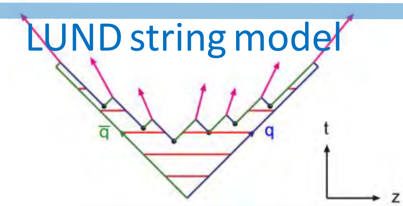

- **String formation in primary NN collisions**

→ decays to pre-hadrons (baryons and mesons)

- **Formation of a QGP state if $\varepsilon > \varepsilon_{critical}$:**

Dissolution of pre-hadrons → DQPM

→ massive quarks/gluons and mean-field energy

(quasi-)elastic collisions :

$$q+q \to q+q \quad g+q \to g+q$$
$$q+\bar{q} \to q+\bar{q} \quad g+\bar{q} \to g+\bar{q}$$
$$\bar{q}+\bar{q} \to \bar{q}+\bar{q} \quad g+g \to g+g$$

inelastic collisions:

$$q+\bar{q} \to g$$
$$g \to q+\bar{q}$$

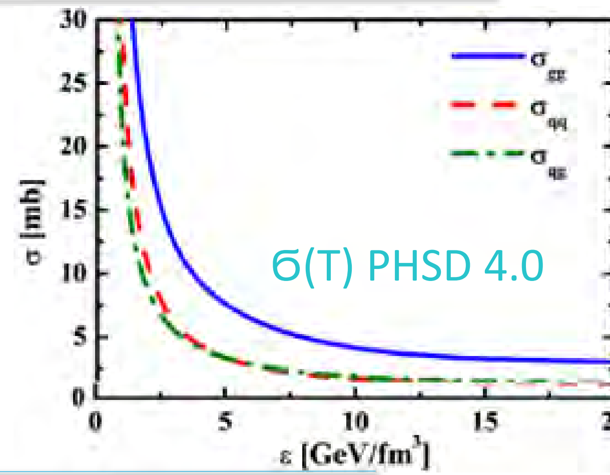

- **Hadronization to colorless off-shell mesons and baryons**

$$g \to q+\bar{q}, \quad q+\bar{q} \leftrightarrow meson \ ('\ string\ ')$$
$$q+q+q \leftrightarrow baryon \ ('\ string\ ')$$

Strict 4-momentum and quantum number conservation

- **Hadron-string interactions – off-shell HSD**

Extraction of (T, μ_B) in PHSD

For each space-time cell of the PHSD:

- **Calculate the local energy density ε^{PHSD} and baryon density n_B^{PHSD}**

1) Energy density ε^{PHSD}

In each space-time cell of the PHSD, the energy-momentum tensor is calculated by the formula:

$$T^{\mu\nu} = \sum_i \frac{p_i^\mu p_i^\nu}{E_i}$$

Diagonalization of the energy-momentum tensor to get the energy density and pressure components expressed in the local rest frame (LRF)

$$T^{\mu\nu} = \begin{pmatrix} T^{00} & T^{01} & T^{02} & T^{03} \\ T^{10} & T^{11} & T^{12} & T^{13} \\ T^{20} & T^{21} & T^{22} & T^{23} \\ T^{30} & T^{31} & T^{32} & T^{33} \end{pmatrix} \Rightarrow \begin{pmatrix} \epsilon^{LRF} & 0 & 0 & 0 \\ 0 & P_x^{LRF} & 0 & 0 \\ 0 & 0 & P_y^{LRF} & 0 \\ 0 & 0 & 0 & P_z^{LRF} \end{pmatrix} \Rightarrow \varepsilon^{PHSD}$$

Xu et al., Phys.Rev. C96 (2017), 024902

2) Net-baryon density n_B^{PHSD} $\Rightarrow$

$$n_B = \gamma_E \left(J_B^0 - \vec{\beta}_E \cdot \vec{J}_B\right) = \frac{J_B^0}{\gamma_E}$$

Net-baryon current: $J_B^\mu = \sum_i \frac{p_i^\mu}{E_i} \frac{(q_i - \bar{q}_i)}{3}$

Eckart velocity $\vec{\beta}_E = \vec{J}_B / J_B^0$

Extraction of (T, μ_B) in PHSD

For **each space-time cell** of the PHSD:

- Calculate the local energy density ε^{PHSD} and baryon density n_B^{PHSD}
- use lQCD relations (up to 6th order):

$$\begin{cases} \dfrac{n_B}{T^3} \approx \chi_2^B(T)\left(\dfrac{\mu_B}{T}\right) + \ldots \\ \Delta\epsilon/T^4 \approx \dfrac{1}{2}\left(T\dfrac{\partial\chi_2^B(T)}{\partial T} + 3\chi_2^B(T)\right)\left(\dfrac{\mu_B}{T}\right)^2 + \ldots \end{cases}$$

Use baryon number susceptibilities χ_n from lQCD

➔ obtain (T, μ_B) by solving the system of coupled equations using ε^{PHSD} and n_B^{PHSD}

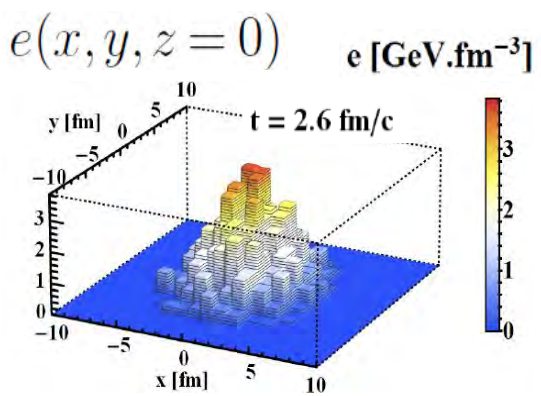

Input:

ε^{PHSD} and n_B^{PHSD}

Output:

T, μ_B

Illustration for HIC ($\sqrt{s_{NN}} = 17$ GeV)

The **temperature** profile in (x; y) **Baryon chemical potential** profile in (x;y)
at midrapidity ($|y_{cell}|$< 1) at 1 and 4 fm/c

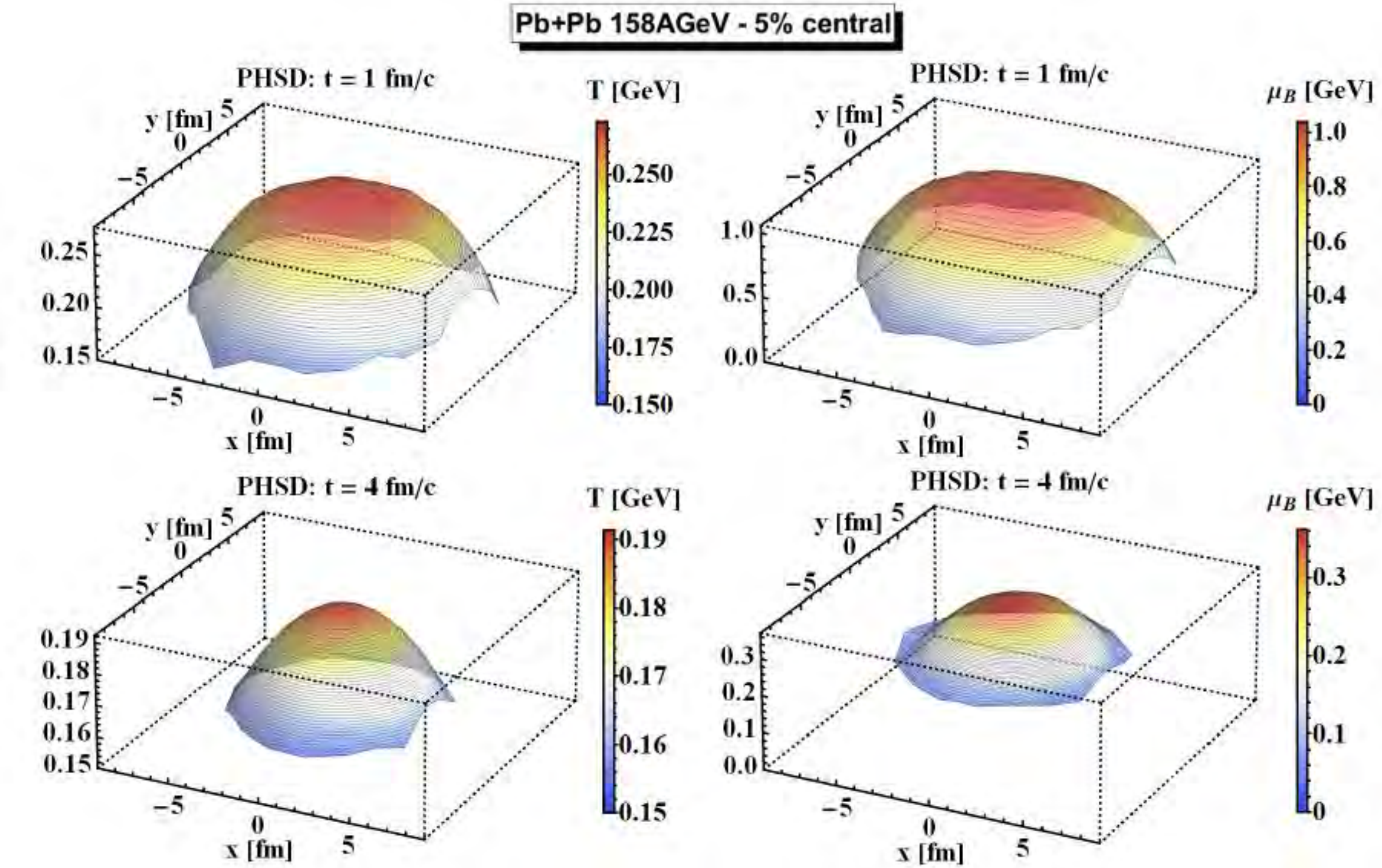

Illustration for HIC ($\sqrt{s_{NN}} = 17$ GeV)

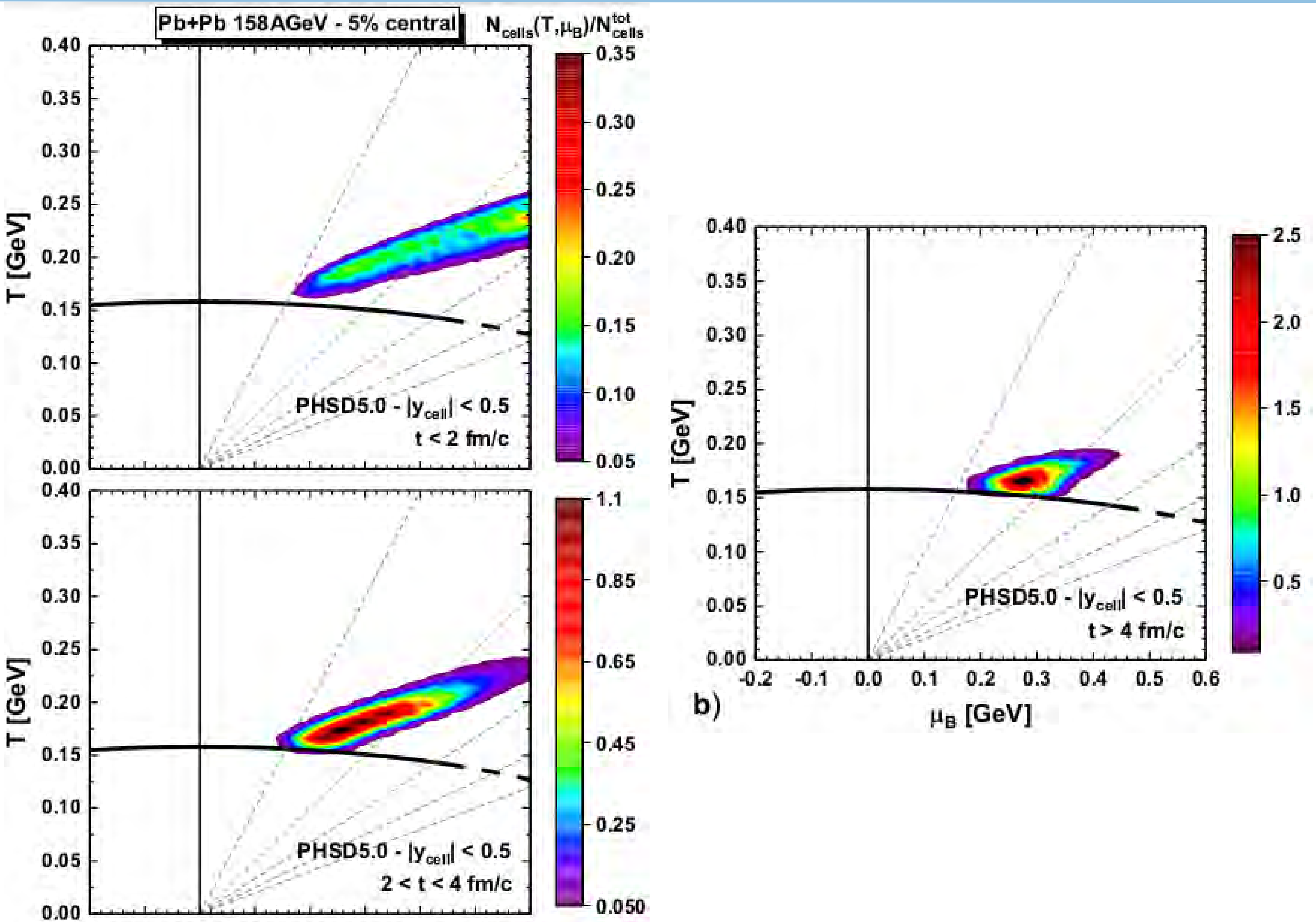

Traces of the QGP at finite μ_B in observables in high energy heavy-ion collisions

Results for HIC

- **Comparison between three different results:**

1) **PHSD 4.0 : only $\sigma(T)$ and $M(T)$**
2) **PHSD 5.0 : with $\sigma\left(\sqrt{s}, T, \mu_B = 0\right)$ and $M(T, \mu_B = 0)$**
3) **PHSD 5.0 : with $\sigma\left(\sqrt{s}, T, \mu_B\right)$ and $M(T, \mu_B)$**

Results for HIC ($\sqrt{s_{NN}} = 200$ GeV)

High-μ_B regions are probed at low $\sqrt{s_{NN}}$ or high rapidity regions

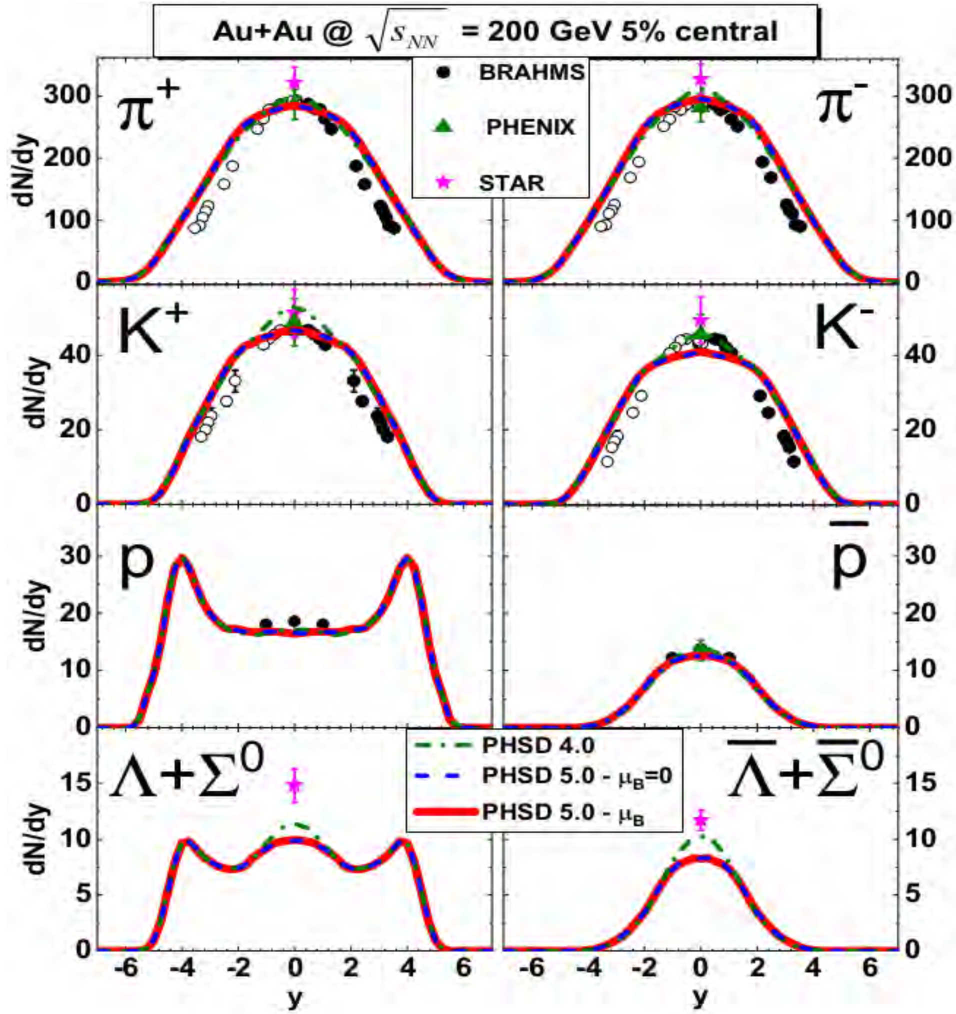

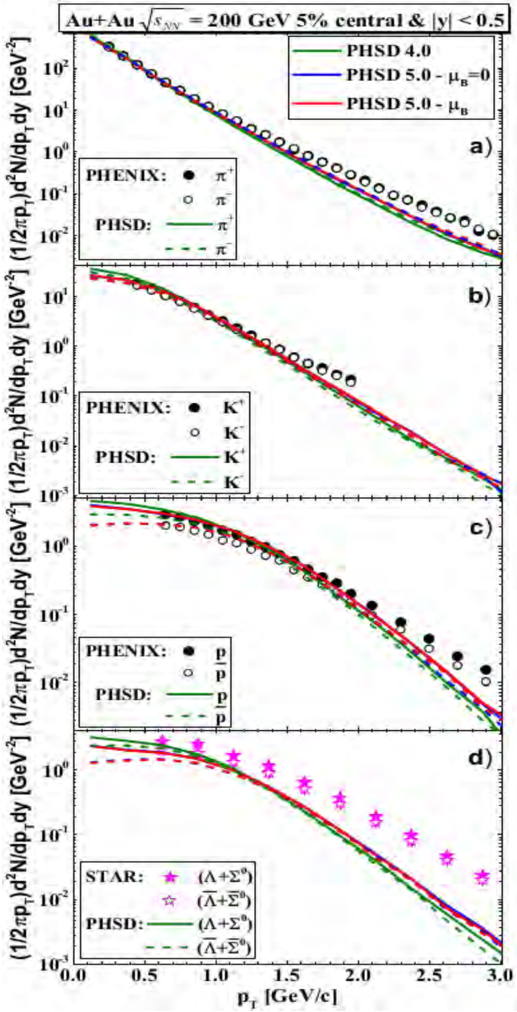

Results for HIC ($\sqrt{s_{NN}} = 17$ GeV)

High-μ_B regions are probed at low $\sqrt{s_{NN}}$ or high rapidity regions
But, QGP fraction is small at low $\sqrt{s_{NN}}$:

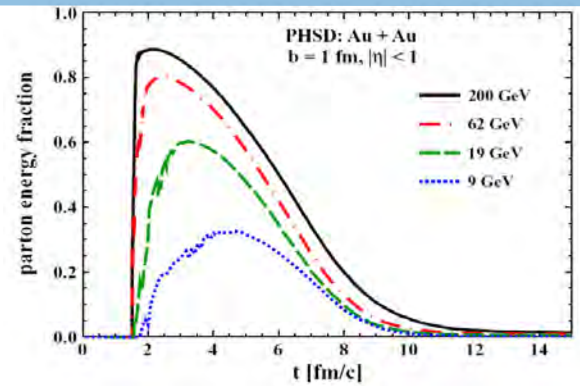

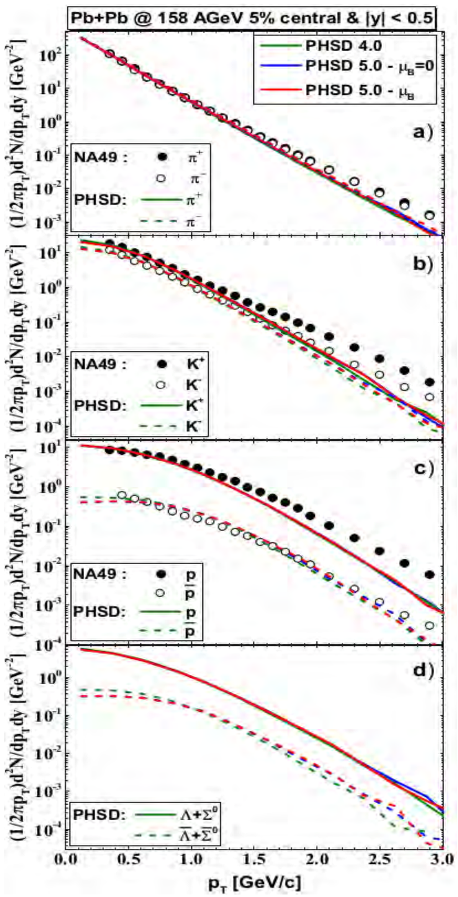

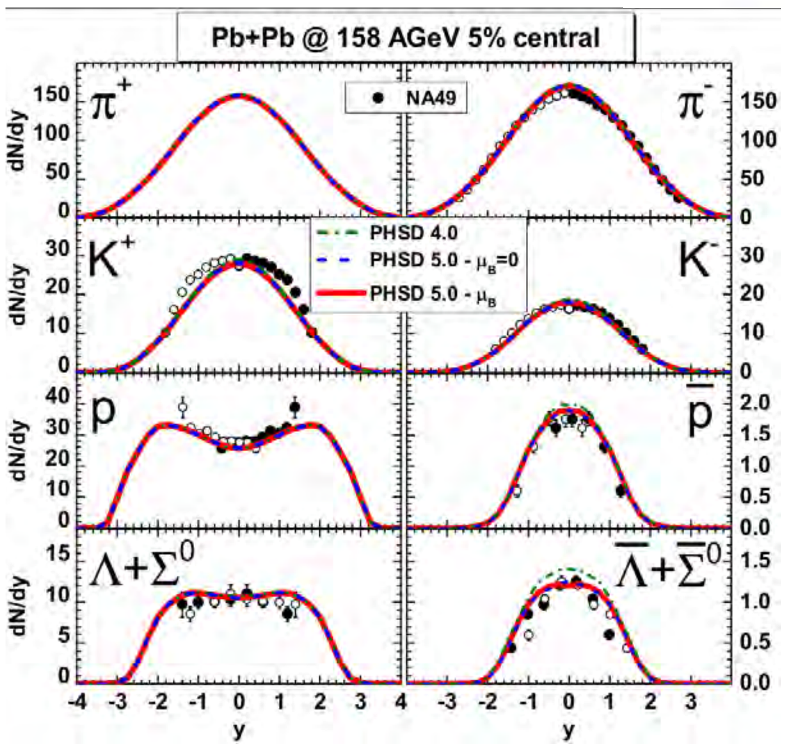

Anisotropic flow coefficients

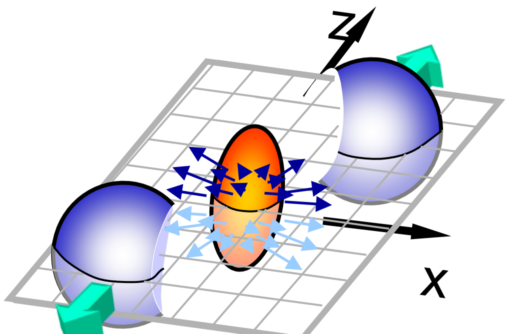

$$\frac{dN}{d\varphi} \propto \left(1 + 2\sum_{n=1}^{+\infty} v_n \cos\left[n(\varphi - \psi_n)\right]\right)$$

$$v_n = \left\langle \cos n\left(\varphi - \psi_n\right)\right\rangle, \quad n = 1,2,3..,$$

Anisotropic flow = correlations with respect to the reaction plane

$$v_n = \langle \cos(n(\phi - \Psi_r))\rangle$$

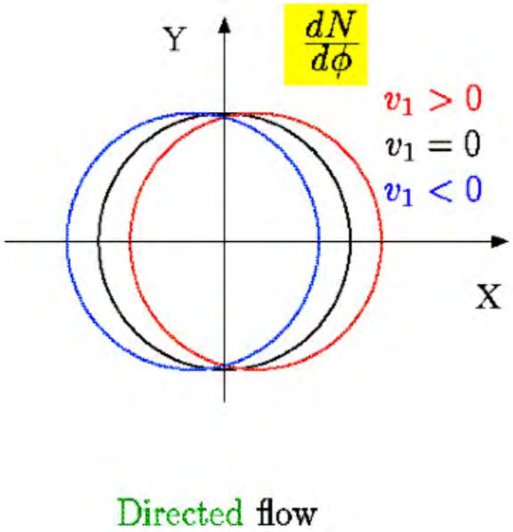

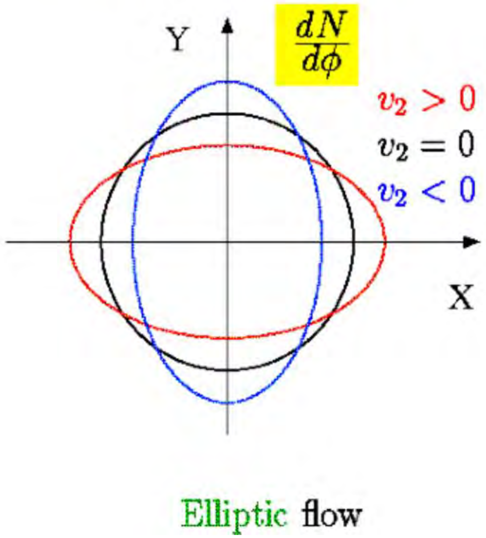

Elliptic flow ($\sqrt{s_{NN}} = 200\ GeV\ vs\ 27GeV$)

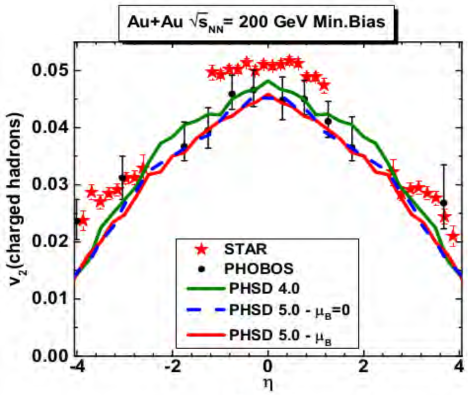

a)

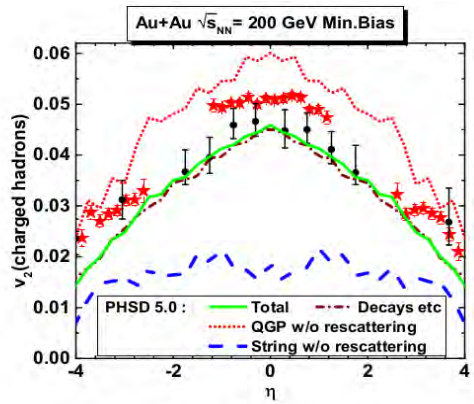

b)

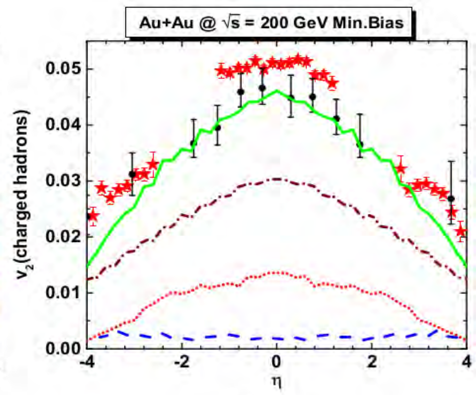

c)

No visible effects of μ_B dependence

200GeV, 10-20% central

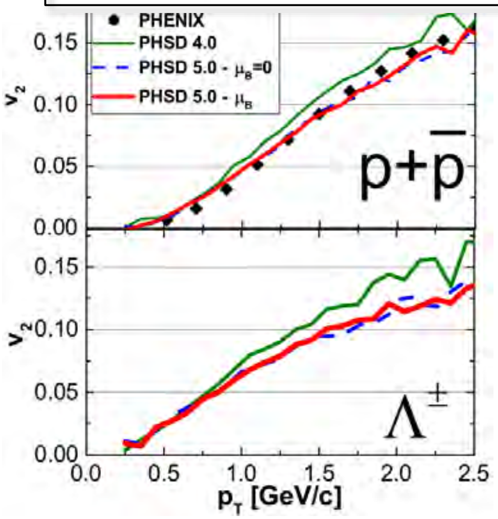

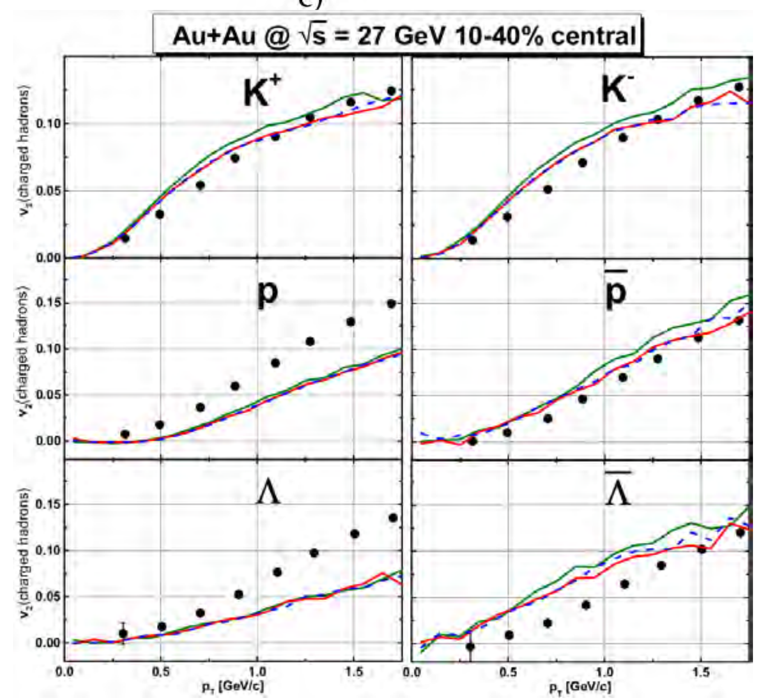

Directed flow ($\sqrt{s_{NN}} = 200\ GeV\ vs\ 27\ GeV$)

$\sqrt{s_{NN}} = 200\ GeV, 10-40\%\ centr$

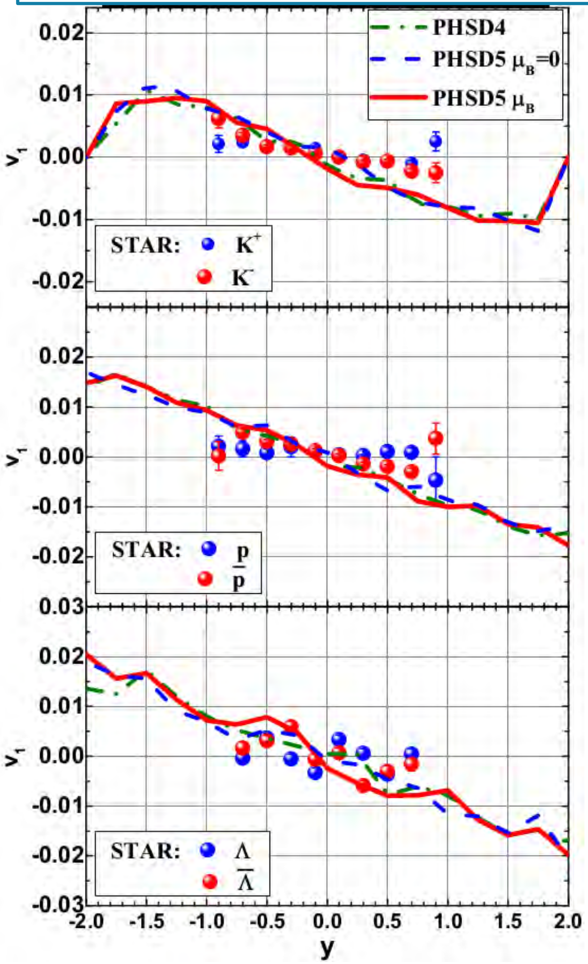

$\sqrt{s_{NN}} = 27\ GeV, 10-40\%\ centr$

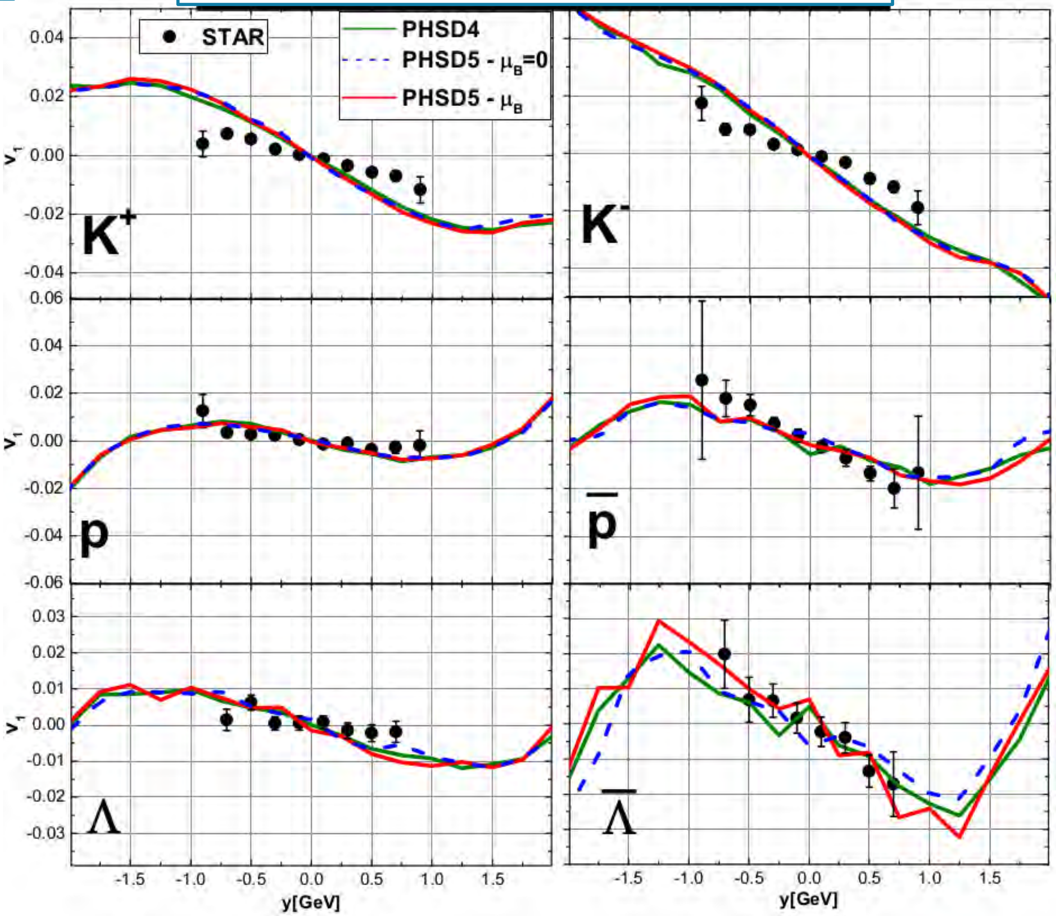

No visible effects of μ_B dependence

Transport coefficients: baryon diffusion coefficient

- **Relaxation Time Approximation**

$$\kappa_B^{\mathrm{RTA}}(T,\mu_B) = \frac{1}{3}\sum_{i=q,\bar{q}}\int \frac{d^3p}{(2\pi)^3}\mathbf{p}^4\tau_i(\mathbf{p},T,\mu_B)$$

$$\frac{d_i(1\pm f_i)f_i}{E_i^2}\left(b_a - \frac{n_B E_i}{\epsilon + p}\right)^2$$

Baryon diffusion depends on the baryon charge->
Reduces proton v2 and increases antiproton v2

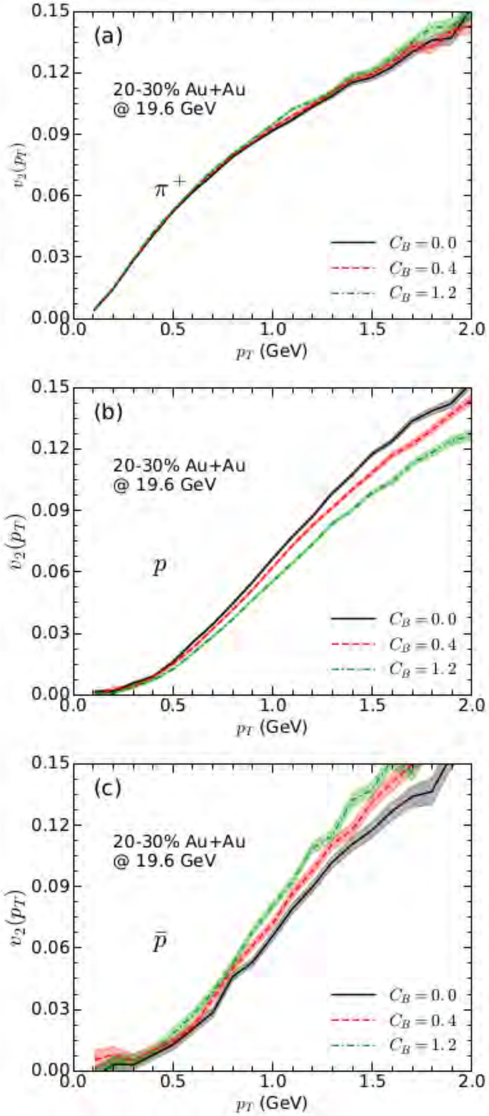

G. S. Denicol et al, PRC 98. 034916 (2018)

Transport coefficients: shear viscosity

- **Kubo formalism**

$$\eta^{\mathrm{Kubo}}(T,\mu_q) = -\int \frac{d^4p}{(2\pi)^4}\, p_x^2 p_y^2 \sum_{i=q,\bar{q},g} d_i\, \frac{\partial f_i(\omega)}{\partial \omega}\, \rho_i(\omega,\mathbf{p})^2$$

$$= \frac{1}{15T}\int \frac{d^4p}{(2\pi)^4}\, \mathbf{p}^4 \sum_{i=q,\bar{q},g} d_i\, \left((1\pm f_i(\omega)) f_i(\omega)\right) \rho_i(\omega,\mathbf{p})^2$$

- **Relaxation Time Approximation**

$$\eta^{\mathrm{RTA}}(T,\mu_q) = \frac{1}{15T}\int \frac{d^3p}{(2\pi)^3} \sum_{i=q,\bar{q},g} \left(\frac{\mathbf{p}^4}{E_i^2\, \boxed{\Gamma_i(\mathbf{p}_i,T,\mu_q)}}\, d_i\, \left((1\pm f_i(E_i)) f_i(E_i)\right)\right)$$

Collisional rate

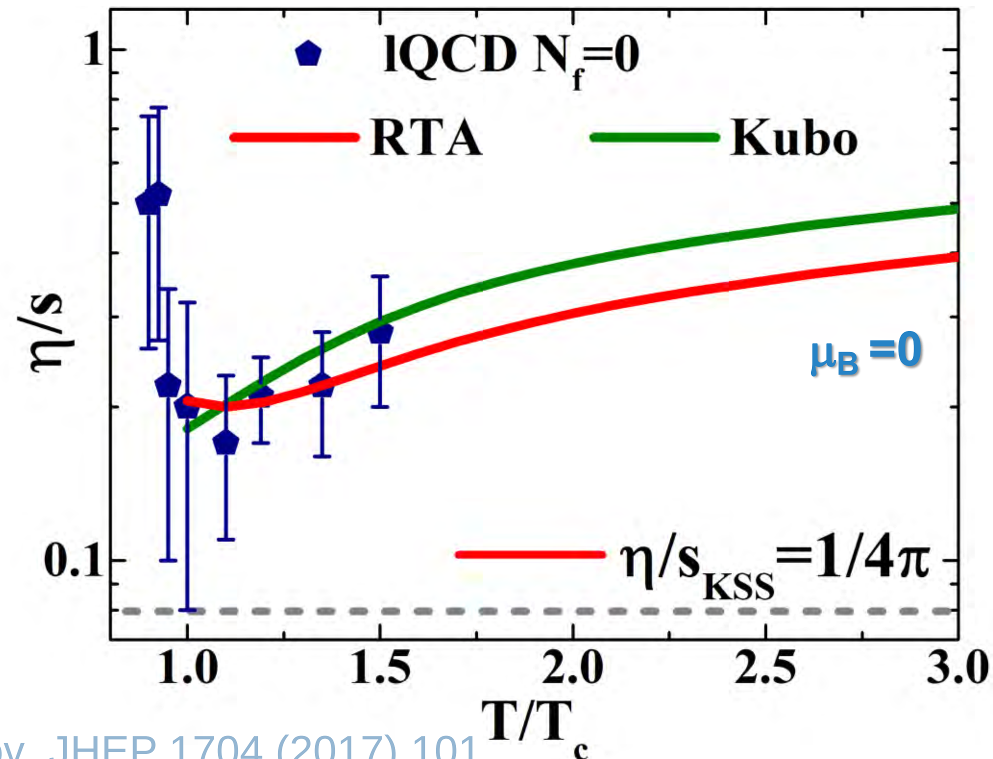

Lattice: N. Astrakhantsev, V. Braguta, A. Kotov JHEP 1704 (2017) 101

DQPM: Time-like and ‚space-like‘ energy densities

Time/space-like part of energy-momentum tensor $T_{\mu\nu}$ for quarks and gluons:

$$T^{\pm}_{00,x}(T) = \tilde{T}r^{\pm}_{x}\ \omega$$

x: gluons, quarks, antiquarks

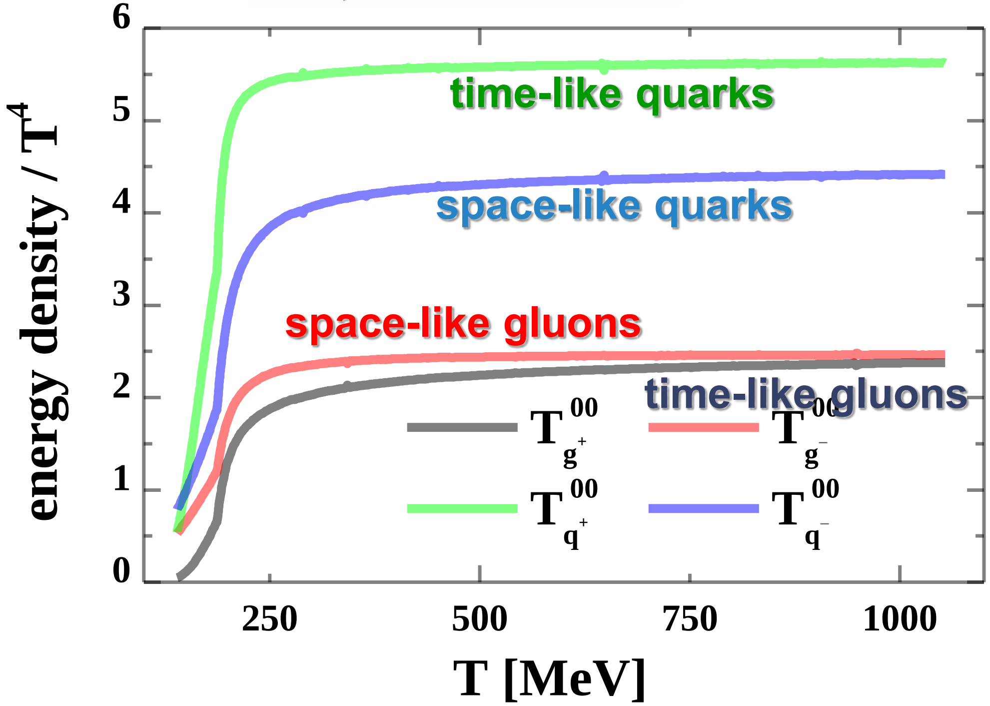

- space-like energy density of quarks and gluons = ~1/3 of total energy density
- space-like energy density dominates for gluons
- space-like parts are identified with potential energy densities

Cassing, NPA 791 (2007) 365: NPA 793 (2007)

DQPM EoS at finite (T, μ_B)

- **Taylor series of thermodynamic quantities in terms of (μ_B/T)**
- **With the 6[nd] order susceptibility. Example 2[nd] order:**

$$\Delta P/T^4 = \frac{P(T,\mu_B) - P(T,0)}{T^4} \approx \frac{1}{2}\chi_2^B(T)\left(\frac{\mu_B}{T}\right)^2$$

$$\frac{n_B}{T^3} = \left.\frac{\partial(P/T^4)}{\partial(\mu_B/T)}\right|_T \approx \chi_2^B(T)\left(\frac{\mu_B}{T}\right)$$

$$\Delta s/T^3 = \frac{s(T,\mu_B) - s(T,0)}{T^3} = \frac{1}{T^3}\left.\frac{\partial \Delta P}{\partial T}\right|_{\mu_B}$$

$$= T\left.\frac{\partial(\Delta P/T^4)}{\partial T}\right|_{\mu_B} + 4(\Delta P/T^4) \approx \frac{1}{2}\left(T\frac{\partial \chi_2^B(T)}{\partial T} + 2\chi_2^B(T)\right)\left(\frac{\mu_B}{T}\right)^2$$

$$\Delta\epsilon/T^4 = \frac{\epsilon(T,\mu_B) - \epsilon(T,0)}{T^4}$$

$$= \Delta s/T^3 - \Delta P/T^4 + \left(\frac{\mu_B}{T}\right)\frac{n_B}{T^3} \approx \frac{1}{2}\left(T\frac{\partial \chi_2^B(T)}{\partial T} + 3\chi_2^B(T)\right)\left(\frac{\mu_B}{T}\right)^2$$

A. Bazavov, Phys. Rev. D 96, 054504(2017)

Extraction of (T, μ_B) in PHSD

- **In each space-time cell of the PHSD, the energy-momentum tensor is calculated by the formula:**

$$T^{\mu\nu} = \sum_i \frac{p_i^\mu p_i^\nu}{E_i}$$

- **Diagonalization of the energy-momentum tensor to get the energy density and pressure components expressed in the local rest frame (LRF)**

$$T^{\mu\nu} = \begin{pmatrix} T^{00} & T^{01} & T^{02} & T^{03} \\ T^{10} & T^{11} & T^{12} & T^{13} \\ T^{20} & T^{21} & T^{22} & T^{23} \\ T^{30} & T^{31} & T^{32} & T^{33} \end{pmatrix} \Rightarrow \begin{pmatrix} \epsilon^{LRF} & 0 & 0 & 0 \\ 0 & P_x^{LRF} & 0 & 0 \\ 0 & 0 & P_y^{LRF} & 0 \\ 0 & 0 & 0 & P_z^{LRF} \end{pmatrix}$$

Xu et al., Phys.Rev. C96 (2017), 024902

For each space-time cell of the PHSD:

- **Calculate the local energy density ε^{PHSD} and baryon density n_B^{PHSD}**
- **use lQCD relations (up to 6th order):**

$$\begin{cases} \dfrac{n_B}{T^3} \approx \chi_2^B(T)\left(\dfrac{\mu_B}{T}\right) + \ldots \\ \Delta\epsilon/T^4 \approx \dfrac{1}{2}\left(T\dfrac{\partial\chi_2^B(T)}{\partial T} + 3\chi_2^B(T)\right)\left(\dfrac{\mu_B}{T}\right)^2 + \ldots \end{cases}$$

➔ **obtain (T, μ_B) by solving the system of coupled equations using ε^{PHSD} and n_B^{PHSD}**

Isentropic trajectories for (T, μ_B)

- Correspondance $s/n_B \leftrightarrow$ collisional energy

s/n_B = 420 ↔ 200 GeV
= 144 ↔ 62.4 GeV
= 94 ↔ 39 GeV
= 70 ↔ 15 GeV
= 51 ↔ 19.6 GeV
= 30 ↔ 14.5 GeV

DQPM

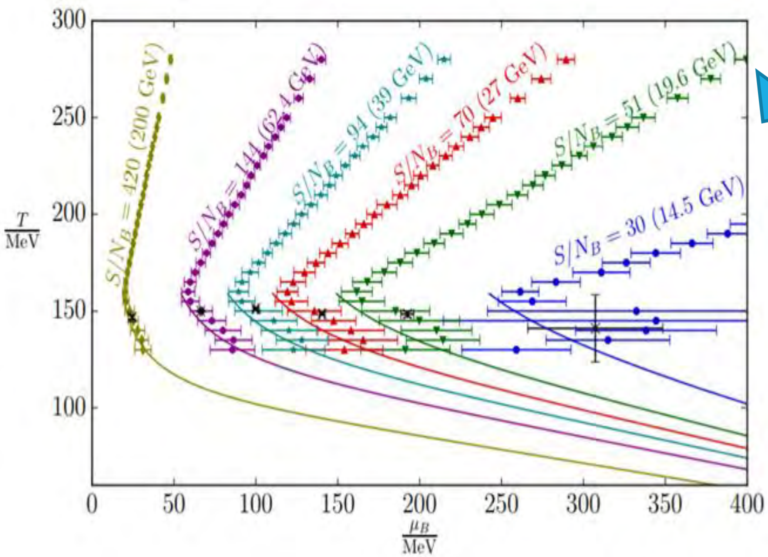

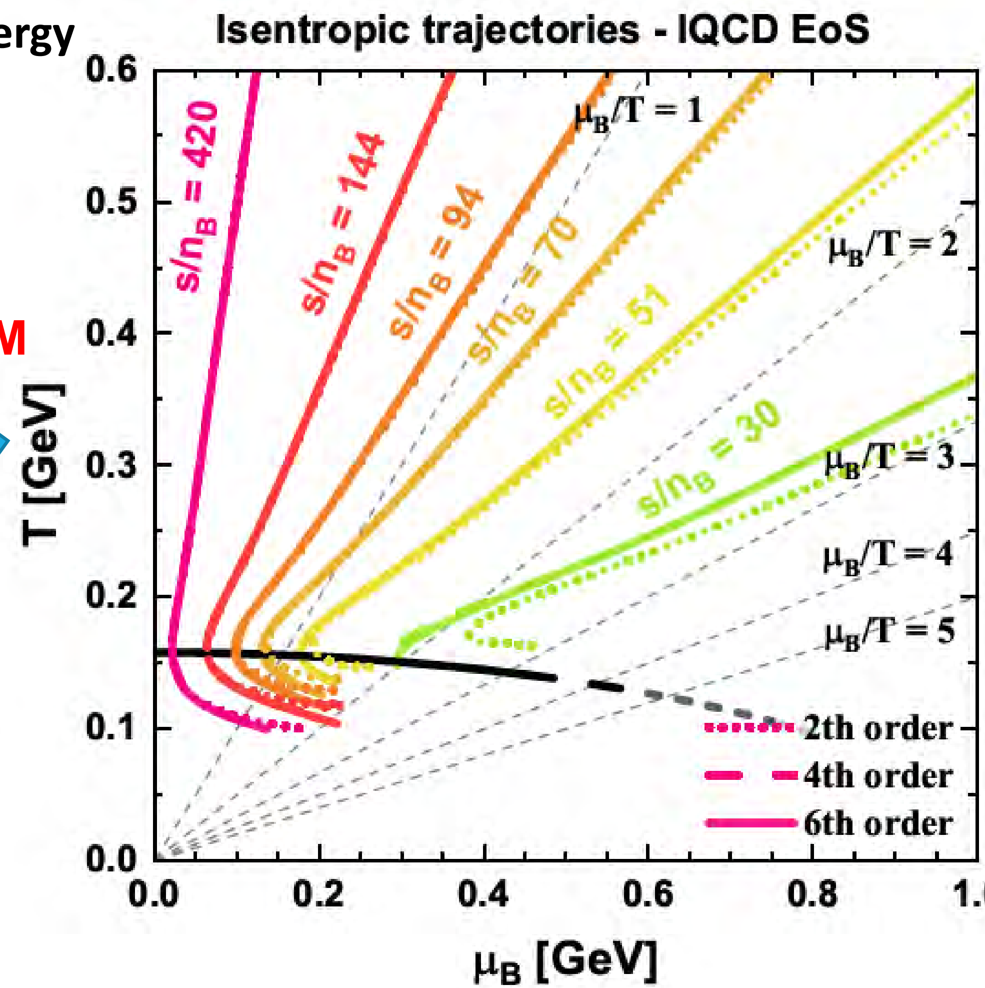

- Safe for $(\mu_B/T) < 3$

lQCD: WB, PoS CPOD2017 (2018) 032

P. Moreau et al., arXiv:1903.10157, PRC (2019)

QuasiParticle model

❖ **How to construct a quasi-particle model:**

1) assume the properties of quasi-particles ➔ some model parameters involved

2) determine the thermal properties of the system from

Grand canonical potential Ω in propagator (D,S) representation (2PI):

$$\beta\Omega[D,S] = \underbrace{\frac{1}{2}\mathrm{Tr}[\ln D^{-1} - \Pi D]}_{\text{bosons}} - \underbrace{\mathrm{Tr}[\ln S^{-1} + \Sigma S]}_{\text{fermions}} + \Phi[D,S]$$

Self-energies:

$$\frac{\delta\Phi}{\delta D} = \frac{1}{2}\Pi$$

$$\frac{\delta\Phi}{\delta S} = -\Sigma$$

Cf. J.P. Blaizot et al, PRD 63 (2001) 065003

i.e. determine entropy *S*, pressure P etc. for QP:

$$\Omega/V = -P \qquad d\Omega = -SdT - PdV - Nd\mu \qquad S = -\frac{\partial\Omega}{\partial T} \qquad N = -\frac{\partial\Omega}{\partial\mu} \qquad P = -\frac{\partial\Omega}{\partial V}$$

3) fit S, P from QP to S, P from lQCD ➔ fix the model parameters

➔ Properties of quasi-particles

Energy-momentum tensor in PHSD

- **Diagonalization of the energy-momentum tensor to get the energy density and pressure components expressed in the local rest frame (LRF)**

$$T^{\mu\nu}\ (x_\nu)_i = \lambda_i\ (x^\mu)_i = \lambda_i\ g^{\mu\nu}\ (x_\nu)_i$$

- **Landau-matching condition:** Xu et al., Phys.Rev. C96 (2017), 024902

$$T^{\mu\nu} u_\nu = \epsilon u^\mu = (\epsilon g^{\mu\nu}) u_\nu$$

- **Evaluation of the characteristic polynomial:**

$$P(\lambda) = \begin{vmatrix} T^{00}-\lambda & T^{01} & T^{02} & T^{03} \\ T^{10} & T^{11}+\lambda & T^{12} & T^{13} \\ T^{20} & T^{21} & T^{22}+\lambda & T^{23} \\ T^{30} & T^{31} & T^{32} & T^{33}+\lambda \end{vmatrix}$$

- **The four solutions λ_i are identified to $(e, -P_1, -P_2, -P_3)$**

The pressure components P_i do not necessarily correspond to (P_x, P_y, P_z)

Extraction of (T, μ_B) in PHSD

- **Correction for the medium anisotropy to extract values for (T, μ_B)**

$$\epsilon^{\rm anis} = \epsilon^{\rm EoS} \; r(x)$$

$$P_\perp = P^{\rm EoS} \; [r(x) + 3xr'(x)]$$

$$P_{||} = P^{\rm EoS} \; [r(x) - 6xr'(x)]$$

$$r(x) = \begin{cases} \dfrac{x^{-1/3}}{2}\left[1 + \dfrac{x \,\text{arctanh}\sqrt{1-x}}{\sqrt{1-x}}\right] & \text{for } x \le 1 \\ \dfrac{x^{-1/3}}{2}\left[1 + \dfrac{x \arctan\sqrt{x-1}}{\sqrt{x-1}}\right] & \text{for } x \ge 1 \end{cases}$$

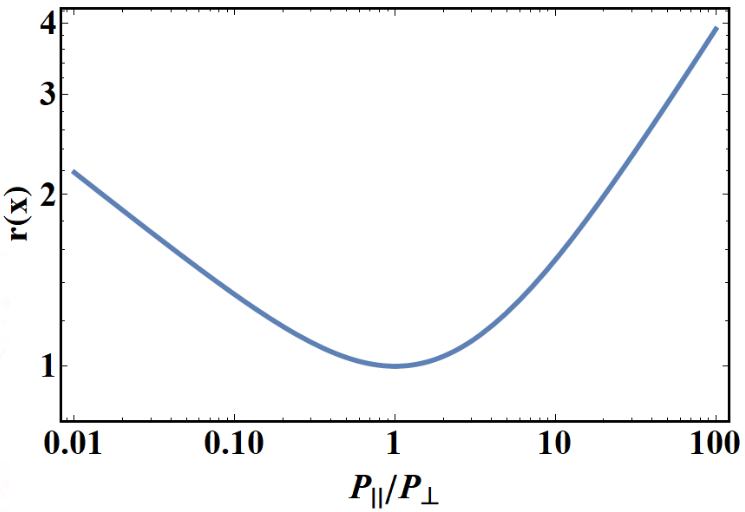

Ryblewski, Florkowski, Phys.Rev. C85 (2012) 064901

- **We have to solve the following system in PHSD:**

$$\begin{cases} \epsilon^{\rm EoS}(T, \mu_B) = \epsilon^{\rm PHSD}/r(x) \\ n_B^{\rm EoS}(T, \mu_B) = n_B^{\rm PHSD} \end{cases}$$

Done by Newton-Raphson method

Models of Heavy-Ion Collisions

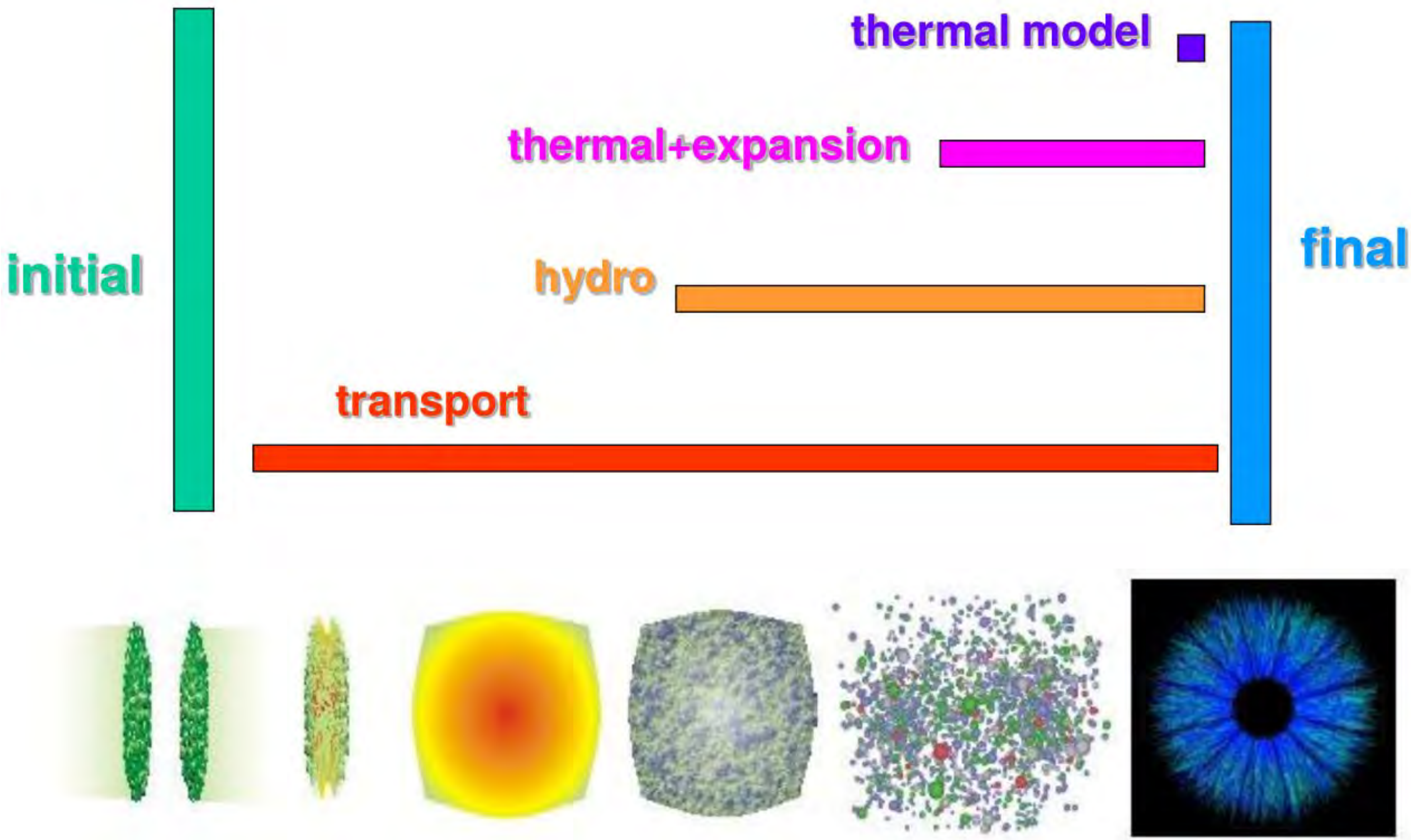

DQPM: q, qbar, g elastic/inelastic scattering (leading order)

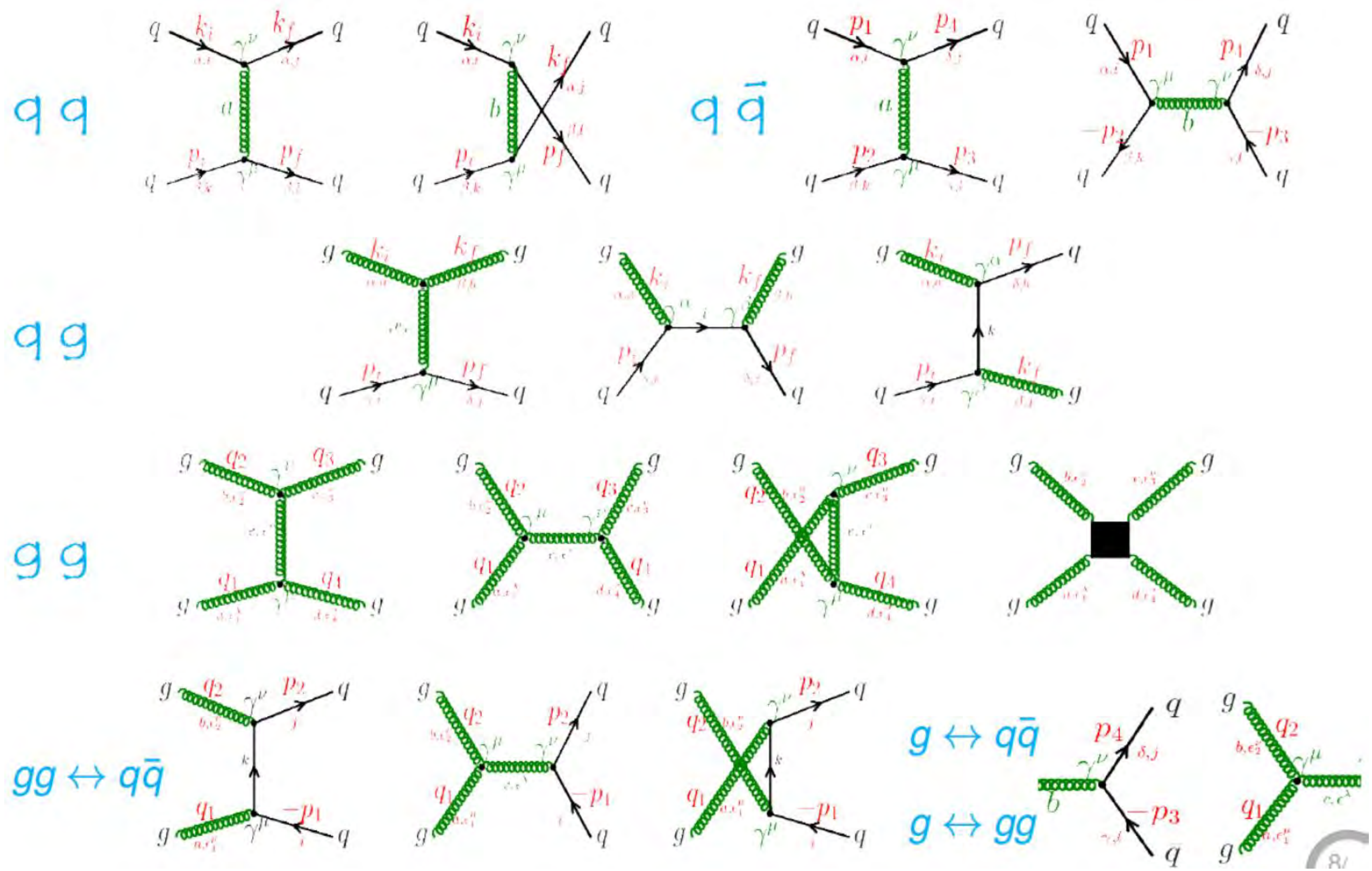

Di-jets in e-p (e-A) collisions from high energy correlators

Farid Salazar

February 28th, 2020

The Galileo Galilei Institute For Theoretical Physics

Outline

- Nuclear matter at high energies: The Color Glass Condensate
- Eikonal scattering, deep inelastic scattering and the dipole correlator
- Di-jets and the quadrupole correlator
- Cross section and elliptic anisotropy
- Outlook

Nuclear matter at high energies

Nuclear matter at high energies

- At high energies (small-x) the dominant degrees of freedom are gluons.

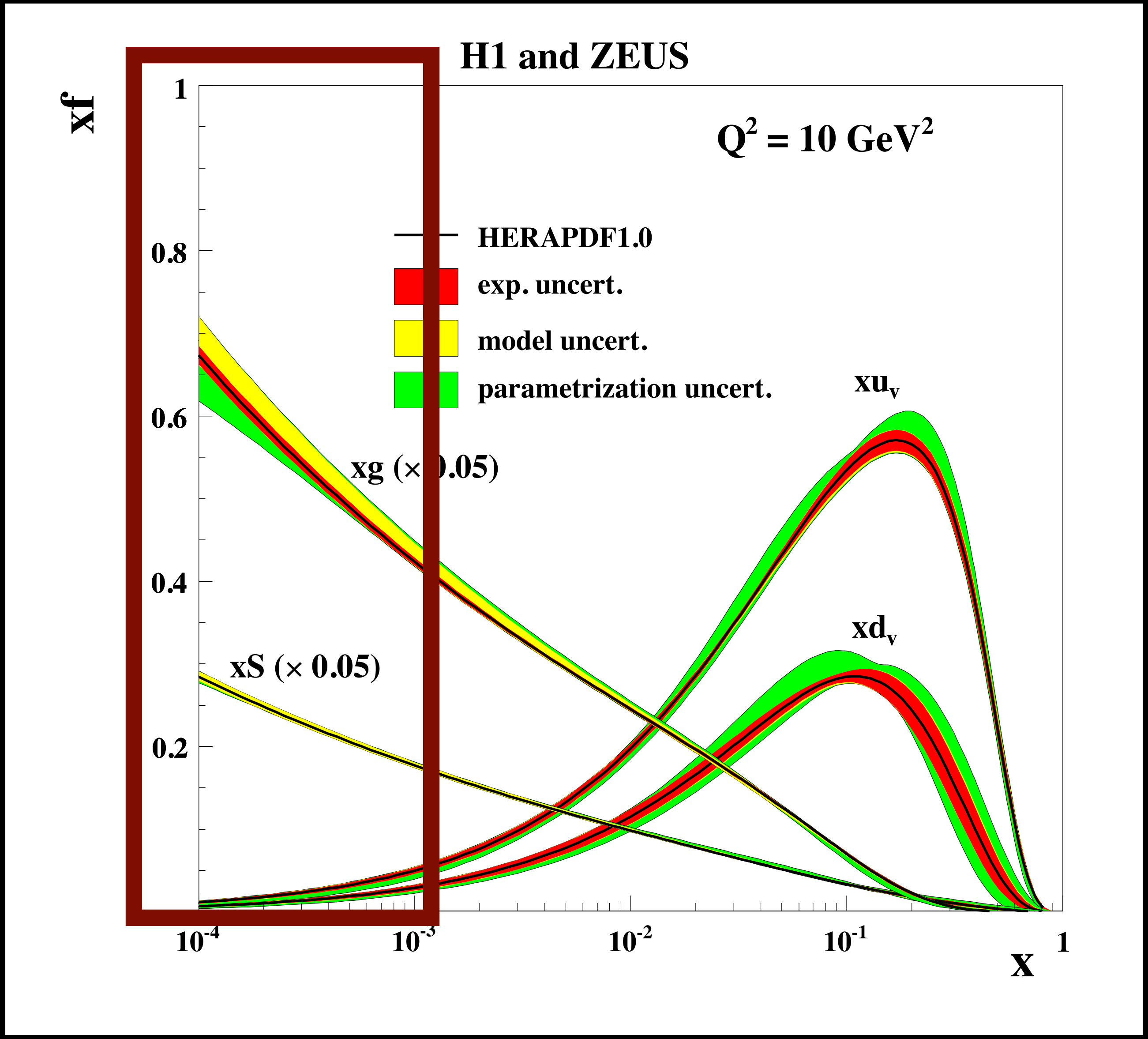

Deep inelastic scattering

longitudinal momentum fraction

Center of mass energy

$$x \sim Q^2/s$$

Photon's virtuality (transverse resolution)

The Color Glass Condensate: Stochastic Yang-Mills

- **Small-x: gluons with a high occupation number.**

  Classical field: $A^{\mu,a}$

$$[D_\nu, F^{\mu\nu}] = J^\mu$$

- **Large-x: frozen, localized (time dilation and length contraction)**

Static eikonal color sources:

$$J^{\mu,a} = \delta^{\mu,+}\rho^a(x^-, x_\perp)$$

$W_\Lambda[\rho]$ **gauge invariant weight functional**

Evaluate correlators in two steps:

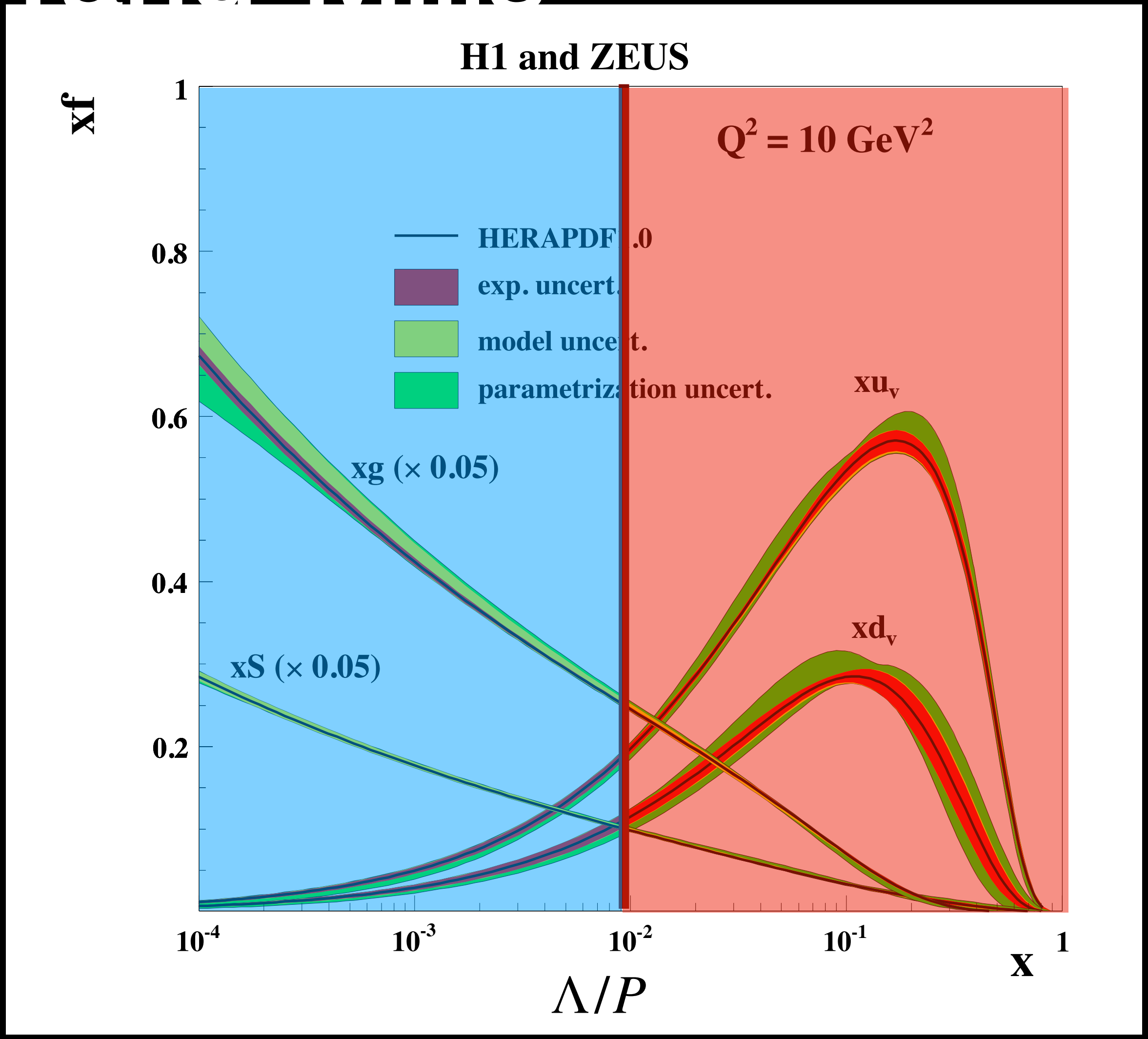

$$\langle\langle \mathcal{O}[\mathcal{A}]\rangle\rangle = \int [\mathcal{D}\rho] W_\Lambda[\rho] \frac{\int^\Lambda [\mathcal{D}A] O[A] e^{iS[\rho,A] - i\int j\cdot A}}{\int^\Lambda \mathcal{D}A e^{iS[\rho,A]}}$$

$$\langle \mathcal{O}[\mathcal{A}]\rangle = \int [\mathcal{D}\rho] W_\Lambda[\rho] \mathcal{O}[\mathcal{A}_{cl}[\rho]]$$

The Color Glass Condensate: JIMWLK Quantum Evolution

$$\langle\langle \mathcal{O}[\mathcal{A}] \rangle\rangle = \int [\mathcal{D}\rho] W_\Lambda[\rho] \frac{\int^\Lambda [\mathcal{D}A] O[A] e^{iS[\rho,A] - i\int j\cdot A}}{\int^\Lambda \mathcal{D}A e^{iS[\rho,A]}}$$

For correlators with momenta $k \ll \Lambda$ quantum corrections logarithmically enhanced (bremsstrahlung) are required.

$$\alpha_s \log(\Lambda/k)$$

$$\langle \mathcal{O}[\mathcal{A}] \rangle_\Lambda = \int [\mathcal{D}\rho] W_\Lambda[\rho]\, \mathcal{O}[\mathcal{A}_{qu}[\rho]]$$

not simple classical Yang-Mills, need to solve path integral

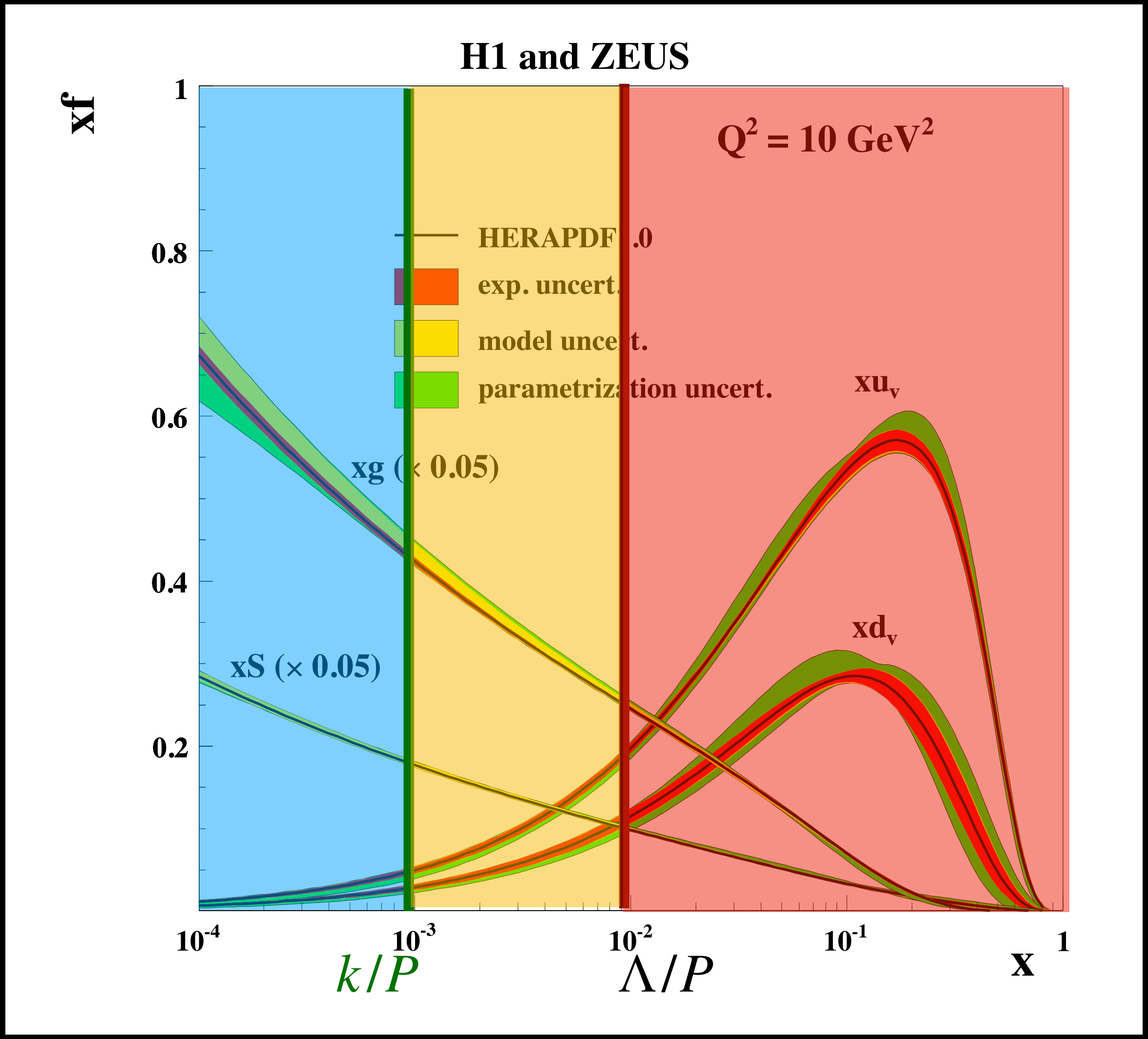

Quantum fluctuations

The Color Glass Condensate: JIMWLK Quantum Evolution

$$\langle\langle \mathcal{O}[\mathcal{A}]\rangle\rangle = \int [\mathcal{D}\rho] W_\Lambda[\rho] \frac{\int^\Lambda [\mathcal{D}A] O[A] e^{iS[\rho,A]-i\int j\cdot A}}{\int^\Lambda \mathcal{D}A e^{iS[\rho,A]}}$$

$$W_\Lambda[\rho] \longrightarrow W_{\Lambda'}[\rho]$$

$$\langle\langle \mathcal{O}[\mathcal{A}]\rangle\rangle = \int [\mathcal{D}\rho] W_{\Lambda'}[\rho] \frac{\int^{\Lambda'} [\mathcal{D}A] O[A] e^{iS[\rho,A]-i\int j\cdot A}}{\int^{\Lambda'} \mathcal{D}A e^{iS[\rho,A]}}$$

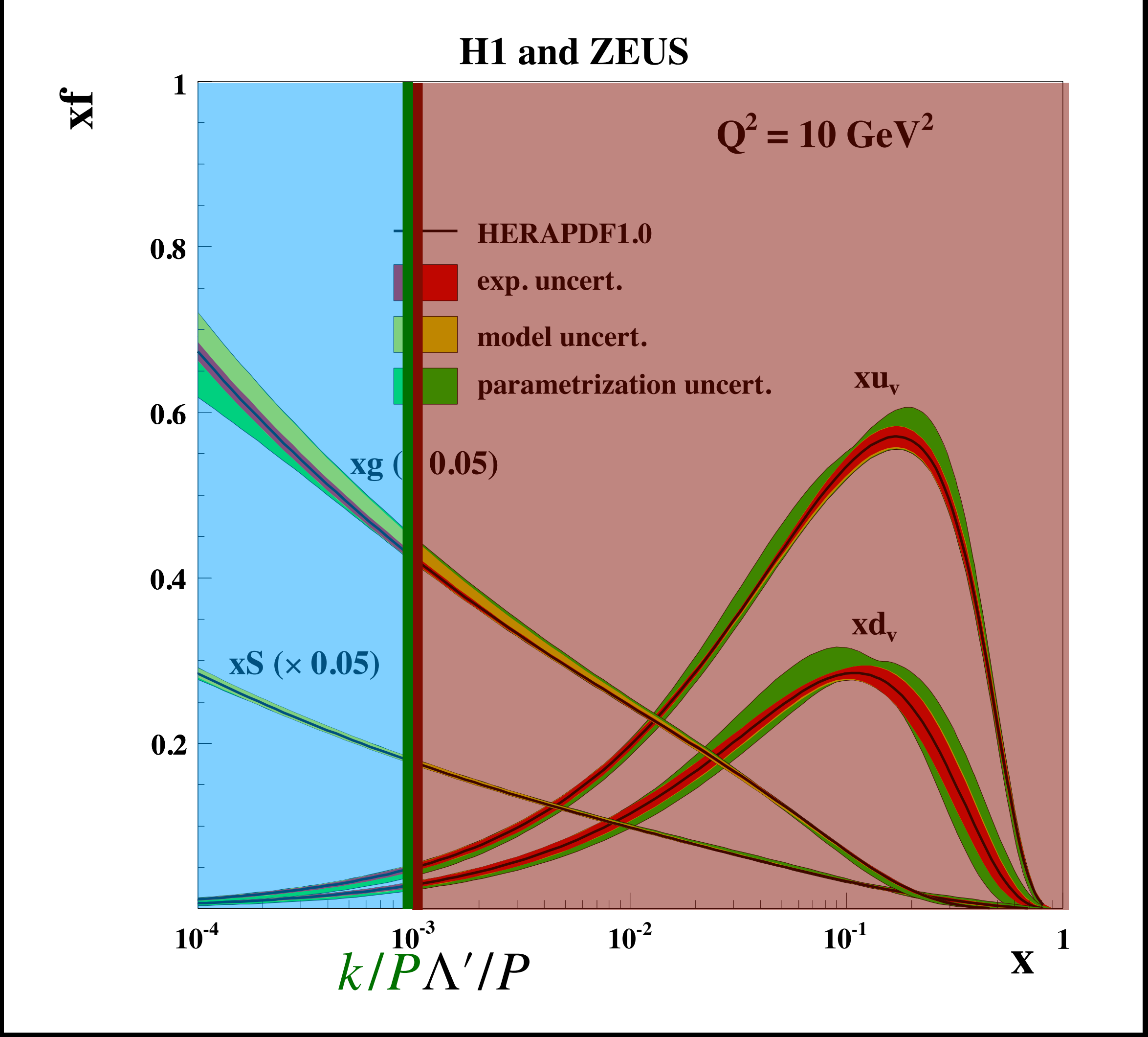

$$\int [\mathcal{D}\rho] W_\Lambda[\rho] \mathcal{O}[\mathcal{A}_{qu}[\rho]] = \int [\mathcal{D}\rho] W_{\Lambda'}[\rho] \mathcal{O}[\mathcal{A}_{cl}[\rho]]$$

Compute classical solution but with renormalized:

$$W_{\Lambda'}[\rho] = \mathcal{H}_{\mathrm{JIMWLK}} \otimes W_\Lambda[\rho]$$

Eikonal scattering, DIS and dipole correlator

Eikonal scattering from classical field: quark

Quark scattering off strong background field

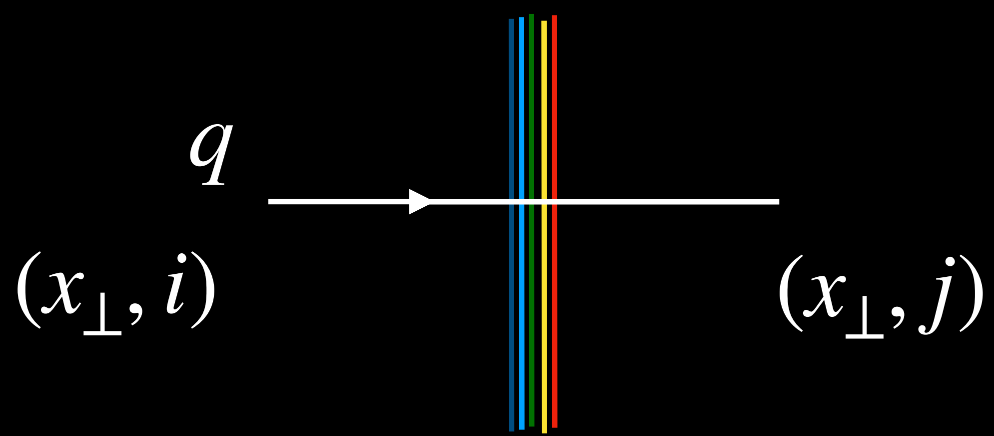

(i, j) color indices in fundamental representation

Color rotation

$$V_{ij}(x_\perp) = \left[\mathcal{P} e^{ig\int dz^- A^{+,a}(x_\perp, z^-) t^a}\right]_{ij}$$

t^a_{ij} **generator in fundamental rep.**

Multiple scattering: path order exponential encodes all multiple gluon exchanges.

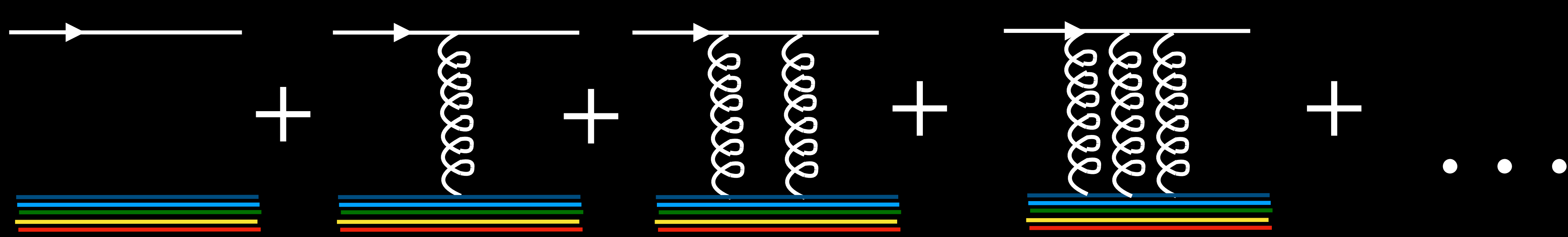

Expansion parameter: $g\rho \sim \mathcal{O}(1)$ **Strong field:** $\rho \sim 1/g$

Deep inelastic scattering

Dipole scatters from shockwave (CGC)

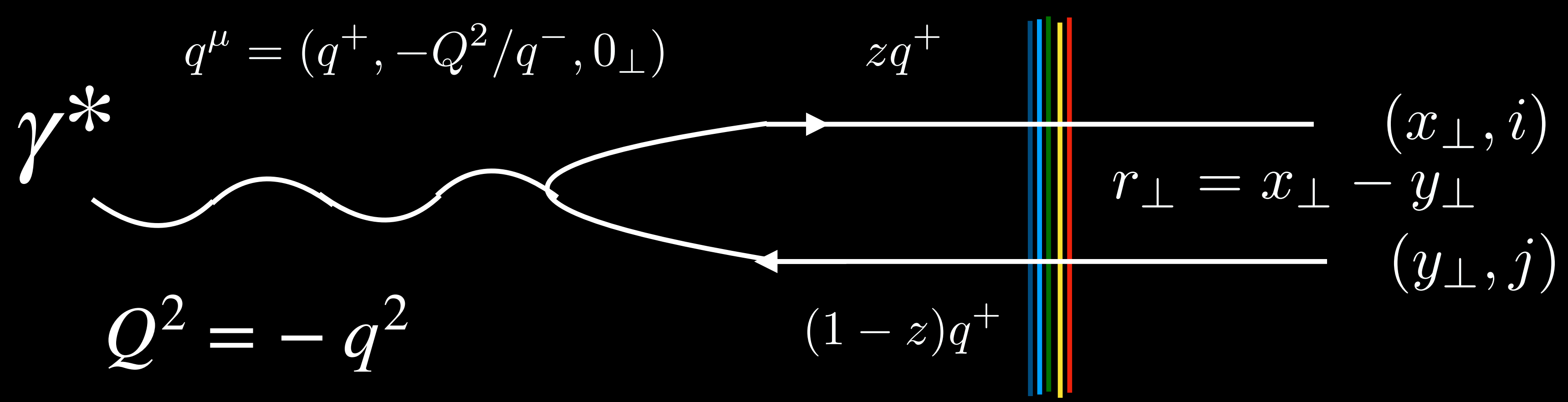

$$\Psi^{\gamma^* \to q\bar{q}}(Q, r_\perp, z)$$

Calculable in QED

$$i\mathcal{M}_{ij}^{q\bar{q}A}(r_\perp, b_\perp) = \frac{1}{N_c}\left[1_{ij} - \left[V(x_\perp)V^\dagger(y_\perp)\right]_{ij}\right]$$

QCD dynamics

Deep inelastic scattering

Dipole scatters from shockwave (CGC)

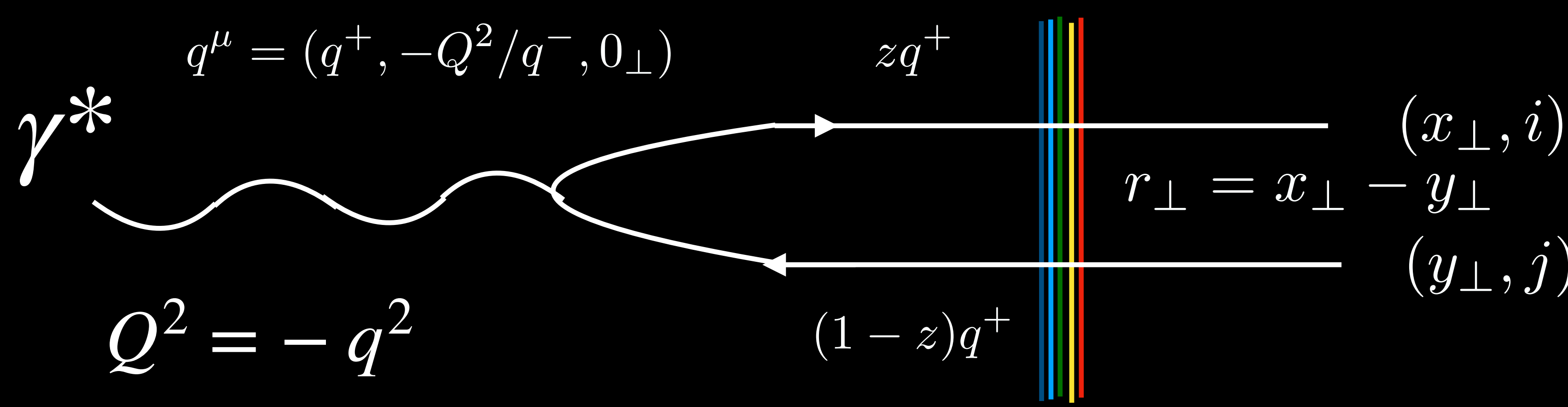

$$\Psi^{\gamma^* \to q\bar{q}}(Q, r_\perp, z) \qquad \frac{1}{N_c}\left[1_{ij} - \left[V(x_\perp)V^\dagger(y_\perp)\right]_{ij}\right]$$

Total DIS cross section:

$$\sigma_{tot}^{q\bar{q}A}(Q^2, x) = \int \frac{d^2 r_\perp}{4\pi} \int_0^1 \frac{dz}{z(1-z)} \left|\Psi^{\gamma^* \to q\bar{q}}(Q, x_\perp - y_\perp, z)\right|^2 \sigma^{q\bar{q}A}(r_\perp, x)$$

Optical theorem:

$$\sigma^{q\bar{q}A}(r_\perp, x) = 2\int d^2 b_\perp D\left(b_\perp + \frac{1}{2}r_\perp, b_\perp - \frac{1}{2}r_\perp, x\right)$$

$$D(x_\perp, y_\perp, x) = 1 - \frac{1}{N_c}\left\langle tr V(x_\perp)V^\dagger(y_\perp)\right\rangle_x$$

The dipole correlator

$$\mathcal{D}(x_\perp, y_\perp)_x = 1 - \frac{1}{N_c} tr(V(x_\perp)V^\dagger(y_\perp))$$

$$D(x_\perp, y_\perp)_x = 1 - \frac{1}{N_c}\left\langle tr(V(x_\perp)V^\dagger(y_\perp))\right\rangle_x$$

$$= \int [\mathcal{D}\rho] W_x[\rho] \left[1 - \frac{1}{N_c} tr(V(x_\perp)V^\dagger(y_\perp))\right]$$

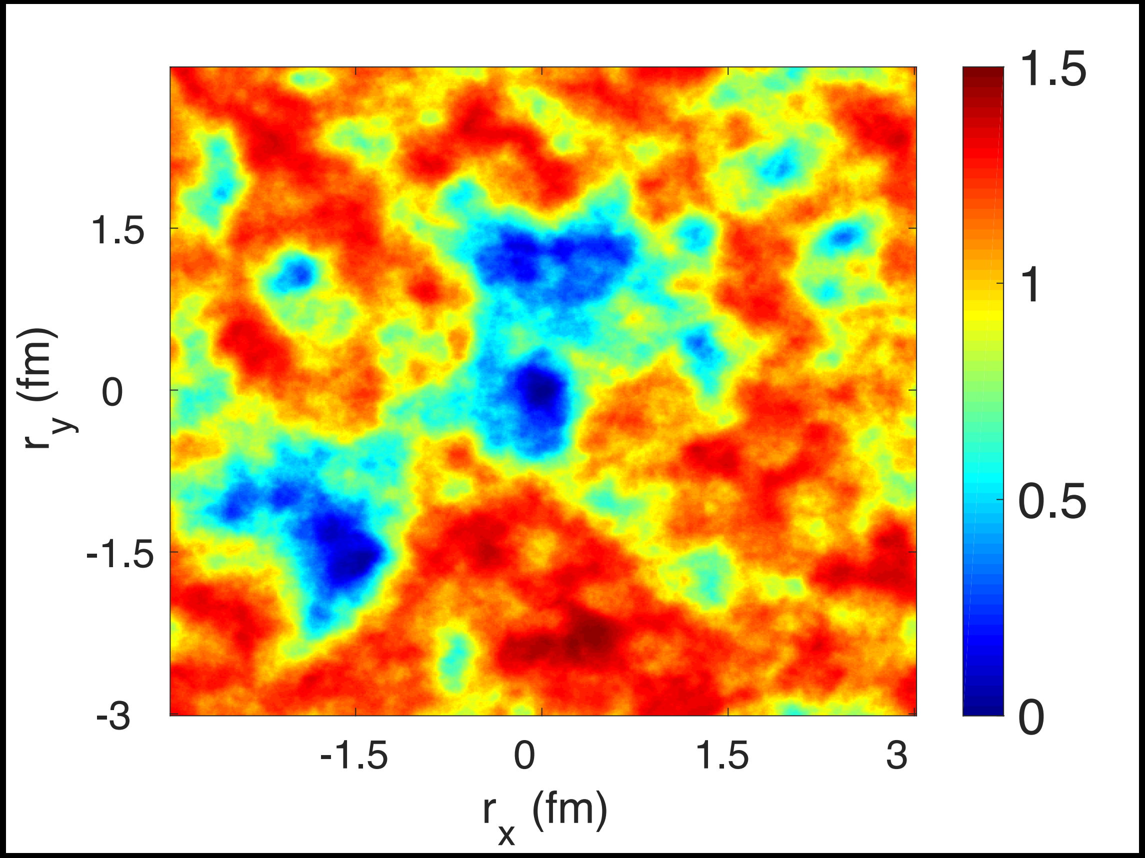

"Dipole amplitude" for one color charge configuration $\mathcal{D}(r_\perp, 0)$

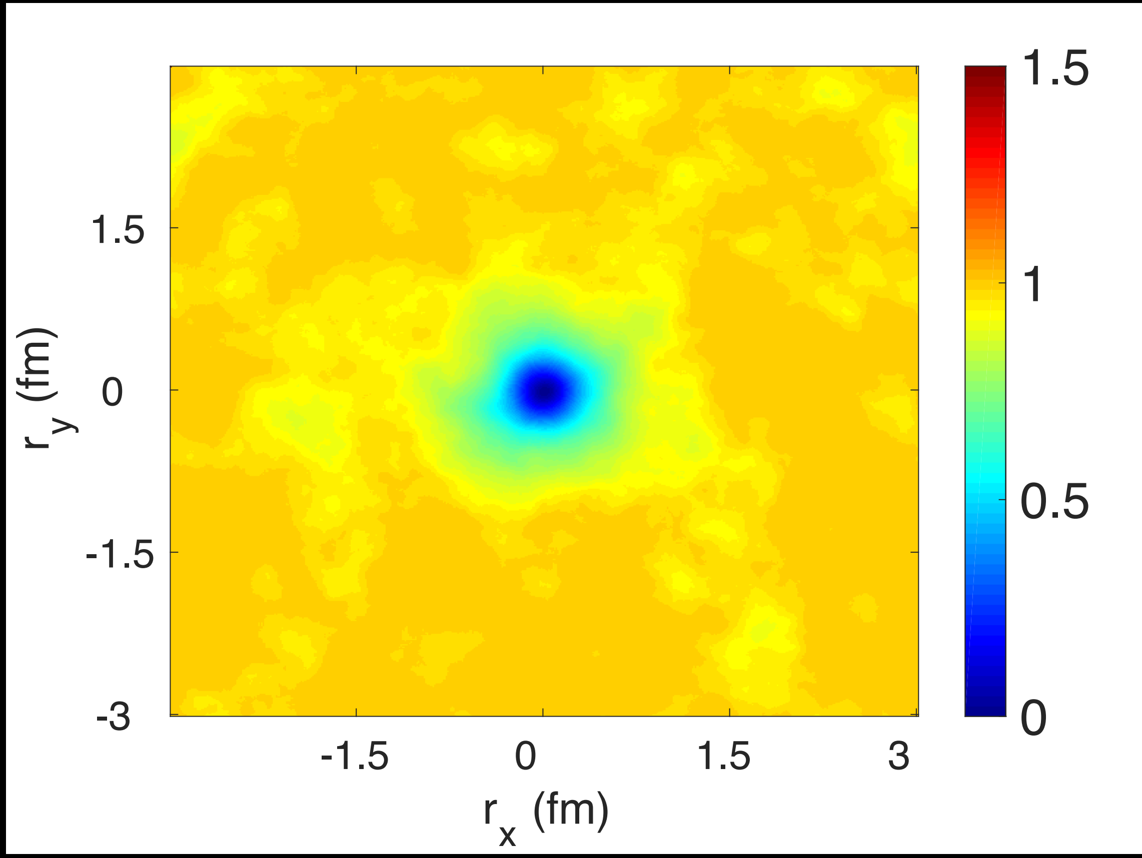

"Dipole amplitude" averaged over multiple charge configurations $D(r_\perp, 0)$

MV model: $\langle \rho^a(x_\perp)\rho^b(y_\perp)\rangle = \mu^2 \delta^{ab}\delta^{(2)}(x_\perp - y_\perp)$

The dipole correlator

$$\mathcal{D}(x_\perp, y_\perp)_x = 1 - \frac{1}{N_c} tr(V(x_\perp)V^\dagger(y_\perp))$$

$$D(x_\perp, y_\perp)_x = 1 - \frac{1}{N_c}\left\langle tr(V(x_\perp)V^\dagger(y_\perp))\right\rangle_x$$

$$= \int [\mathcal{D}\rho] W_x[\rho] \left[1 - \frac{1}{N_c} tr(V(x_\perp)V^\dagger(y_\perp))\right]$$

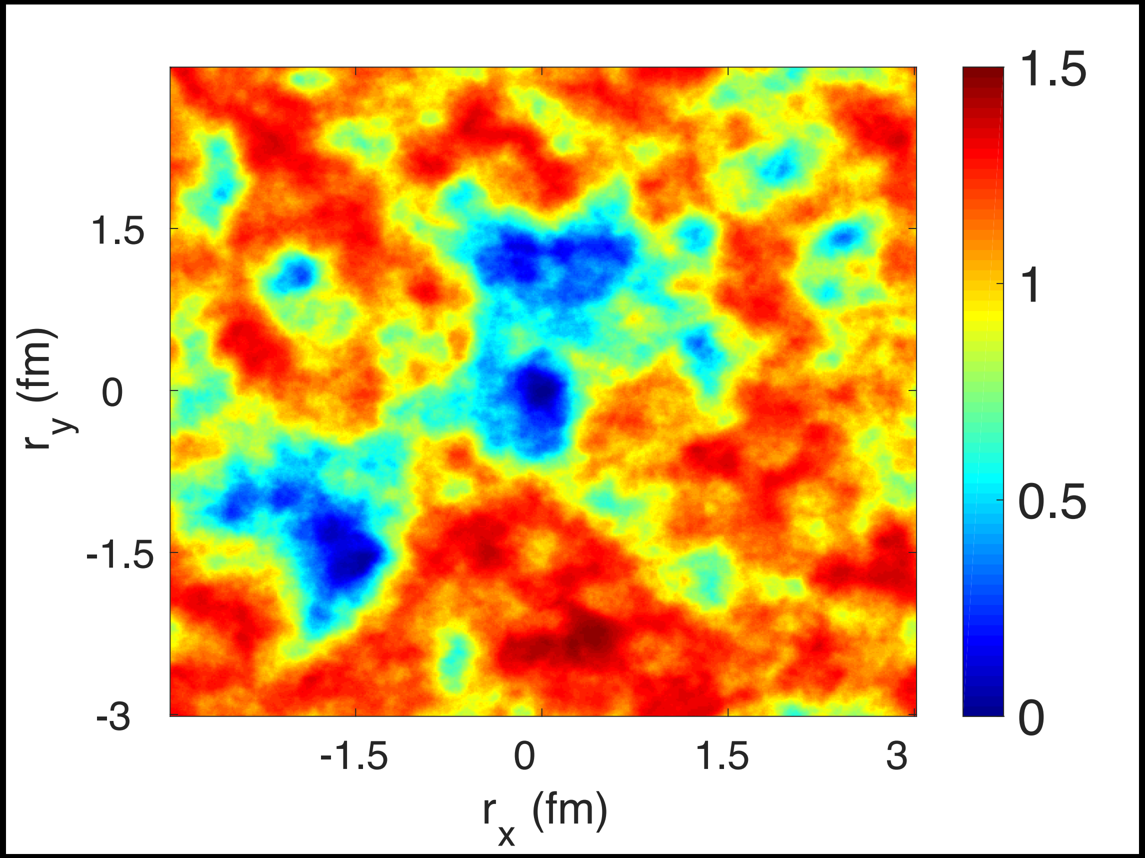

"Dipole amplitude" for one color charge configuration $\mathcal{D}(r_\perp, 0)$

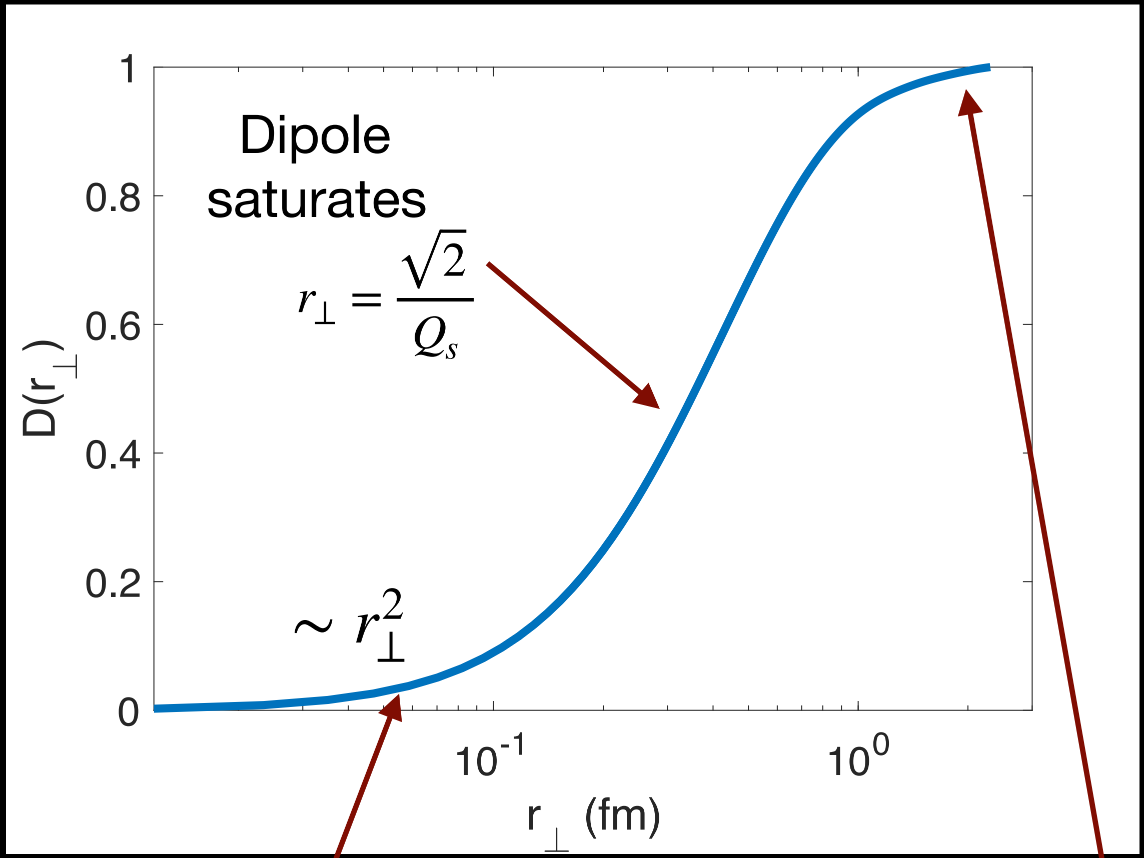

Color transparency

Black-disk

Saturation scale grows with density $Q_s^2 \sim \mu^2$

The dipole correlator

Energy evolution

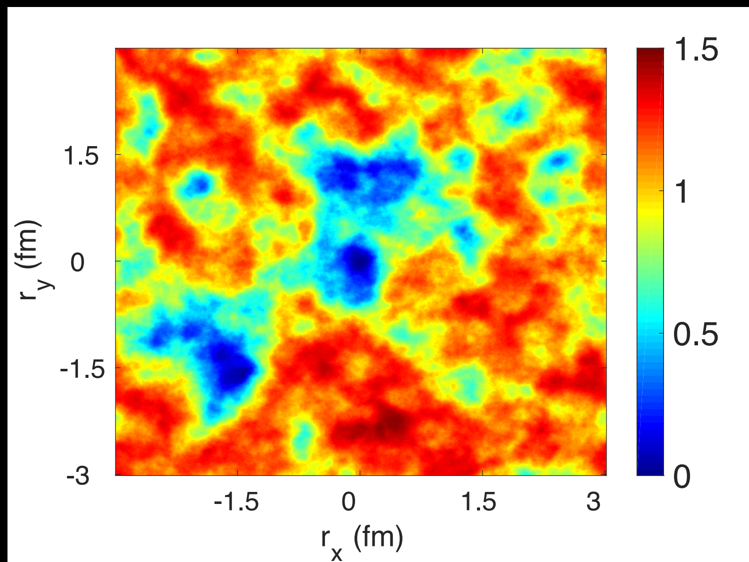

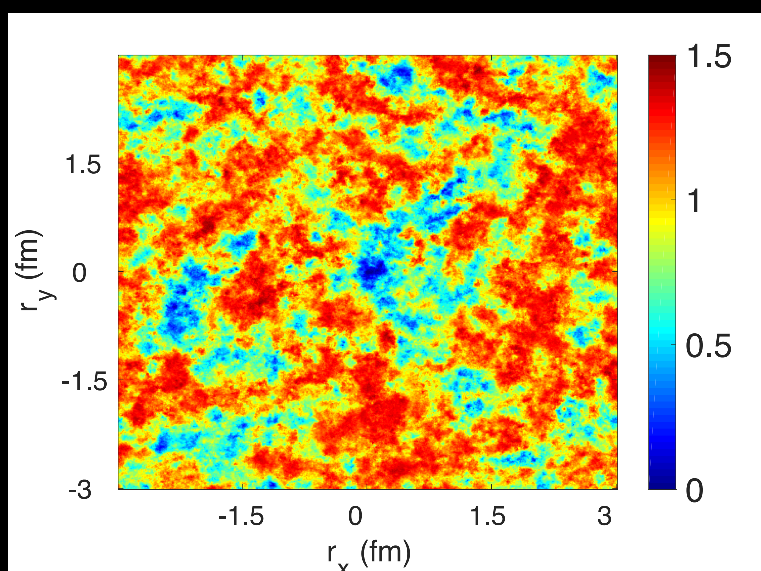

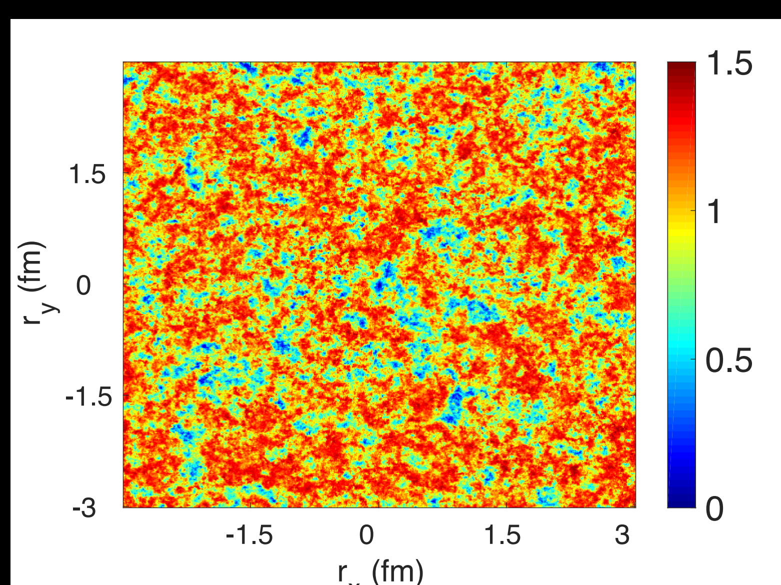

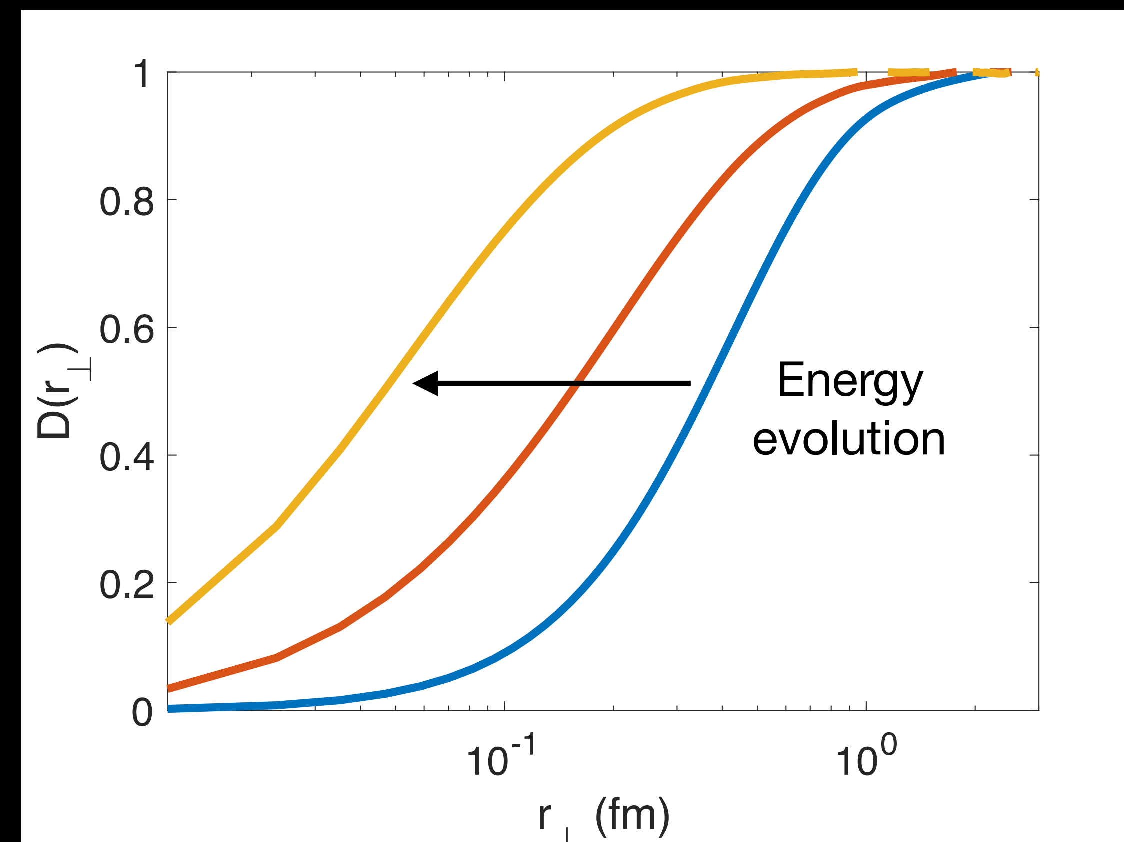

At higher energies dipole saturation occurs at smaller dipole sizes.

$$Q_s^2 \sim (1/x)^\lambda \sim s^\lambda \qquad \lambda \sim 0.3$$

$\alpha_s(Q_s) \ll 1$ weak coupling

Di-jets and the quadrupole correlator

Di-jet production in ep (eA)

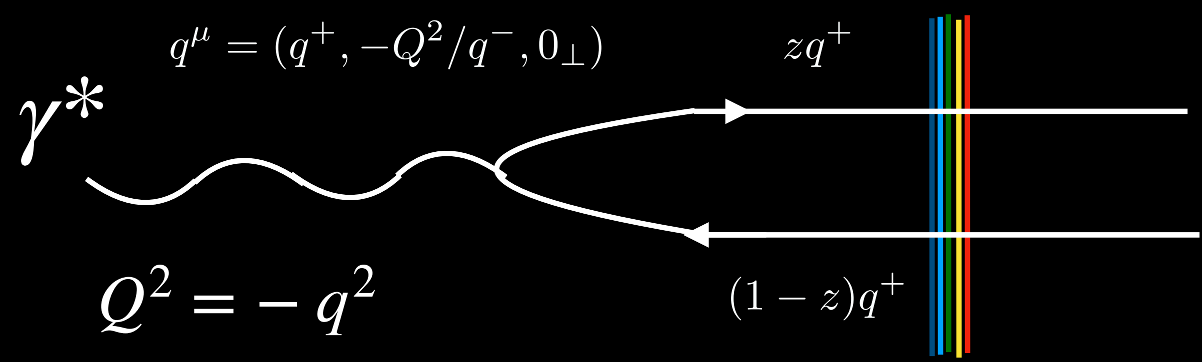

Inclusive dijet

two jets + anything else

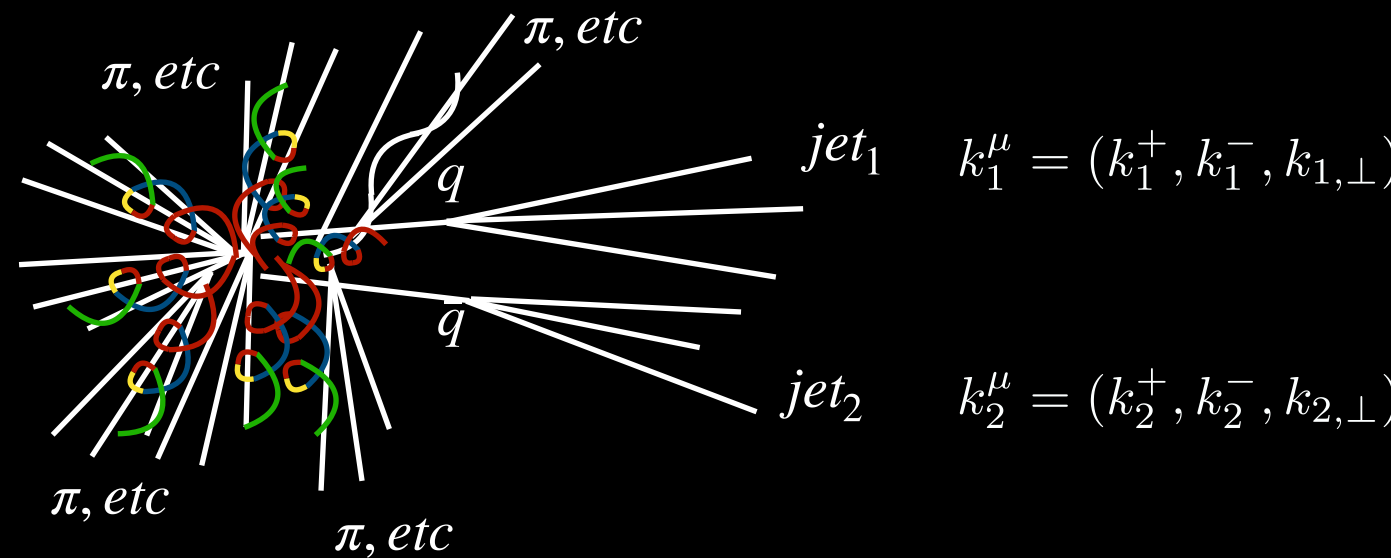

Convenient choice of coordinates

$$P_\perp = z_2 k_{1,\perp} + z_1 k_{2,\perp}$$

$$\Delta_\perp = k_{1,\perp} - k_{2,\perp}$$

Momenta in the transverse plane

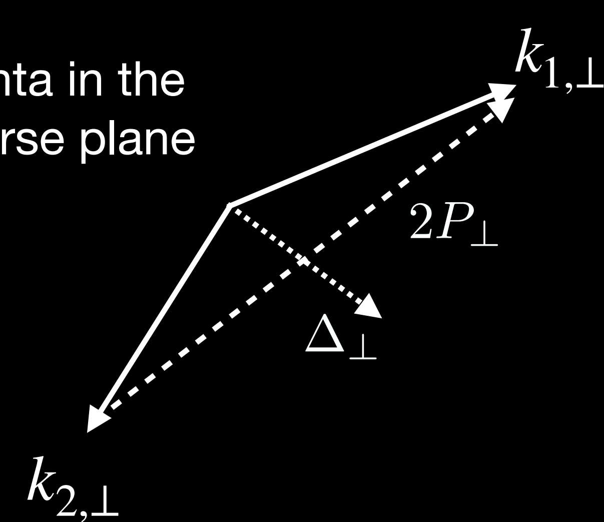

Di-jet production in ep (eA)

Amplitude **Conjugate amplitude**

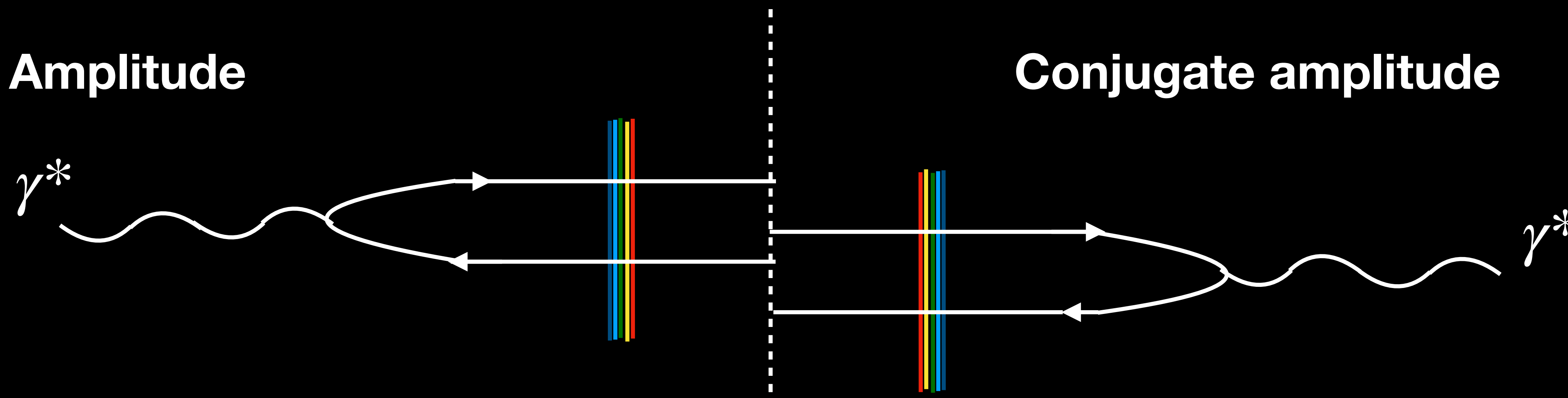

$$\Psi^{\gamma^*\to q\bar{q}}(Q, r_\perp, z) \qquad \Psi^{\gamma^*\to q\bar{q}}(Q, r'_\perp, z)$$

$$\left[1_{ij} - \left[V(x_\perp)V^\dagger(y_\perp)\right]_{ij}\right] \times \left[1_{ij} - \left[V(x'_\perp)V^\dagger(y'_\perp)\right]_{ij}\right]$$

$$\frac{d\sigma^{\gamma^* p(A)\to q\bar{q}X}}{d\Pi} \sim \int d^2r_\perp d^2b_\perp d^2r'_\perp d^2b'_\perp e^{-iP_\perp\cdot(r_\perp - r'_\perp)} e^{-\Delta_\perp\cdot(b_\perp - b'_\perp)} \Psi(r_\perp)\Psi^*(r'_\perp)$$
$$\times\, Q\left(b_\perp + \frac{1}{2}r_\perp, b_\perp - \frac{1}{2}r_\perp; b'_\perp - \frac{1}{2}r'_\perp, b'_\perp + \frac{1}{2}r'_\perp\right)$$

$$Q(x_1, x_2; x_3, x_4) \equiv 1 - \frac{1}{N_c}\left\langle tr\left[V(x_1)V^\dagger(x_2)\right]\right\rangle - \frac{1}{N_c}\left\langle tr\left[V(x_3)V^\dagger(x_4)\right]\right\rangle$$
$$+\frac{1}{N_c}\left\langle tr\left[V(x_1)V^\dagger(x_2)V(x_3)V^\dagger(x_4)\right]\right\rangle$$

Sensitive to color charge fluctuations

Sensitive to quadrupole!

Richer color structure

A familiar limit: back-to-back jets and TMD factorization

In the back-to-back limit $P_\perp \gg \Delta_\perp$ expand the quadrupole for small dipole ($r_\perp$, $r'_\perp$) sizes:

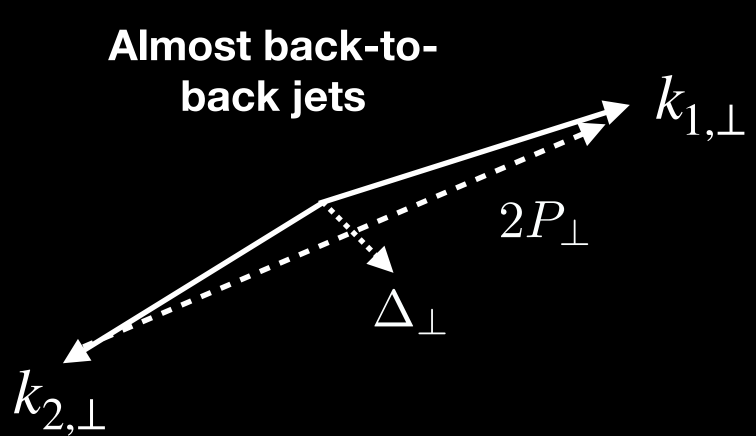

$$Q\left(b_\perp + \frac{1}{2}r_\perp, b_\perp - \frac{1}{2}r_\perp; b'_\perp - \frac{1}{2}r'_\perp, b'_\perp + \frac{1}{2}r'_\perp\right)$$

$$\downarrow$$

$$r^i_\perp r'^j_\perp \left\langle Tr\left[V_{b_\perp}\partial^i V^\dagger_{b_\perp} V_{b'_\perp}\partial^j V^\dagger_{b'_\perp}\right]\right\rangle$$

hard part

$$\frac{d\sigma^{\gamma^* p(A)\to q\bar{q}X}}{d\Pi} \sim \mathcal{H}^{\gamma * g\to q\bar{q}}(P_\perp, Q^2)\left[\alpha_s x G(x,\Delta_\perp) + \mathcal{C}(P,Q^2)\alpha_s x h(x,\Delta_\perp)\cos(2\phi)\right]$$

hard part

unpolarized

linearly polarized

gluon Weizsacker-Williams TMD

Multi-gluon correlations and evidence of saturation from dijet measurements at an Electron Ion Collider

arxiv: 1912.05586
(soon to be published at PRL)

Björn Schenke
Niklas Müller
Heikki Mäntysaari

Technical aspects (not discussed): Non-linear Gaussian approximation for quadrupole operator, Balitsky-Kovchegov small-x evolution, initial dipole fit to HERA DIS data

Angle $\theta_{P\Delta}$ averaged cross section

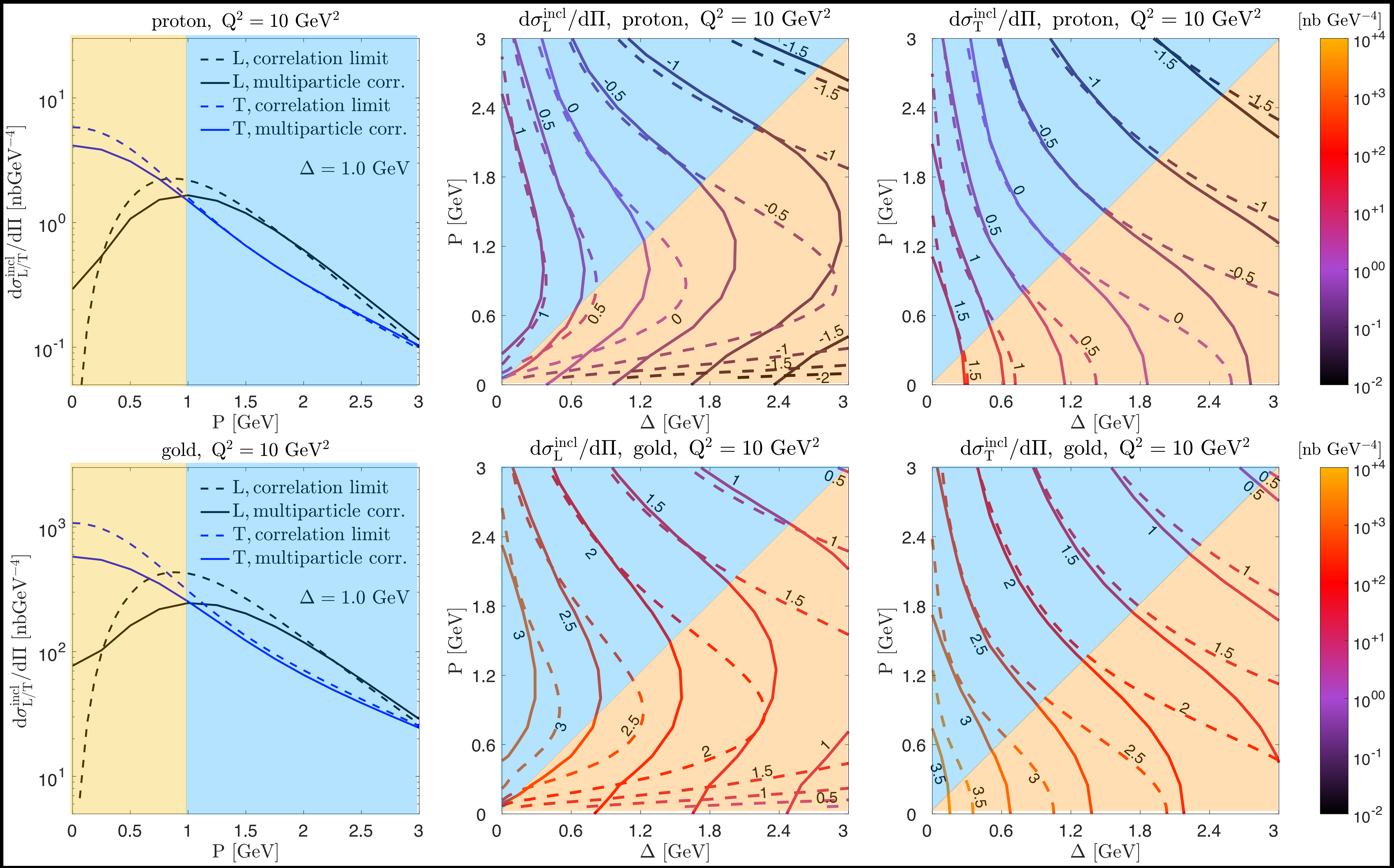

Region $\Delta_\perp < P_\perp$ TMD regime

Region $P_\perp < \Delta_\perp$ full multi-gluon correlation

Expected deviation from TMD limit, enhanced at $P_\perp \sim Q_s$ (stronger for Gold)

Elliptic anisotropy in $\theta_{P\Delta}$

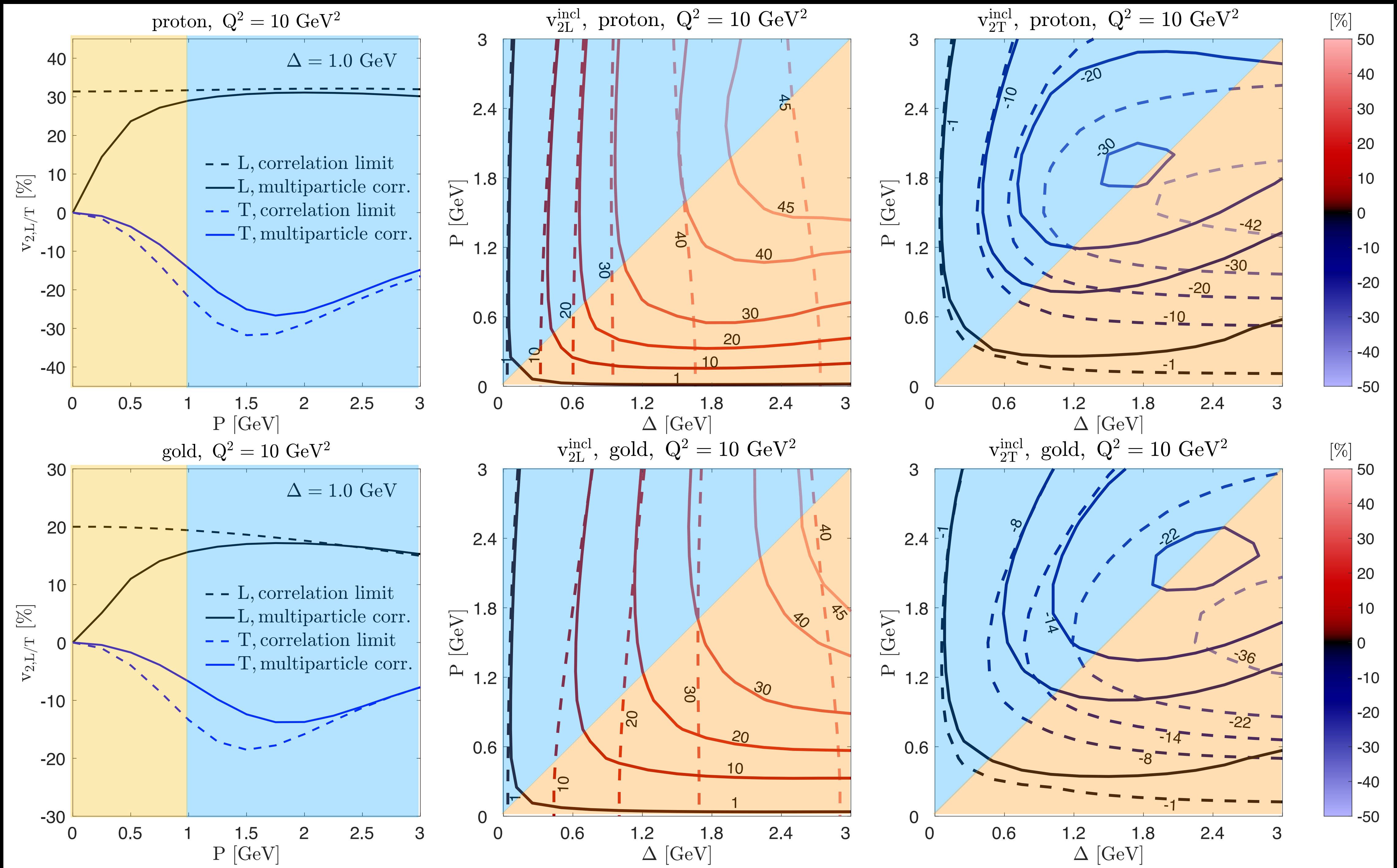

Region $\Delta_\perp < P_\perp$ TMD regime

Region $P_\perp < \Delta_\perp$ full multi-gluon correlation

Large elliptic anisotropies, generated by color charge correlations, slightly stronger for full multi-gluon correlations.

Outlook

- Full JIMWLK evolution (beyond the Gaussian, mean field approximation)
- Fragmentation (Pythia, convolution with fragmentation functions)
- Next-to-leading order corrections (impact factors and JIMWLK/BK at NLO)

Thank you!

УНИВЕРЗИТЕТ У БЕОГРАДУ
ИНСТИТУТ ЗА ФИЗИКУ | БЕОГРАД
ИНСТИТУТ ОД НАЦИОНАЛНОГ ЗНАЧАЈА ЗА РЕПУБЛИКУ СРБИЈУ

The Galileo Galilei Institute For Theoretical Physics
Centro Nazionale di Studi Avanzati dell'Istituto Nazionale di Fisica Nucleare
Arcetri, Firenze

Generalization of high-$p_\perp$ particle's energy loss to a finite value of radiated energy

Bojana Ilic (Blagojevic)

Institute of Physics Belgrade

University of Belgrade

The soft-gluon approximation

- **The soft-gluon approximation (*sg*) definition – radiated gluon takes away only a small amount of initial parton's energy $x = \frac{\omega}{E} \ll 1$.**

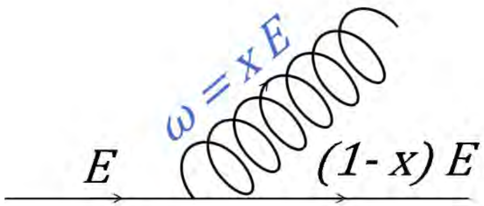

- **Widely-used assumption in calculating radiative energy loss of high $p_\perp$ particle traversing QGP**

ASW (PRD 69:114003), **BDMPS** (NPB 484:265), **BDMPS-Z** (JETP Lett. 65:615), **GLV** (NPB 594:371), **DGLV** (NPA 733:265), **HT** (NPA 696:788);

M. Djordjevic, PRC, 80:064909 (2009), **M. Djorjevic and U. Heinz**, PRL 101:022302 (2008)

B. Blagojevic, M. Djordjevic and M. Djordjevic,
Phys. Rev. C 99, no. 2, 024901 (2019)

Why do we test validity of the soft-gluon approximation?

- Considerable medium induced radiative energy loss obtained by different models → inconsistent with *sg* approximation?
- Sg approximation used in our Dynamical energy loss model. (M. Djordjevic and M. D. PLB 734:286 (2014))
- Our dynamical energy loss model reported robust agreement with comprehensive set of experimental R_{AA} data → implies model applicability.

(M. Djordjevic and M. D., PLB 734:286 (2014); PRC 90:034910 (2014), M. Djordjevic, M. D. and B. Blagojevic, PLB 737:298 (2014); M. Djordjevic, PRL 112:042302 (2014), M. Djordjevic and M. D., PRC 92:024918 (2015))

  - It breaks-down for:
    - $5 < p_\perp < 10$ GeV
    - Primarily for gluon-jets

B. Blagojevic, M. Djordjevic and M. Djordjevic,
Phys. Rev. C 99, no. 2, 024901 (2019)

Relaxing the soft-gluon approximation

- **Beyond soft-gluon approximation (*bsg*) in DGLV: x finite**

- **<u>DGLV formalism assumes:</u>**

B. Blagojevic, M. Djordjevic and M. Djordjevic,
Phys. Rev. C 99, no. 2, 024901 (2019)

Relaxing the soft-gluon approximation

- **Beyond soft-gluon approximation (*bsg*) in DGLV: x finite**
- **<u>DGLV formalism assumes:</u>**

Finite size (L) optically thin QGP medium

B. Blagojevic, M. Djordjevic and M. Djordjevic,
Phys. Rev. C 99, no. 2, 024901 (2019)

Relaxing the soft-gluon approximation

- **Beyond soft-gluon approximation (*bsg*) in DGLV: x finite**

- **DGLV formalism assumes:**

Finite size (L) optically thin QGP medium

Static color-screened Yukawa potential:

(M. Gyulassy, P. Levai and I. Vitev, NPB 594:371 (2001))

Static scattering centers $V_n = 2\pi\delta(q_n^0)v(\vec{\boldsymbol{q}}_n)e^{-i\vec{\boldsymbol{q}}_n\cdot\vec{\boldsymbol{x}}_n}T_{a_n}(R)\otimes T_{a_n}(n)$

$$v(\vec{\boldsymbol{q}}_n) = \frac{4\pi\alpha_s}{\vec{\boldsymbol{q}}_n^2+\mu^2}$$

B. Blagojevic, M. Djordjevic and M. Djordjevic, Phys. Rev. C 99, no. 2, 024901 (2019)

Relaxing the soft-gluon approximation

- **Beyond soft-gluon approximation (*bsg*) in DGLV: x finite**

- **<u>DGLV formalism assumes:</u>**

Finite size (L) optically thin QGP medium

Static color-screened Yukawa potential:

(M. Gyulassy, P. Levai and I. Vitev, NPB 594:371 (2001))

Static scattering centers $V_n = 2\pi\delta(q_n^0)v(\vec{\boldsymbol{q}}_n)e^{-i\vec{\boldsymbol{q}}_n\cdot\vec{\boldsymbol{x}}_n}T_{a_n}(R)\otimes T_{a_n}(n)$

$$v(\vec{\boldsymbol{q}}_n) = \frac{4\pi\alpha_s}{\vec{\boldsymbol{q}}_n^2+\mu^2}$$

Gluons as transversely polarized partons with effective mass

$$m_g = \mu/\sqrt{2}$$

(M. Djordjevic and M. Gyulassy, PRC 68:034914 (2003))

B. Blagojevic, M. Djordjevic and M. Djordjevic,
Phys. Rev. C 99, no. 2, 024901 (2019)

Calculations beyond soft-gluon approximation

0^{th} order

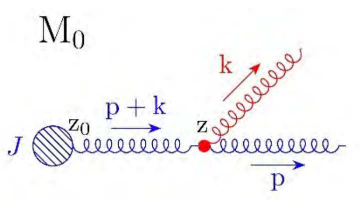

Interaction with one scatterer

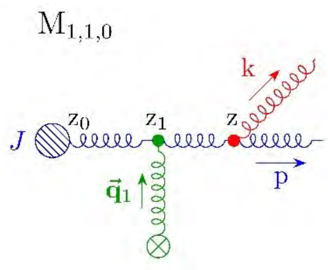

Interaction with two scatterers in contact limit

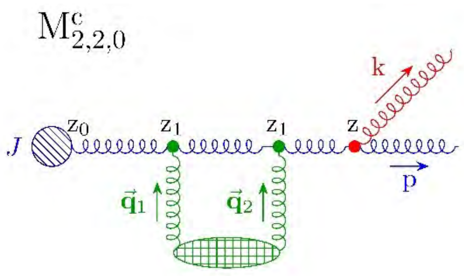

- **Assumptions:**

B. Blagojevic, M. Djordjevic and M. Djordjevic,
Phys. Rev. C 99, no. 2, 024901 (2019)

Calculations beyond soft-gluon approximation

0^{th} order

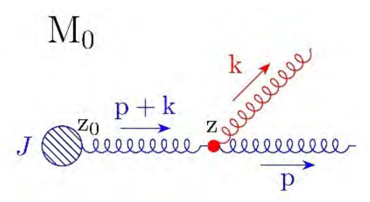

Interaction with one scatterer

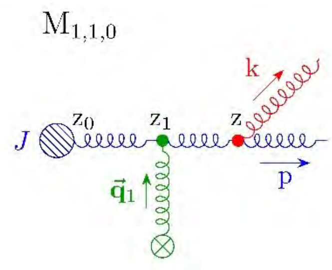

Interaction with two scatterers in contact limit

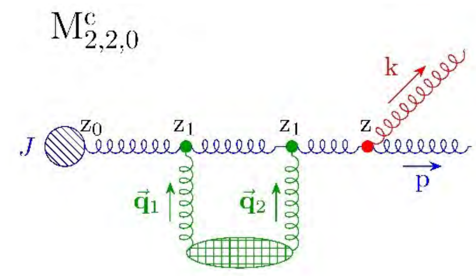

- **Assumptions:**

- **Initial gluon propagates along the longitudinal axis**

  (consistently for all diagrams!)

B. Blagojevic, M. Djordjevic and M. Djordjevic,
Phys. Rev. C 99, no. 2, 024901 (2019)

Calculations beyond soft-gluon approximation

0th order

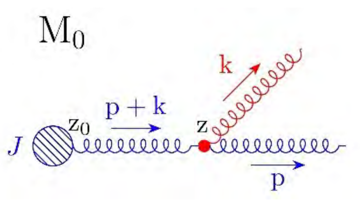

Interaction with one scatterer

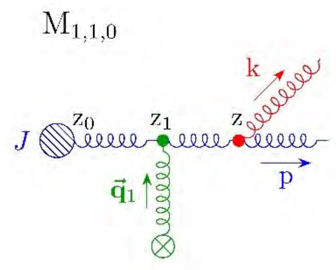

Interaction with two scatterers in contact limit

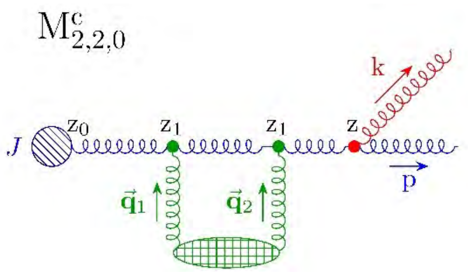

- **Assumptions:**

- **Initial gluon propagates along the longitudinal axis**

  (consistently for all diagrams!)

- **The soft-rescattering (eikonal) approximation**

B. Blagojevic, M. Djordjevic and M. Djordjevic,
Phys. Rev. C 99, no. 2, 024901 (2019)

Calculations beyond soft-gluon approximation

0th order

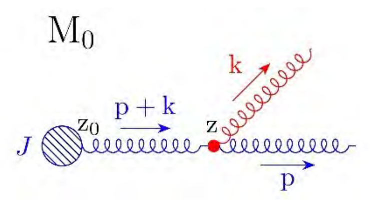

Interaction with one scatterer

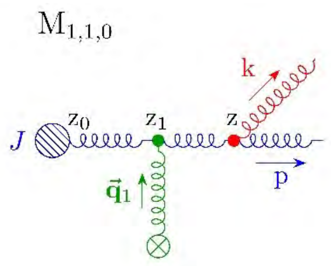

Interaction with two scatterers in contact limit

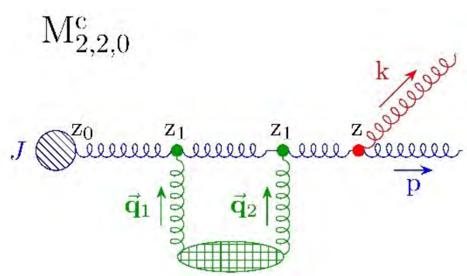

- **Assumptions:**

- **Initial gluon propagates along the longitudinal axis**

  (consistently for all diagrams!)

- **The soft-rescattering (eikonal) approximation**

- **The 1st order in opacity approximation**

(M. Gyulassy, P. Levai and I. Vitev, PLB 538:282 (2002))

B. Blagojevic, M. Djordjevic and M. Djordjevic,
Phys. Rev. C 99, no. 2, 024901 (2019)

Calculations beyond soft-gluon approximation

$$M_0 = J_a(p+k)e^{i(p+k)x_0}(-2ig_s)(1-x+x^2) \times \frac{\boldsymbol{\epsilon}\cdot\mathbf{k}}{\mathbf{k}^2+m_g^2(1-x+x^2)}(T^c)_{da}$$

No interactions with QGP medium

$$M_{1,1,0} = J_a(p+k)e^{i(p+k)x_0}(-i)(1-x+x^2)(T^cT^{a_1})_{da}T_{a_1}\int\frac{d^2\mathbf{q}_1}{(2\pi)^2}v(0,\mathbf{q}_1)e^{-i\mathbf{q}_1\cdot\mathbf{b}_1} \times(-2ig_s)\frac{\boldsymbol{\epsilon}\cdot(\mathbf{k}-x\mathbf{q}_1)}{(\mathbf{k}-x\mathbf{q}_1)^2+m_g^2(1-x+x^2)}e^{\frac{i}{2\omega}\left(\mathbf{k}^2+\frac{x}{1-x}(\mathbf{k}-\mathbf{q}_1)^2+\frac{m_g^2(1-x+x^2)}{1-x}\right)(z_1-z_0)}$$

$$M_{1,0,0} = J_a(p+k)e^{i(p+k)x_0}(-i)(1-x+x^2)(T^{a_1}T^c)_{da}T_{a_1}\int\frac{d^2\mathbf{q}_1}{(2\pi)^2}v(0,\mathbf{q}_1)e^{-i\mathbf{q}_1\cdot\mathbf{b}_1} \times(2ig_s)\frac{\boldsymbol{\epsilon}\cdot\mathbf{k}}{\mathbf{k}^2+\chi}\left(e^{\frac{i}{2\omega}\left(\mathbf{k}^2+\frac{x}{1-x}(\mathbf{k}-\mathbf{q}_1)^2+\frac{\chi}{1-x}\right)(z_1-z_0)}-e^{-\frac{i}{2\omega}\frac{x}{1-x}\left(\mathbf{k}^2-(\mathbf{k}-\mathbf{q}_1)^2\right)(z_1-z_0)}\right)$$

$$M_{1,0,1} = J_a(p+k)e^{i(p+k)x_0}(-i)(1-x+x^2)[T^c,T^{a_1}]_{da}T_{a_1}\int\frac{d^2\mathbf{q}_1}{(2\pi)^2}v(0,\mathbf{q}_1)e^{-i\mathbf{q}_1\cdot\mathbf{b}_1} \times(2ig_s)\frac{\boldsymbol{\epsilon}\cdot(\mathbf{k}-\mathbf{q}_1)}{(\mathbf{k}-\mathbf{q}_1)^2+\chi}\left(e^{\frac{i}{2\omega}\left(\mathbf{k}^2+\frac{x}{1-x}(\mathbf{k}-\mathbf{q}_1)^2+\frac{\chi}{1-x}\right)(z_1-z_0)}-e^{\frac{i}{2\omega}\left(\mathbf{k}^2-(\mathbf{k}-\mathbf{q}_1)^2\right)(z_1-z_0)}\right)$$

One interaction with QGP medium

Symmetric under the exchange of radiated (k) and final gluon (p).

Recovers *sg* result for $x \ll 1$.

B. Blagojevic, M. Djordjevic and M. Djordjevic, Phys. Rev. C 99, no. 2, 024901 (2019)

Calculations beyond soft-gluon approximation

$$M^c_{2,2,0} = -J_a(p+k)e^{i(p+k)x_0}(T^cT^{a_2}T^{a_1})_{da}T_{a_2}T_{a_1}(1-x+x^2)(-i)\int\frac{d^2\mathbf{q}_1}{(2\pi)^2}(-i)\int\frac{d^2\mathbf{q}_2}{(2\pi)^2}v(0,\mathbf{q}_1)v(0,\mathbf{q}_2)e^{-i(\mathbf{q}_1+\mathbf{q}_2)\cdot\mathbf{b}_1}$$
$$\times\frac{1}{2}(2ig_s)\frac{\boldsymbol{\epsilon}\cdot(\mathbf{k}-x(\mathbf{q}_1+\mathbf{q}_2))}{(\mathbf{k}-x(\mathbf{q}_1+\mathbf{q}_2))^2+\chi}e^{\frac{i}{2\omega}(\mathbf{k}^2+\frac{x}{1-x}(\mathbf{k}-\mathbf{q}_1-\mathbf{q}_2)^2+\frac{\chi}{1-x})(z_1-z_0)}$$

$$M^c_{2,0,3} = J_a(p+k)e^{i(p+k)x_0}[[T^c,T^{a_2}],T^{a_1}]_{da}T_{a_2}T_{a_1}(1-x+x^2)(-i)\int\frac{d^2\mathbf{q}_1}{(2\pi)^2}(-i)\int\frac{d^2\mathbf{q}_2}{(2\pi)^2}v(0,\mathbf{q}_1)v(0,\mathbf{q}_2)e^{-i(\mathbf{q}_1+\mathbf{q}_2)\cdot\mathbf{b}_1}$$
$$\times\frac{1}{2}(2ig_s)\frac{\boldsymbol{\epsilon}\cdot(\mathbf{k}-\mathbf{q}_1-\mathbf{q}_2)}{(\mathbf{k}-\mathbf{q}_1-\mathbf{q}_2)^2+\chi}\left(e^{\frac{i}{2\omega}(\mathbf{k}^2+\frac{x}{1-x}(\mathbf{k}-\mathbf{q}_1-\mathbf{q}_2)^2+\frac{\chi}{1-x})(z_1-z_0)}-e^{\frac{i}{2\omega}(\mathbf{k}^2-(\mathbf{k}-\mathbf{q}_1-\mathbf{q}_2)^2)(z_1-z_0)}\right)$$

$$M^c_{2,0,0} = J_a(p+k)e^{i(p+k)x_0}(T^{a_2}T^{a_1}T^c)_{da}T_{a_2}T_{a_1}(1-x+x^2)(-i)\int\frac{d^2\mathbf{q}_1}{(2\pi)^2}(-i)\int\frac{d^2\mathbf{q}_2}{(2\pi)^2}v(0,\mathbf{q}_1)v(0,\mathbf{q}_2)e^{-i(\mathbf{q}_1+\mathbf{q}_2)\cdot\mathbf{b}_1}$$
$$\times\frac{1}{2}(2ig_s)\frac{\boldsymbol{\epsilon}\cdot\mathbf{k}}{\mathbf{k}^2+\chi}\left(e^{\frac{i}{2\omega}(\mathbf{k}^2+\frac{x}{1-x}(\mathbf{k}-\mathbf{q}_1-\mathbf{q}_2)^2+\frac{\chi}{1-x})(z_1-z_0)}-e^{\frac{i}{2\omega}\frac{x}{1-x}((\mathbf{k}-\mathbf{q}_1-\mathbf{q}_2)^2-\mathbf{k}^2)(z_1-z_0)}\right)$$

$$M^c_{2,0,1} = J_a(p+k)e^{i(p+k)x_0}(T^{a_2}[T^c,T^{a_1}])_{da}T_{a_2}T_{a_1}(1-x+x^2)(-i)\int\frac{d^2\mathbf{q}_1}{(2\pi)^2}(-i)\int\frac{d^2\mathbf{q}_2}{(2\pi)^2}v(0,\mathbf{q}_1)v(0,\mathbf{q}_2)e^{-i(\mathbf{q}_1+\mathbf{q}_2)\cdot\mathbf{b}_1}$$
$$\times(2ig_s)\frac{\boldsymbol{\epsilon}\cdot(\mathbf{k}-\mathbf{q}_1)}{(\mathbf{k}-\mathbf{q}_1)^2+\chi}\left(e^{\frac{i}{2\omega}(\mathbf{k}^2+\frac{x}{1-x}(\mathbf{k}-\mathbf{q}_1-\mathbf{q}_2)^2+\frac{\chi}{1-x})(z_1-z_0)}-e^{\frac{i}{2\omega}(\mathbf{k}^2-\frac{(\mathbf{k}-\mathbf{q}_1)^2}{1-x}+\frac{x}{1-x}(\mathbf{k}-\mathbf{q}_1-\mathbf{q}_2)^2)(z_1-z_0)}\right)$$

$$M^c_{2,0,2} = J_a(p+k)e^{i(p+k)x_0}(T^{a_1}[T^c,T^{a_2}])_{da}T_{a_2}T_{a_1}(1-x+x^2)(-i)\int\frac{d^2\mathbf{q}_1}{(2\pi)^2}(-i)\int\frac{d^2\mathbf{q}_2}{(2\pi)^2}v(0,\mathbf{q}_1)v(0,\mathbf{q}_2)e^{-i(\mathbf{q}_1+\mathbf{q}_2)\cdot\mathbf{b}_1}$$
$$\times(2ig_s)\frac{\boldsymbol{\epsilon}\cdot(\mathbf{k}-\mathbf{q}_2)}{(\mathbf{k}-\mathbf{q}_2)^2+\chi}\left(e^{\frac{i}{2\omega}(\mathbf{k}^2+\frac{x}{1-x}(\mathbf{k}-\mathbf{q}_1-\mathbf{q}_2)^2+\frac{\chi}{1-x})(z_1-z_0)}-e^{\frac{i}{2\omega}(\mathbf{k}^2-\frac{(\mathbf{k}-\mathbf{q}_2)^2}{1-x}+\frac{x}{1-x}(\mathbf{k}-\mathbf{q}_1-\mathbf{q}_2)^2)(z_1-z_0)}\right)$$

Two interactions with QGP medium

Symmetric under the exchange of k and p gluons.

Recovers *sg* result for $x \ll 1$.

Two negligible amplitudes are omitted.

B. Blagojevic, M. Djordjevic and M. Djordjevic,
Phys. Rev. C 99, no. 2, 024901 (2019)

Calculations beyond soft-gluon approximation

$$\frac{x d^3 N_g^{(0)}}{dx d\mathbf{k}^2} = \frac{\alpha_s}{\pi} \frac{C_2(G)\, \mathbf{k}^2}{(\mathbf{k}^2 + m_g^2(1-x+x^2))^2} \times \frac{(1-x+x^2)^2}{1-x}$$

Reduces to well-known Altarelli-Parisi (G. Altarelli and G. Parisi, NPB 126:298 (1977)) **result for massless particles.**

Single gluon radiation spectrum beyond soft-gluon approximation:

$$\frac{dN_g^{(1)}}{dx} = \frac{C_2(G)\alpha_s}{\pi} \frac{L}{\lambda} \frac{(1-x+x^2)^2}{x(1-x)} \int \frac{d^2\mathbf{q}_1}{\pi} \frac{\mu^2}{(\mathbf{q}_1^2+\mu^2)^2} \int d\mathbf{k}^2$$
$$\times \Bigg\{ \frac{(\mathbf{k}-\mathbf{q}_1)^2+\chi}{(\frac{4x(1-x)E}{L})^2 + ((\mathbf{k}-\mathbf{q}_1)^2+\chi)^2} \Big(2\frac{(\mathbf{k}-\mathbf{q}_1)^2}{(\mathbf{k}-\mathbf{q}_1)^2+\chi} - \frac{\mathbf{k}\cdot(\mathbf{k}-\mathbf{q}_1)}{\mathbf{k}^2+\chi} - \frac{(\mathbf{k}-\mathbf{q}_1)\cdot(\mathbf{k}-x\mathbf{q}_1)}{(\mathbf{k}-x\mathbf{q}_1)^2+\chi} \Big)$$
$$+ \frac{\mathbf{k}^2+\chi}{(\frac{4x(1-x)E}{L})^2 + (\mathbf{k}^2+\chi)^2} \Big(\frac{\mathbf{k}^2}{\mathbf{k}^2+\chi} - \frac{\mathbf{k}\cdot(\mathbf{k}-x\mathbf{q}_1)}{(\mathbf{k}-x\mathbf{q}_1)^2+\chi} \Big) + \Big(\frac{(\mathbf{k}-x\mathbf{q}_1)^2}{((\mathbf{k}-x\mathbf{q}_1)^2+\chi)^2} - \frac{\mathbf{k}^2}{(\mathbf{k}^2+\chi)^2} \Big) \Bigg\}$$

$$\chi = m_g^2(1-x+x^2)$$

B. Blagojevic, M. Djordjevic and M. Djordjevic, Phys. Rev. C 99, no. 2, 024901 (2019)

Introduction of effective gluon mass in *bsg* radiative energy loss expression for the first time!

Comparison of analytical expressions $\left(\frac{dN_g^{(1)}}{dx}\right)$

Beyond soft-gluon approximation:

$$f_{bsg}(\boldsymbol{k},\boldsymbol{q}_1,x)=\frac{(1-x+x^2)^2}{x(1-x)}\left\{\left(2\frac{(\boldsymbol{k}-\boldsymbol{q}_1)^2}{(\boldsymbol{k}-\boldsymbol{q}_1)^2+\chi}-\frac{\boldsymbol{k}\cdot(\boldsymbol{k}-\boldsymbol{q}_1)}{\boldsymbol{k}^2+\chi}-\frac{(\boldsymbol{k}-\boldsymbol{q}_1)\cdot(\boldsymbol{k}-x\boldsymbol{q}_1)}{(\boldsymbol{k}-x\boldsymbol{q}_1)^2+\chi}\right)\frac{(\boldsymbol{k}-\boldsymbol{q}_1)^2+\chi}{\left(\frac{4x(1-x)E}{L}\right)^2+\left((\boldsymbol{k}-\boldsymbol{q}_1)^2+\chi\right)^2}\right.$$

$$\left.+\frac{\boldsymbol{k}^2+\chi}{\left(\frac{4x(1-x)E}{L}\right)^2+\left(\boldsymbol{k}^2+\chi\right)^2}\left(\frac{\boldsymbol{k}^2}{\boldsymbol{k}^2+\chi}-\frac{\boldsymbol{k}\cdot(\boldsymbol{k}-x\boldsymbol{q}_1)}{(\boldsymbol{k}-x\boldsymbol{q}_1)^2+\chi}\right)+\left(\frac{(\boldsymbol{k}-x\boldsymbol{q}_1)^2}{((\boldsymbol{k}-x\boldsymbol{q}_1)^2+\chi)^2}-\frac{\boldsymbol{k}^2}{(\boldsymbol{k}^2+\chi)^2}\right)\right\}$$

$$\chi = m_g^2(1-x+x^2)$$

Soft-gluon approximation:

$$f_{sg}(\boldsymbol{k},\boldsymbol{q}_1,x)=\frac{1}{x}\frac{(\boldsymbol{k}-\boldsymbol{q}_1)^2+m_g^2}{\left(\frac{4xE}{L}\right)^2+((\boldsymbol{k}-\boldsymbol{q}_1)^2+m_g^2)^2}2\left(\frac{(\boldsymbol{k}-\boldsymbol{q}_1)^2}{(\boldsymbol{k}-\boldsymbol{q}_1)^2+m_g^2}-\frac{\boldsymbol{k}\cdot(\boldsymbol{k}-\boldsymbol{q}_1)}{\boldsymbol{k}^2+m_g^2}\right)$$

M. Djordjevic and M. Gyulassy, NPA 733:265 (2004)

Only this term remains in *sg* and reduces to:

B. Blagojevic, M. Djordjevic and M. Djordjevic, Phys. Rev. C 99, no. 2, 024901 (2019)

Bsg **expression is clearly different and significantly more complex than its *sg* analogon!**

Comparison of numerical predictions between *bsg* and *sg*

B. Blagojevic, M. Djordjevic and M. Djordjevic,
Phys. Rev. C 99, no. 2, 024901 (2019)

Comparison of numerical predictions between *bsg* and *sg*

1. **Fractional radiative energy loss $\Delta E^{(1)}/E$ and number of radiated gluons $N_g^{(1)}$**

B. Blagojevic, M. Djordjevic and M. Djordjevic,
Phys. Rev. C 99, no. 2, 024901 (2019)

Comparison of numerical predictions between *bsg* and *sg*

1. **Fractional radiative energy loss $\Delta E^{(1)}/E$ and number of radiated gluons $N_g^{(1)}$**
2. **Fractional differential radiative energy loss $\frac{1}{E}\frac{dE^{(1)}}{dx}$ and single gluon radiation spectrum $\frac{dN_g^{(1)}}{dx}$**

B. Blagojevic, M. Djordjevic and M. Djordjevic, Phys. Rev. C 99, no. 2, 024901 (2019)

Comparison of numerical predictions between *bsg* and *sg*

1. **Fractional radiative energy loss $\Delta E^{(1)}/E$ and number of radiated gluons $N_g^{(1)}$**
2. **Fractional differential radiative energy loss $\frac{1}{E}\frac{dE^{(1)}}{dx}$ and single gluon radiation spectrum $\frac{dN_g^{(1)}}{dx}$**
3. **Angular averaged nuclear modification factor R_{AA}**

B. Blagojevic, M. Djordjevic and M. Djordjevic,
Phys. Rev. C 99, no. 2, 024901 (2019)

Effect of relaxing *sga* on integrated variables

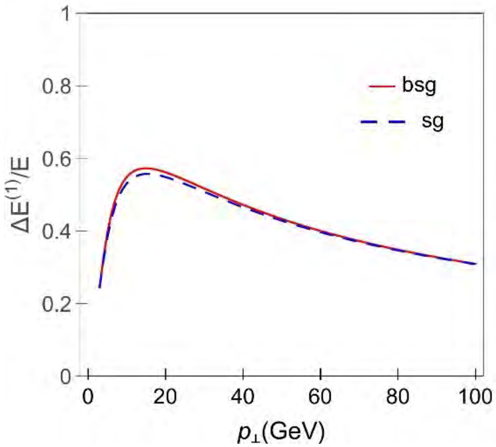

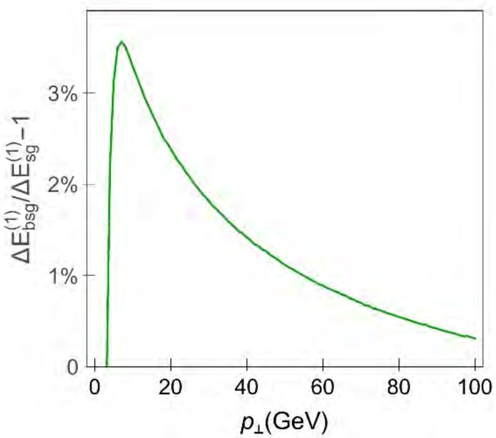

Finite x slightly increases $\Delta E^{(1)}/E$ up to $\approx$ 3% compared to *sg* .

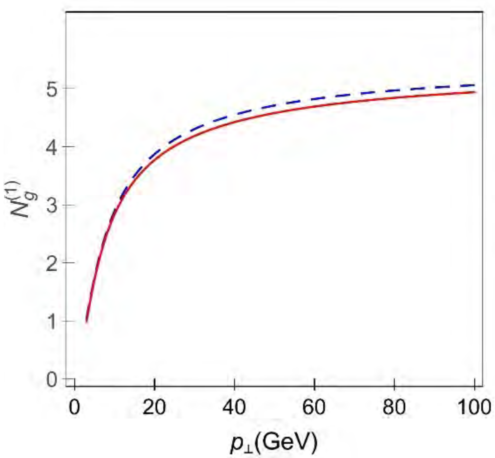

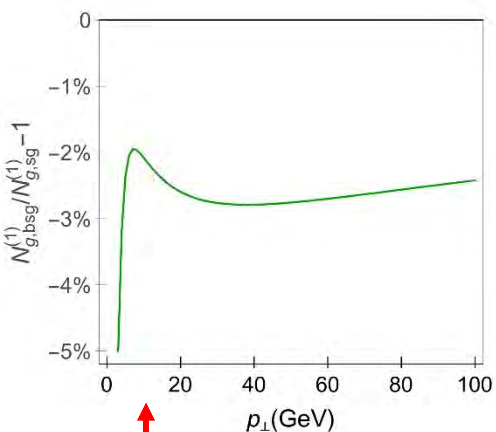

$\approx$ 10 GeV

Finite x slightly decreases $N_g^{(1)}$ (peaks at $\approx -2\%$) compared to *sg* .

Surprisingly, effect on $\Delta E^{(1)}/E$ and $N_g^{(1)}$ is small and of an opposite sign!

B. Blagojevic, M. Djordjevic and M. Djordjevic, Phys. Rev. C 99, no. 2, 024901 (2019)

Effect of relaxing *sga* on differential variables

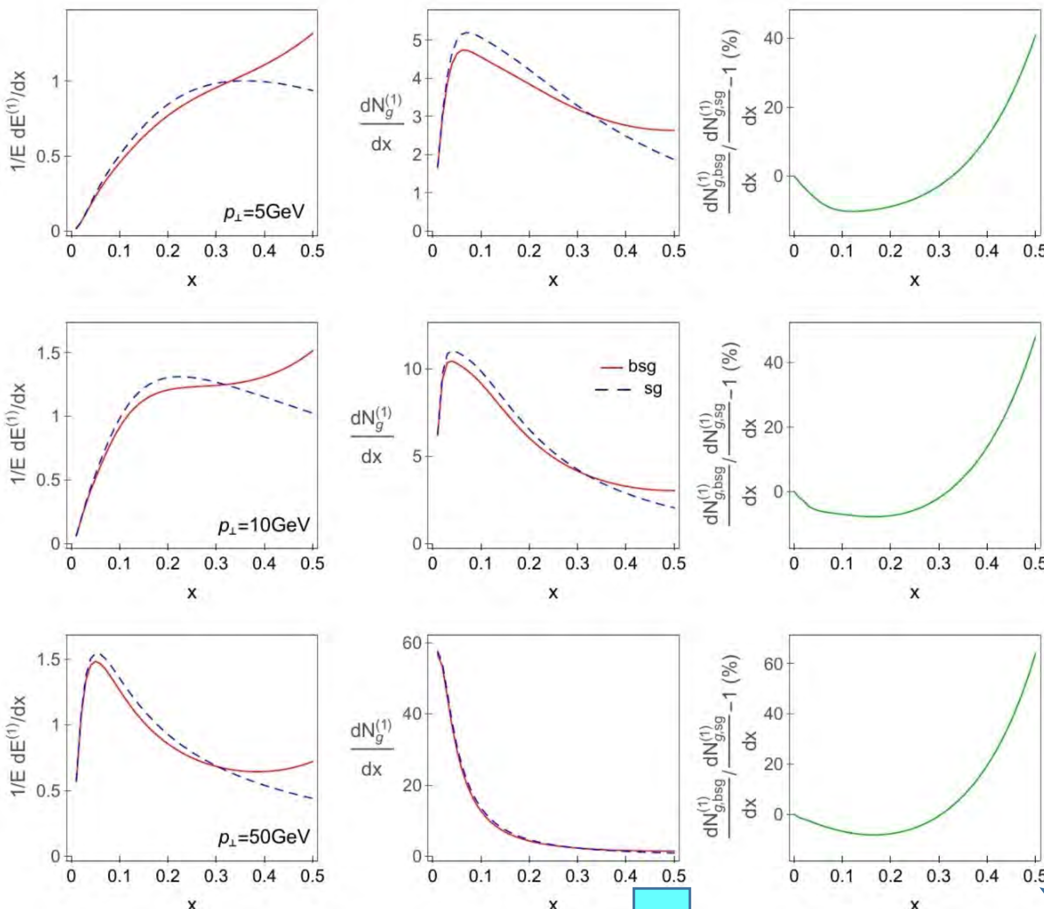

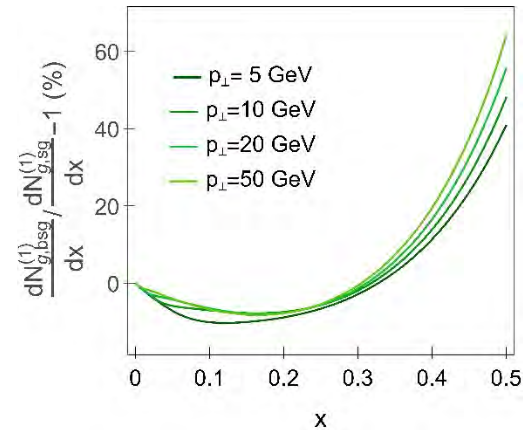

Nearly the same effect on $dN_g^{(1)}/dx$ (for $0 < x \leq 0.4$) independently of $p_\perp$.

The effect on $dE^{(1)}/dx$ and $dN_g^{(1)}/dx$ is small for $x \leq 0.4$, while enhances to a notable value with increasing x.

Computational formalism for bare gluon suppression

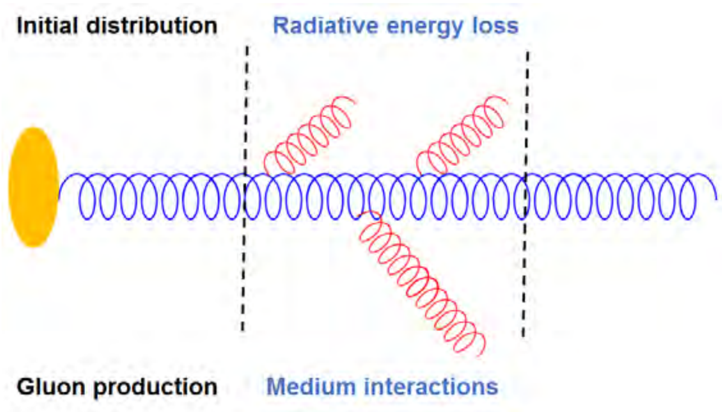

1. Initial gluon $p_\perp$ spectrum
2. Radiative energy loss

- Gluon production: Initial $p_\perp$ distribution

(Z.B. Kang, I. Vitev and H. Xing, PLB 718:482 (2012); R. Sharma, I. Vitev and B.W. Zhang, PRC 80:054902 (2009))

- Radiative energy loss in finite size static QGP medium *beyond soft gluon approximation*

(B. Blagojevic, M. Djordjevic and M. Djordjevic, Phys. Rev. C 99, no. 2, 024901 (2019))

- Multi-gluon fluctuations

(M. Gyulassy, P. Levai and I. Vitev, PLB 538:282 (2002))

- Path-length fluctuations

(S. Wicks, W. Horowitz, M. Djordjevic and M. Gyulassy, NPA 784:426 (2007); A. Dainese, EPJ C 33:495 (2004))

B. Blagojevic, M. Djordjevic and M. Djordjevic, Phys. Rev. C 99, no. 2, 024901 (2019)

Effect of relaxing *sga* on R_{AA}

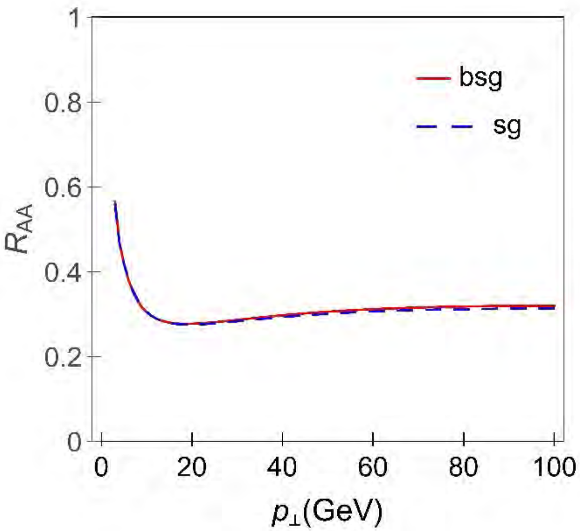

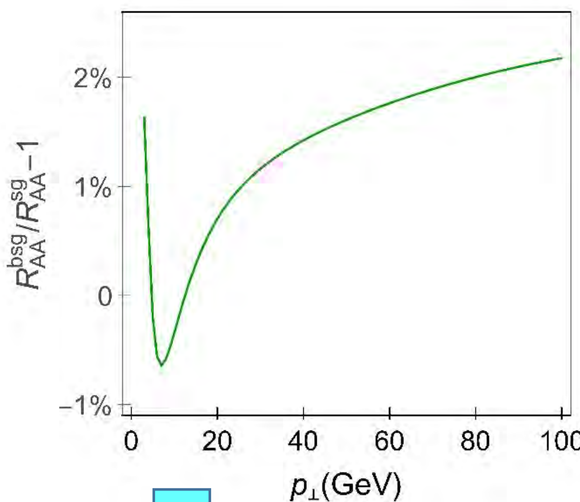

Even smaller effect on R_{AA} compared to all previous variables!

1. **Why is R_{AA} barely affected by this relaxation?**
2. **How the large differential variables discrepancies between *bsg* and *sg* cases at $x > 0.4$ do not influence R_{AA}?**

B. Blagojevic, M. Djordjevic and M. Djordjevic, Phys. Rev. C 99, no. 2, 024901 (2019)

Explanation of negligible effect on R_{AA} (1)

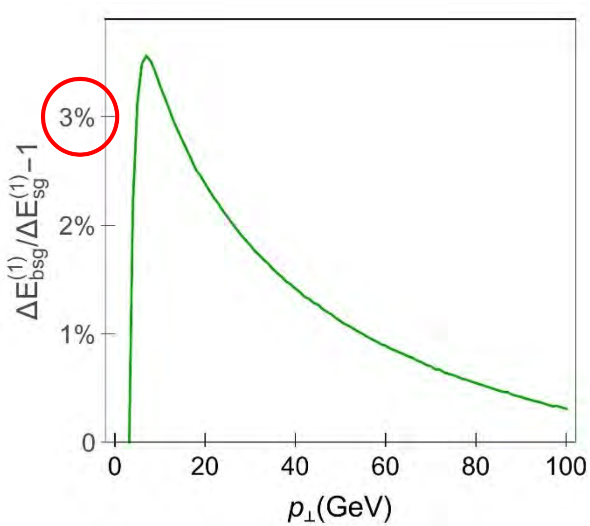

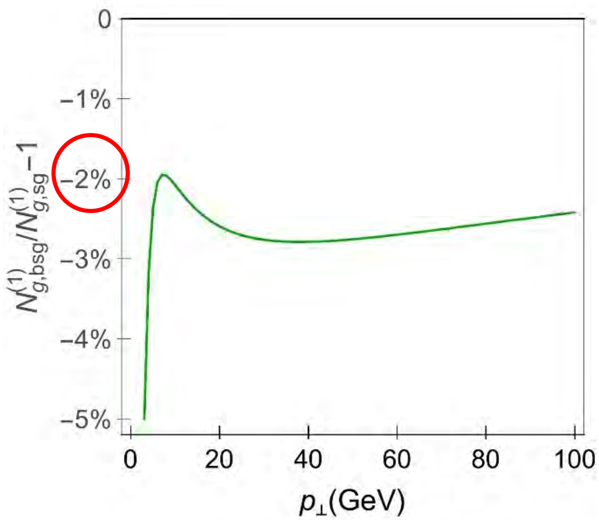

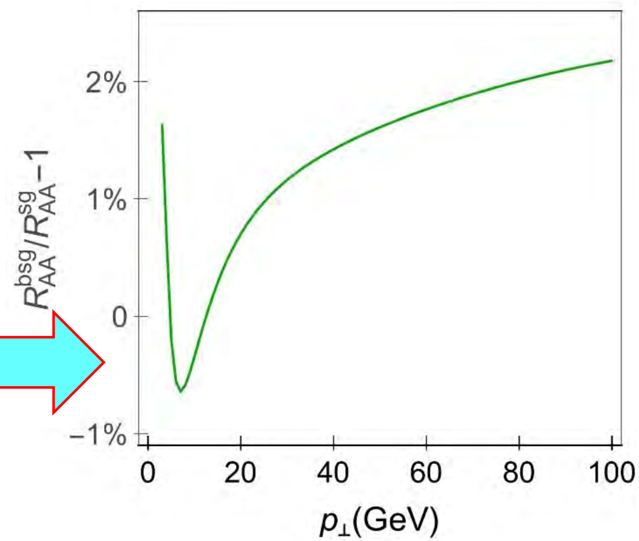

Both $\Delta E^{(1)}/E$ and $N_g^{(1)}$ non-trivially affect R_{AA}.

Interplay of the opposite effects on $\Delta E^{(1)}/E$ and $N_g^{(1)}$ results in negligible R_{AA} change.

B. Blagojevic, M. Djordjevic and M. Djordjevic, Phys. Rev. C 99, no. 2, 024901 (2019)

Explanation of negligible effect on R_{AA} (2)

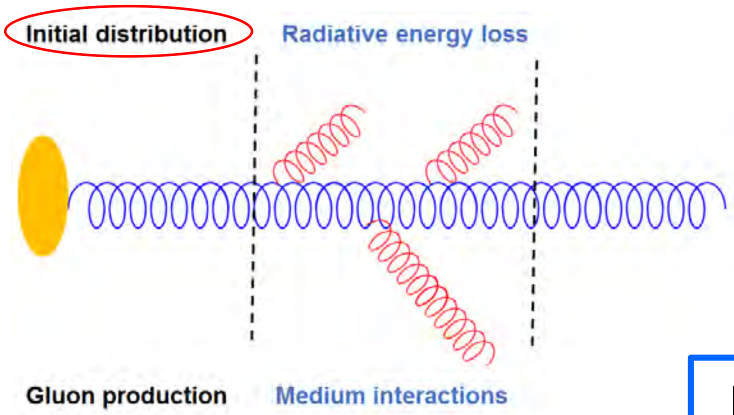

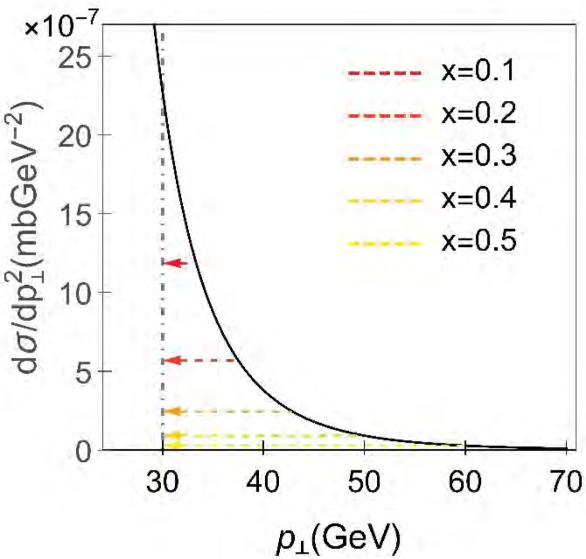

Due to exponentially decreasing initial gluon $p_\perp$ distribution, the $x \leq 0.4$ is the most relevant region for differentiating between *bsg* and *sg* R_{AA}.

In this region *bsg* and *sg* $\frac{dN_g^{(1)}}{dx}$ and $\frac{1}{E}\frac{dE^{(1)}}{dx}$ are within 10%.

Intuitively explains insignificant effect on R_{AA}.

B. Blagojevic, M. Djordjevic and M. Djordjevic, Phys. Rev. C 99, no. 2, 024901 (2019)

Conclusions and outlook

Different theoretical models obtained considerable radiative energy loss questioning the validity of the soft-gluon approximation.

We relaxed the approximation for high $p_\perp$ gluons, which are most affected by it, within DGLV formalism, and although analytical results differ to a great extent in *bsg* and *sg* cases, surprisingly the numerical predictions were nearly indistinguishable.

Consequently, this relaxation should have even smaller impact on high $p_\perp$ quarks.

This implies that soft gluon approximation is well-founded within DGLV formalism.

We expect that the soft-gluon approximation can be reliably applied within the dynamical energy loss formalism, which needs to be rigorously tested in the future.

Thank you for your attention!

In collaboration with: Magdalena Djordjevic and Marko Djordjevic

European Research Council
Established by the European Commission

МИНИСТАРСТВО ПРОСВЕТЕ,
НАУКЕ И ТЕХНОЛОШКОГ РАЗВОЈА

B. Blagojevic, M. Djordjevic and M. Djordjevic,
Phys. Rev. C 99, no. 2, 024901 (2019)

Backup

Generalization on dynamical medium

- Implicitly suggested by robust agreement of our R_{AA} predictions with experimental data
- Only $f(\boldsymbol{k}, \boldsymbol{q}, x)$ depends on x
- $f(\boldsymbol{k}, \boldsymbol{q}, x)$ in soft-gluon approximation is the same in static and in dynamical case

We expect dynamical $f(\boldsymbol{k}, \boldsymbol{q}, x)$ to be modified in the similar manner to the static (DGLV) case.

B. Blagojevic, M. Djordjevic and M. Djordjevic, Phys. Rev. C 99, no. 2, 024901 (2019)

Calculations beyond soft-gluon approximation

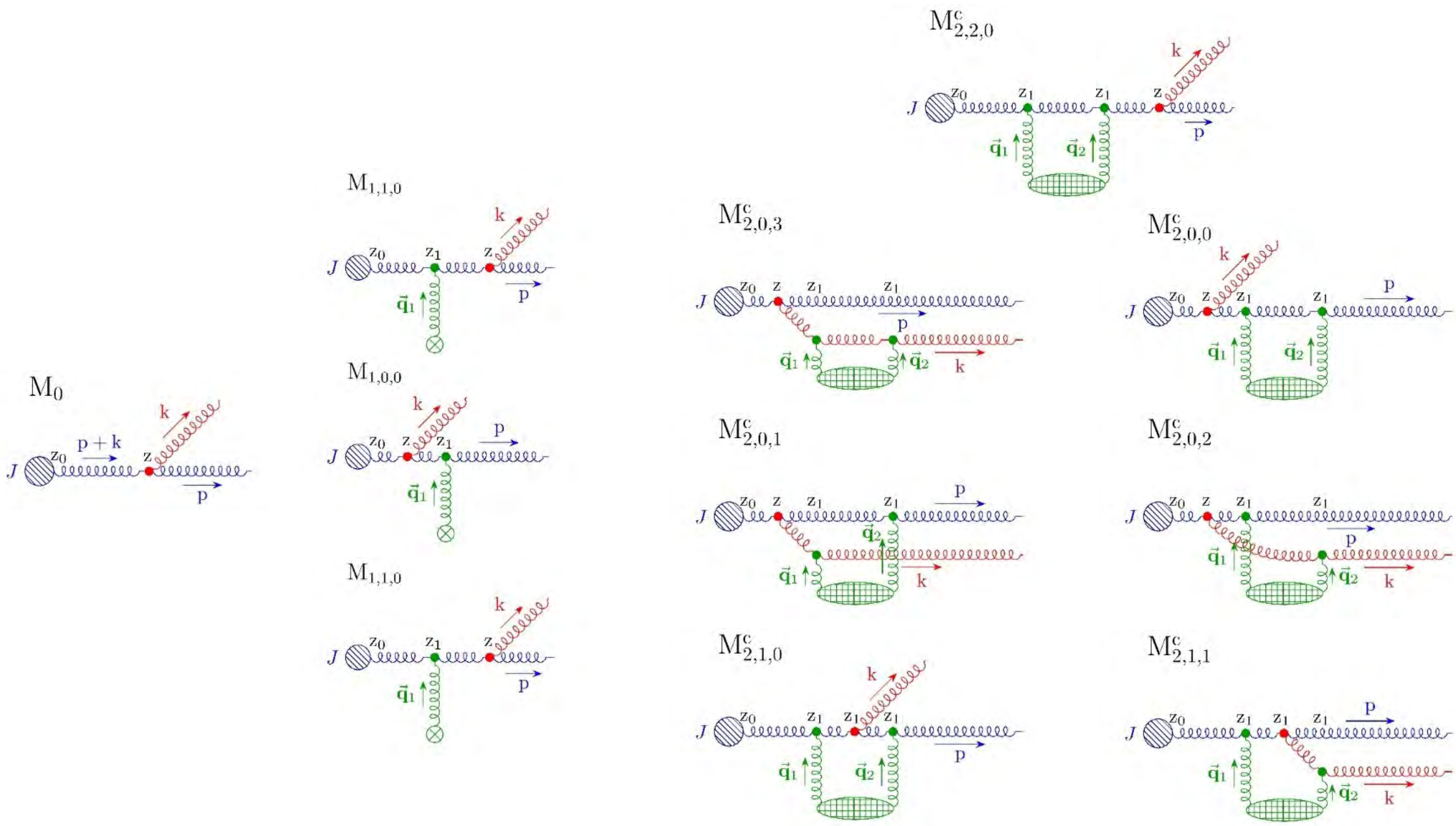

B. Blagojevic, M. Djordjevic and M. Djordjevic,
Phys. Rev. C 99, no. 2, 024901 (2019)

Calculations beyond soft-gluon approximation

Longitudinal initial gluon direction:

No interactions with QGP medium (M_0)

$$p + k = [E^+, E^-, \mathbf{0}]$$

One interaction with QGP medium (M_1)

$$p + k - q_1 = [E^+ - q_{1z}, E^- + q_{1z}, \mathbf{0}]$$

Two interactions with QGP medium (M_2)

$$p + k - q_1 - q_2 = [E^+ - q_{1z} - q_{2z}, E^- + q_{1z} + q_{2z}, \mathbf{0}]$$

$$k = [xE^+, \frac{\mathbf{k}^2 + m_g^2}{xE^+}, \mathbf{k}] \qquad p = [(1-x)E^+, \frac{\mathbf{p}^2 + m_g^2}{(1-x)E^+}, \mathbf{p}]$$

Transverse momenta: $\boldsymbol{p} + \boldsymbol{k} = \mathbf{0}$

Transverse momenta: $\boldsymbol{p} + \boldsymbol{k} \neq \mathbf{0}$

Consistent with longitudinal propagation of initial particle!

Transverse momenta: $\boldsymbol{p} + \boldsymbol{k} = \mathbf{0}$ **in contact-limit**

Transverse gluon polarization:

$$n^\mu = [0,2,0]$$

G. Ovanesyan and I. Vitev, JHEP 1106, 080 (2011)

$$\epsilon(k) \cdot k = 0, \quad \epsilon(k) \cdot n = 0, \quad \epsilon(k)^2 = -1, \quad \epsilon(p+k) \cdot (p+k) = 0, \quad \epsilon(p+k) \cdot n = 0,$$

$$\epsilon(p) \cdot p = 0, \quad \epsilon(p) \cdot n = 0, \quad \epsilon(p)^2 = -1, \quad \epsilon(p+k)^2 = -1.$$

$$\epsilon_i(k) = [0, \frac{2\epsilon_i \cdot \mathbf{k}}{xE^+}, \epsilon_i],$$

$$\epsilon_i(p+k) = [0, 0, \epsilon_i],$$

$$\epsilon_i(p) = [0, \frac{2\epsilon_i \cdot \mathbf{p}}{(1-x)E^+}, \epsilon_i],$$

B. Blagojevic, M. Djordjevic and M. Djordjevic, Phys. Rev. C 99, no. 2, 024901 (2019)

Calculations beyond soft-gluon approximation

$$d^3N_g^{(1)}d^3N_J = \left(\frac{1}{d_T}\,\mathrm{Tr}\,\langle|M_1|^2\rangle + \frac{2}{d_T} Re\,\mathrm{Tr}\,\langle M_2 M_0^*\rangle\right)\frac{d^3\vec{\mathbf{p}}}{(2\pi)^3 2p^0}\frac{d^3\vec{\mathbf{k}}}{(2\pi)^3 2\omega}$$

New!

$$d^3N_J = d_G|J(p+k)|^2\frac{d^3\vec{\mathbf{p}}_J}{(2\pi)^3 2E_J}$$

$$\boxed{\frac{d^3\vec{\mathbf{p}}}{(2\pi)^3 2p^0}\frac{d^3\vec{\mathbf{k}}}{(2\pi)^3 2\omega} = \frac{d^3\vec{\mathbf{p}}_J}{(2\pi)^3 2E_J}\frac{dx d^2\mathbf{k}}{(2\pi)^3 2x(1-x)}}$$

$$\frac{x d^3N_g^{(0)}}{dx d\mathbf{k}^2} = \frac{\alpha_s}{\pi}\frac{C_2(G)\,\mathbf{k}^2}{(\mathbf{k}^2 + m_g^2(1-x+x^2))^2} \times\frac{(1-x+x^2)^2}{1-x}$$

Z. B. Kang, F. Ringer and I. Vitev, JHEP 1703, 146 (2017)

$$\frac{dN_g^{(1)}}{dx} = \frac{C_2(G)\alpha_s}{\pi}\frac{L}{\lambda}\frac{(1-x+x^2)^2}{x(1-x)}\int\frac{d^2\mathbf{q}_1}{\pi}\frac{\mu^2}{(\mathbf{q}_1^2+\mu^2)^2}\int d\mathbf{k}^2$$
$$\times\Big\{\frac{(\mathbf{k}-\mathbf{q}_1)^2+\chi}{(\frac{4x(1-x)E}{L})^2+((\mathbf{k}-\mathbf{q}_1)^2+\chi)^2}\Big(2\frac{(\mathbf{k}-\mathbf{q}_1)^2}{(\mathbf{k}-\mathbf{q}_1)^2+\chi} - \frac{\mathbf{k}\cdot(\mathbf{k}-\mathbf{q}_1)}{\mathbf{k}^2+\chi} - \frac{(\mathbf{k}-\mathbf{q}_1)\cdot(\mathbf{k}-x\mathbf{q}_1)}{(\mathbf{k}-x\mathbf{q}_1)^2+\chi}\Big)$$
$$+\frac{\mathbf{k}^2+\chi}{(\frac{4x(1-x)E}{L})^2+(\mathbf{k}^2+\chi)^2}\Big(\frac{\mathbf{k}^2}{\mathbf{k}^2+\chi} - \frac{\mathbf{k}\cdot(\mathbf{k}-x\mathbf{q}_1)}{(\mathbf{k}-x\mathbf{q}_1)^2+\chi}\Big) + \Big(\frac{(\mathbf{k}-x\mathbf{q}_1)^2}{((\mathbf{k}-x\mathbf{q}_1)^2+\chi)^2} - \frac{\mathbf{k}^2}{(\mathbf{k}^2+\chi)^2}\Big)\Big\}$$

B. Blagojevic, M. Djordjevic and M. Djordjevic, Phys. Rev. C 99, no. 2, 024901 (2019)

$$m_g = m_\infty = \sqrt{\Pi_T(p_0/|\vec{\mathrm{p}}| = 1)} = \mu_E/\sqrt{2}$$

Effective gluon mass

(M. Djordjevic and M. Gyulassy, PRC 68:034914 (2003))

B. Blagojevic, M. Djordjevic and M. Djordjevic,
Phys. Rev. C 99, no. 2, 024901 (2019)

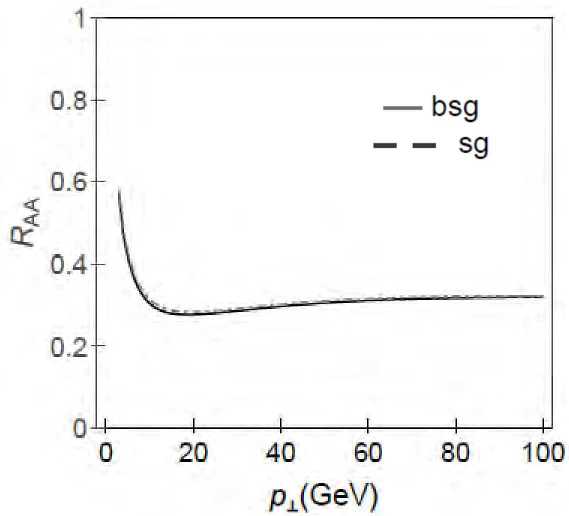

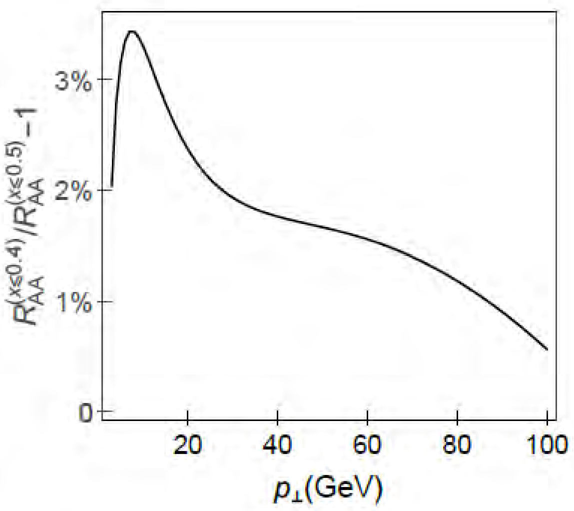

Non-relevance of x > 0.4 region for the importance of relaxing the soft-gluon approximation

B. Blagojevic, M. Djordjevic and M. Djordjevic, Phys. Rev. C 99, no. 2, 024901 (2019)

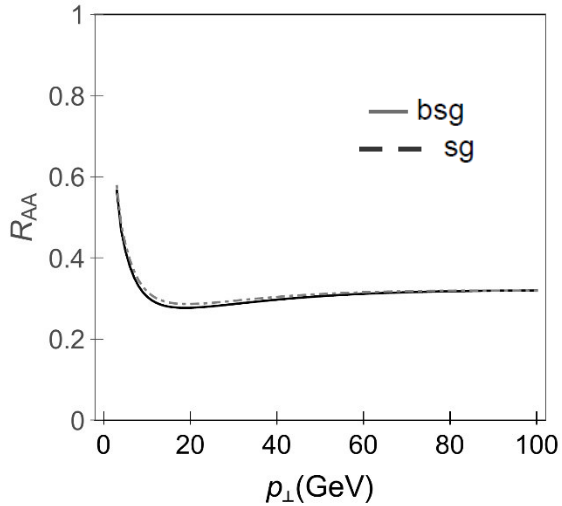

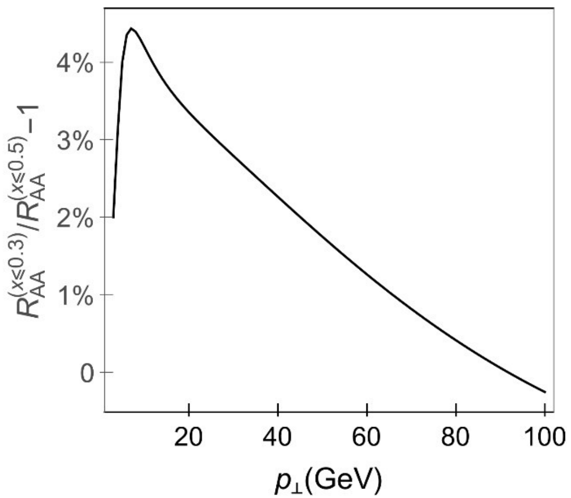

Non-relevance of $x > 0.3$ region for the importance of relaxing the soft-gluon approximation

B. Blagojevic, M. Djordjevic and M. Djordjevic, Phys. Rev. C 99, no. 2, 024901 (2019)

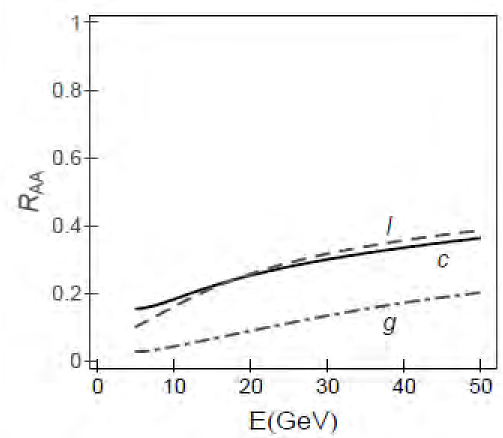

LHC 2.76 TeV

M. Djordjevic, PRL 112:042302 (2014).

B. Blagojevic, M. Djordjevic and M. Djordjevic,
Phys. Rev. C 99, no. 2, 024901 (2019)

$$\frac{d\sigma_{el}}{d^2\mathbf{q}_1} = \frac{C_2(G)C_2(T)}{d_G}\frac{|v(0,\mathbf{q}_1)|^2}{(2\pi)^2}$$

Opacity $= L/\lambda = N\sigma_{el}/A_\perp$

Small transverse momentum transfer elastic cross section (GW)

(M. Gyulassy and X.N. Wang, NPB 420, 583 (1994))

B. Blagojevic, M. Djordjevic and M. Djordjevic, Phys. Rev. C 99, no. 2, 024901 (2019)

Two limits of longitudinal distance distribution

Longitudinal distance between gluon production site and target rescattering site:

Exponential distribution

$$\frac{2}{L}e^{\frac{-2\Delta z}{L}}$$

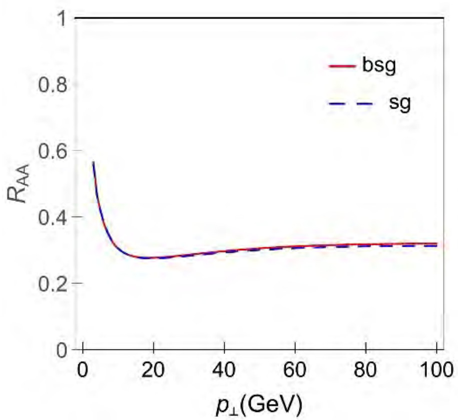

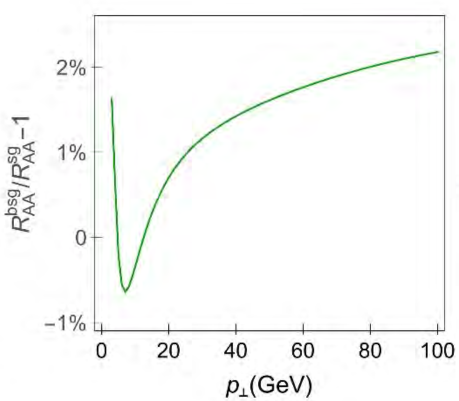

Uniform distribution

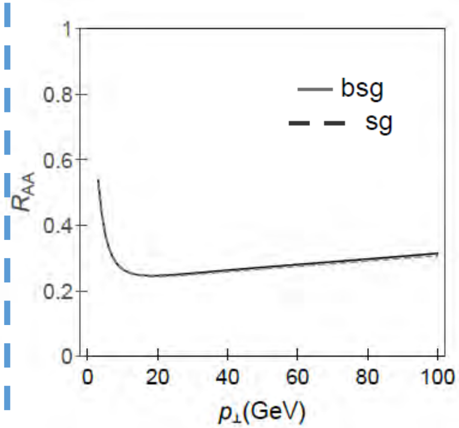

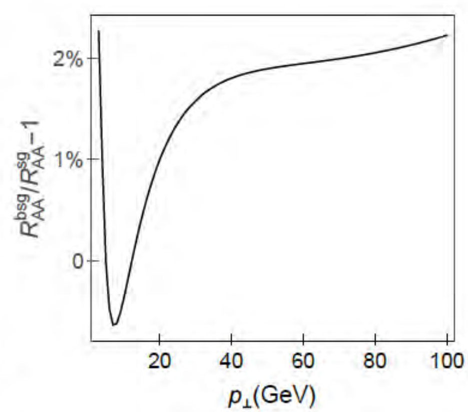

B. Blagojevic, M. Djordjevic and M. Djordjevic,
Phys. Rev. C 99, no. 2, 024901 (2019)

Two limits of longitudinal distance distribution

Exponential distribution

$$\frac{dN_g^{(1)}}{dx} = \frac{C_2(G)\alpha_s}{\pi}\frac{L}{\lambda}\frac{(1-x+x^2)^2}{x(1-x)}\int\frac{d^2\mathbf{q}_1}{\pi}\frac{\mu^2}{(\mathbf{q}_1^2+\mu^2)^2}\int d\mathbf{k}^2$$
$$\times\Big\{\frac{(\mathbf{k}-\mathbf{q}_1)^2+\chi}{(\frac{4x(1-x)E}{L})^2+((\mathbf{k}-\mathbf{q}_1)^2+\chi)^2}\Big(2\frac{(\mathbf{k}-\mathbf{q}_1)^2}{(\mathbf{k}-\mathbf{q}_1)^2+\chi}-\frac{\mathbf{k}\cdot(\mathbf{k}-\mathbf{q}_1)}{\mathbf{k}^2+\chi}-\frac{(\mathbf{k}-\mathbf{q}_1)\cdot(\mathbf{k}-x\mathbf{q}_1)}{(\mathbf{k}-x\mathbf{q}_1)^2+\chi}\Big)$$
$$+\frac{\mathbf{k}^2+\chi}{(\frac{4x(1-x)E}{L})^2+(\mathbf{k}^2+\chi)^2}\Big(\frac{\mathbf{k}^2}{\mathbf{k}^2+\chi}-\frac{\mathbf{k}\cdot(\mathbf{k}-x\mathbf{q}_1)}{(\mathbf{k}-x\mathbf{q}_1)^2+\chi}\Big)+\Big(\frac{(\mathbf{k}-x\mathbf{q}_1)^2}{((\mathbf{k}-x\mathbf{q}_1)^2+\chi)^2}-\frac{\mathbf{k}^2}{(\mathbf{k}^2+\chi)^2}\Big)\Big\}$$

Uniform distribution

$$\frac{dN_g^{(1)}}{dx} = \frac{C_2(G)\alpha_s}{\pi}\frac{L}{\lambda}\frac{(1-x+x^2)^2}{x(1-x)}\int\frac{d^2\mathbf{q}_1}{\pi}\frac{\mu^2}{(\mathbf{q}_1^2+\mu^2)^2}\int d\mathbf{k}^2$$
$$\times\Big\{\Big(1-\frac{\sin\big(\frac{(\mathbf{k}-\mathbf{q}_1)^2+\chi}{2x(1-x)E}L\big)}{\frac{(\mathbf{k}-\mathbf{q}_1)^2+\chi}{2x(1-x)E}L}\Big)\frac{1}{(\mathbf{k}-\mathbf{q}_1)^2+\chi}\Big(2\frac{(\mathbf{k}-\mathbf{q}_1)^2}{(\mathbf{k}-\mathbf{q}_1)^2+\chi}-\frac{\mathbf{k}\cdot(\mathbf{k}-\mathbf{q}_1)}{\mathbf{k}^2+\chi}-\frac{(\mathbf{k}-\mathbf{q}_1)\cdot(\mathbf{k}-x\mathbf{q}_1)}{(\mathbf{k}-x\mathbf{q}_1)^2+\chi}\Big)$$
$$+\Big(1-\frac{\sin\big(\frac{\mathbf{k}^2+\chi}{2x(1-x)E}L\big)}{\frac{\mathbf{k}^2+\chi}{2x(1-x)E}L}\Big)\frac{1}{\mathbf{k}^2+\chi}\Big(\frac{\mathbf{k}^2}{\mathbf{k}^2+\chi}-\frac{\mathbf{k}\cdot(\mathbf{k}-x\mathbf{q}_1)}{(\mathbf{k}-x\mathbf{q}_1)^2+\chi}\Big)+\Big(\frac{(\mathbf{k}-x\mathbf{q}_1)^2}{((\mathbf{k}-x\mathbf{q}_1)^2+\chi)^2}-\frac{\mathbf{k}^2}{(\mathbf{k}^2+\chi)^2}\Big)\Big\}$$

B. Blagojevic, M. Djordjevic and M. Djordjevic,
Phys. Rev. C 99, no. 2, 024901 (2019)

$$R_{AA}(p_\perp) = \frac{dN_{AA}/dp_\perp}{N_{bin} dN_{pp}/dp_\perp}$$

D. Molnar and D. Sun, NPA 932:140; NPA 910:486, T. Renk, PRC 85:044903.

$$\frac{E_f d^3\sigma(g)}{dp_f^3} = \frac{E_i d^3\sigma(g)}{dp_i^3} \otimes P(E_i \to E_f)$$

pQCD convolution

B. Blagojevic, M. Djordjevic and M. Djordjevic, Phys. Rev. C 99, no. 2, 024901 (2019)

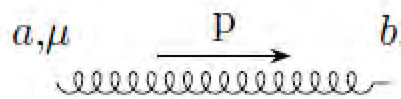

$$= \frac{i\delta_{ab} P_{\mu\nu}}{p^2 - m_g^2 + i\epsilon}$$

$$P_{\mu\nu} = -\left(g_{\mu\nu} - \frac{p_\mu p_\nu n^2 + n_\mu n_\nu p^2 - n_\mu p_\nu (np) - n_\nu p_\mu (np)}{n^2 p^2 - (np)^2}\right)$$

(M. Djordjevic and M. Gyulassy, PRC 68:034914 (2003))

B. Blagojevic, M. Djordjevic and M. Djordjevic,
Phys. Rev. C 99, no. 2, 024901 (2019)

The Galileo Galilei Institute for Theoretical Physics

GGI

Firenze, 28 February 2020

The influence of electromagnetic fields in relativistic proton-nucleus collisions

Lucia Oliva

LO, Pierre Moreau, Vadim Voronyuk and Elena Bratkovskaya

Phys. Rev. C 101 (2020) 014917 [arXiv: 1909.06770]

GOETHE UNIVERSITÄT FRANKFURT AM MAIN

Alexander von Humboldt Stiftung/Foundation

GSI Helmholtzzentrum für Schwerionenforschung GmbH

CRC-TR 211 Strong-interaction matter under extreme conditions

High energy collisions recreate the extreme condition of temperature and density are required to form the

QUARK-GLUON PLASMA (QGP)

- initially expected only in heavy-ion collisions
- small colliding systems as control measurements

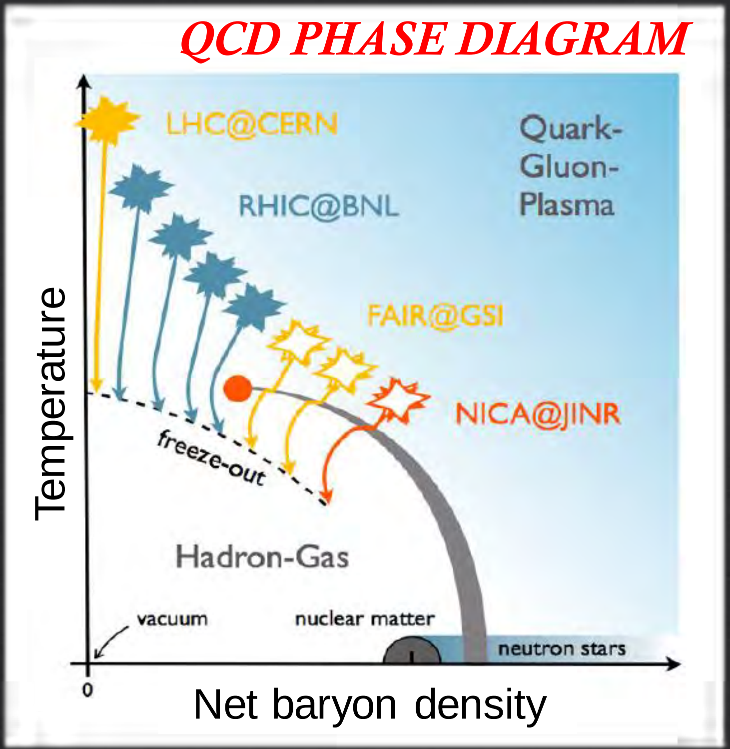

SIGNATURES OF COLLECTIVE FLOW IN SMALL SYSTEMS

p+Pb at LHC

p/d/^{3}He+Au at RHIC

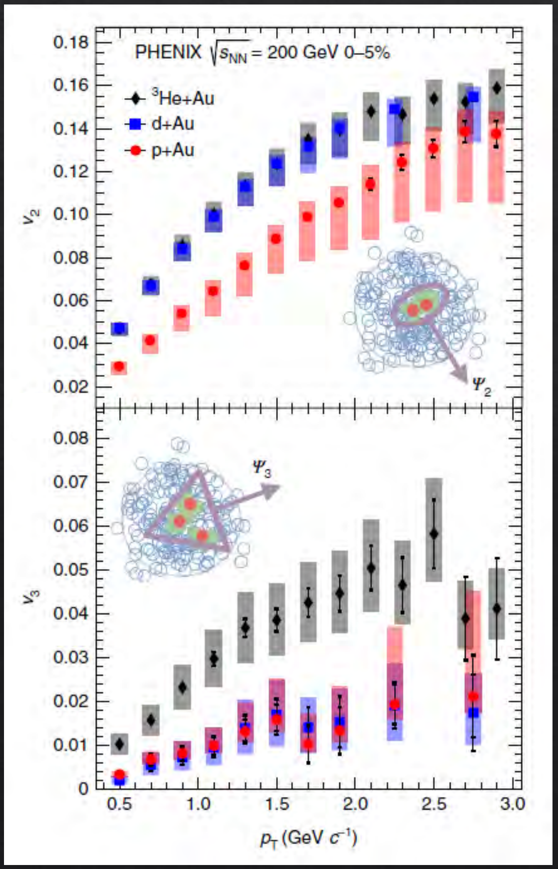

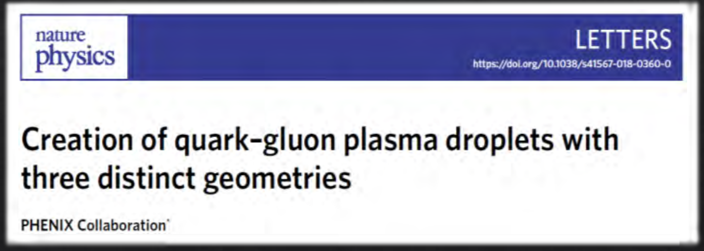
nature physics

LETTERS

https://doi.org/10.1038/s41567-018-0360-0

Creation of quark-gluon plasma droplets with three distinct geometries

PHENIX Collaboration*

PHENIX, Nature Phys. 15 (2019) 214

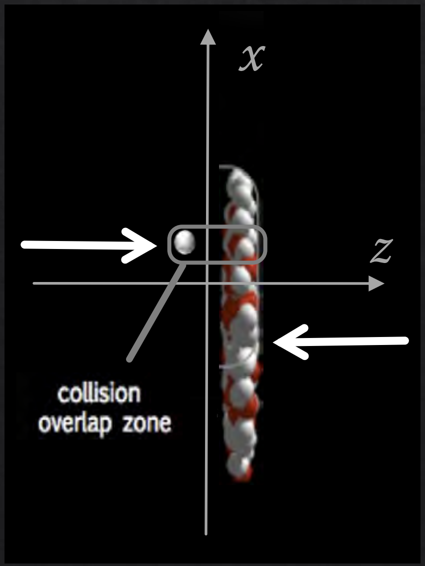

Short-lived droplets of QGP in proton-induced collisions

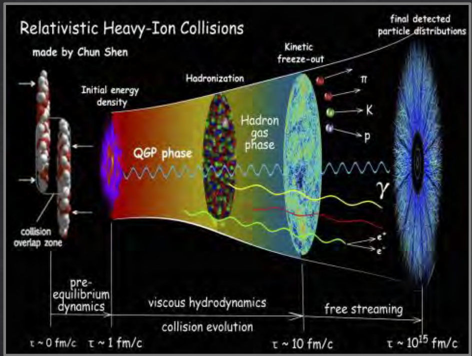

HICs

~ 10^{18}-10^{19} G

magnetars

~ 10^{14}-10^{15} G

laboratory

~ 10^{6} G

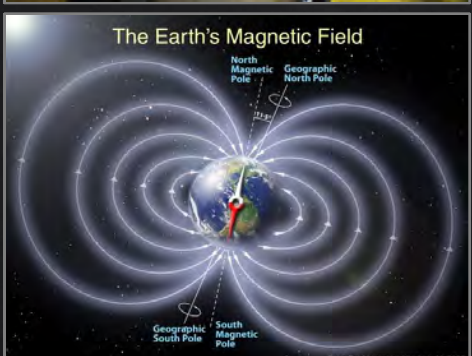

Earth's field

~ 1 G

Many interesting phenomena in HICs driven by the intense electromagnetic fields (EMF) produced since the early stage of the collision

CHIRAL MAGNETIC EFFECT

$$J_m = \frac{e^2}{2\pi^2}\mu_5 \boldsymbol{B}$$

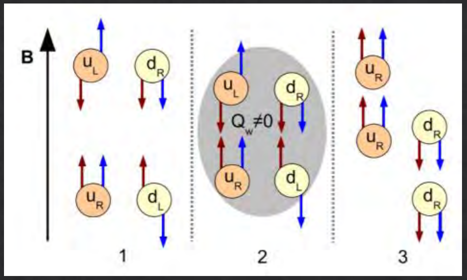

Kharzeev, McLerran and Warringa, NPA 803 (2008) 227

CHARGE-ODD DIRECTED FLOW

$$\boldsymbol{F}_{em} = q(\boldsymbol{E} + \boldsymbol{v} \times \boldsymbol{B}) \quad \rightarrow \quad v_1^+ \neq v_1^-$$

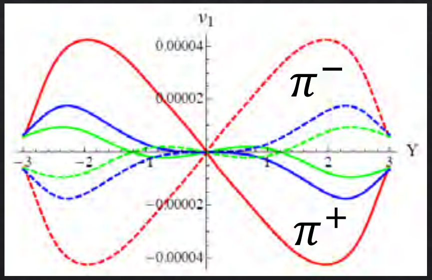

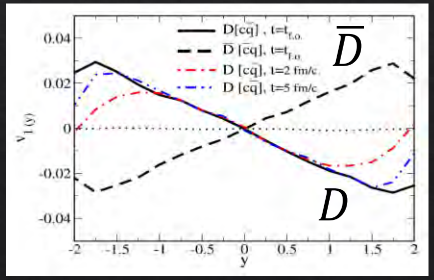

Gursoy, Kharzeev and Rajagopal, PRC 89 (2014) 054905
Voronyuk, Toneev, Voloshin and Cassing, PRC 90 (2014) 064903
Das, Plumari, Greco et al., PLB 768 (2017) 260

EMF in proton-nucleus collisions?

PHSD: Parton-Hadron-String Dynamics

non-equilibrium transport approach to describe large and small colliding systems

talk of O. Soloveva

To study the phase transition from hadronic to partonic matter and QGP properties from a microscopic origin

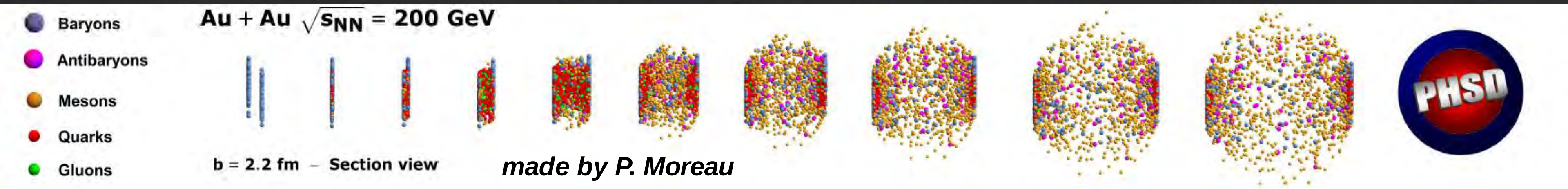

made by P. Moreau

- INITIAL A+A COLLISIONS: nucleon-nucleon collisions lead to the formation of strings that decay to pre-hadrons
- FORMATION OF QGP: if energy density $\varepsilon > \varepsilon_C$ pre-hadrons dissolve in massive quarks and gluons + mean-field potential
- PARTONIC STAGE: evolution based on off-shell transport equations with the DQPM defining parton spectral functions
- HADRONIZATION: massive off-shell partons with broad spectral functions hadronize to off-shell baryons and mesons
- HADRONIC PHASE: evolution based on the off-shell transport equations with hadron-hadron interactions

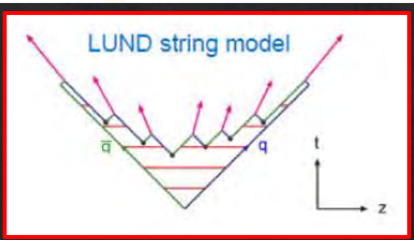

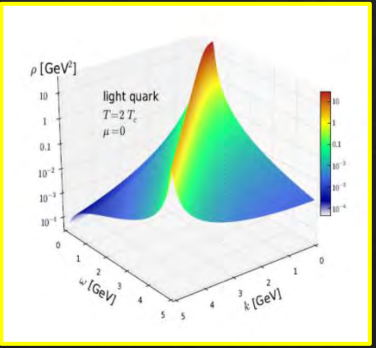

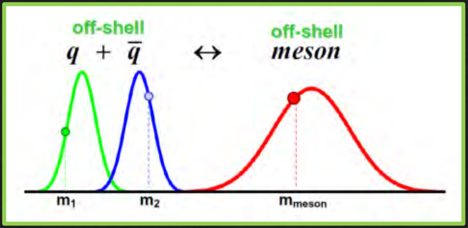

Cassing and Bratkovskaya, PRC 78 (2008) 034919; NPA831 (2009) 215
Cassing, EPJ ST 168 (2009) 3; NPA856 (2011) 162

PHSD + electromagnetic fields

PHSD includes the dynamical formation and evolution of the retarded electomagnetic field (EMF) and its influence on quasi-particle dynamics

Voronyuk *et al.* (HSD), PRC 83 (2011) 054911; Toneev *et al.* (PHSD), PRC 86 (2012) 064907

$$\left\{\frac{\partial}{\partial t} + \left(\frac{\mathbf{p}}{p_0} + \nabla_{\mathbf{p}} U\right)\nabla_{\mathbf{r}} + \left(-\nabla_{\mathbf{r}} U + e\mathbf{E} + e\mathbf{v}\times\mathbf{B}\right)\nabla_{\mathbf{p}}\right\} f = C_{\mathrm{coll}}(f, f_1, \ldots, f_N)$$

Lorentz force

TRANSPORT EQUATIONS

consistent solution of particle and field evolution equations

charge distribution

electric current

$$\nabla\cdot\mathbf{B} = 0 \qquad \nabla\times\mathbf{E} = -\frac{\partial\mathbf{B}}{\partial t} \qquad \nabla\cdot\mathbf{E} = 4\pi\rho \qquad \nabla\times\mathbf{B} = \frac{\partial\mathbf{E}}{\partial t} + \frac{4\pi}{c}\mathbf{j}$$

MAXWELL EQUATIONS

$$e\mathbf{E}(t,\mathbf{r}) = \alpha_{em}\frac{1-\beta^2}{\left[(\mathbf{R}\cdot\boldsymbol{\beta})^2 + R^2(1-\beta^2)\right]^{3/2}}\mathbf{R}$$

$$e\mathbf{B}(t,\mathbf{r}) = \boldsymbol{\beta}\times e\mathbf{E}(t,\mathbf{r})$$

single freely moving charge

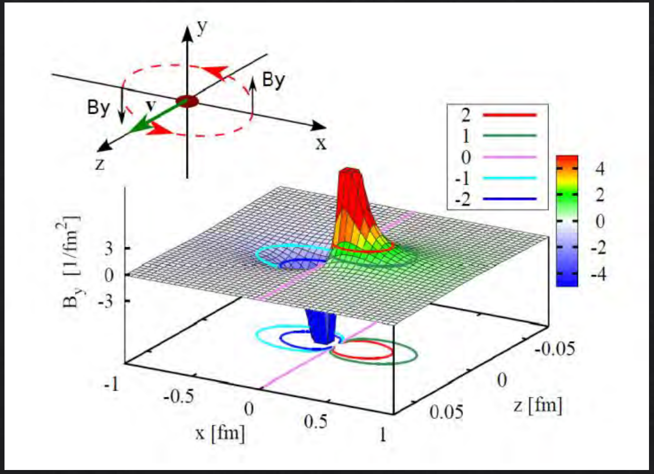

Electromagnetic fields in symmetric systems

in a nuclear collision the magnetic field is a superposition of solenoidal fields from different moving charges

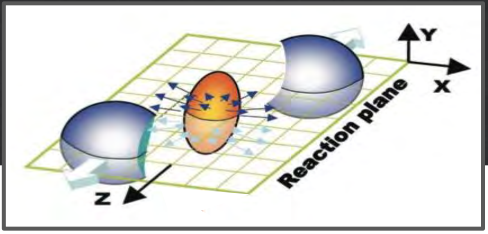

Au+Au @RHIC 200 GeV – b = 10 fm

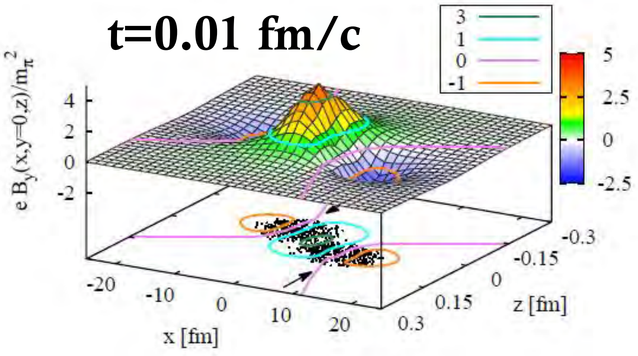

Voronyuk *et al*. (HSD), PRC 83 (2011) 054911

Electromagnetic fields in symmetric systems

in a nuclear collision the magnetic field is a superposition of solenoidal fields from different moving charges

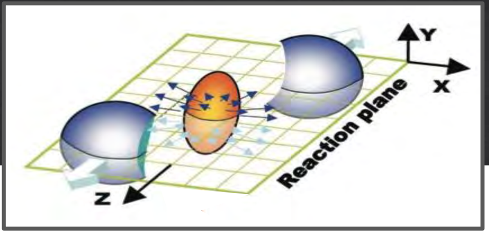

Au+Au @RHIC 200 GeV – b = 10 fm

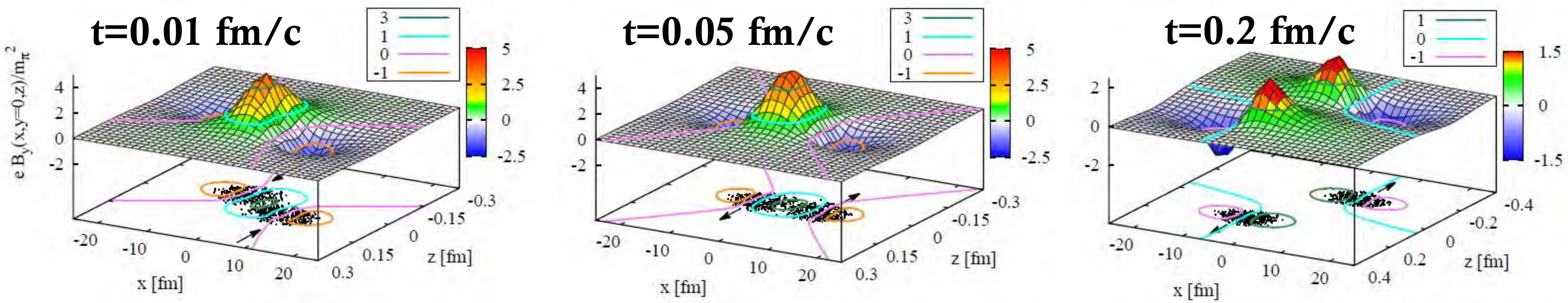

MAGNETIC FIELD

- dominated by the y-component
- maximal strength reached during nuclear overlapping time
- only due to spectators up to $t \sim 1$ fm/c
- drops down by three orders of magnitude and become comparable with that from participants

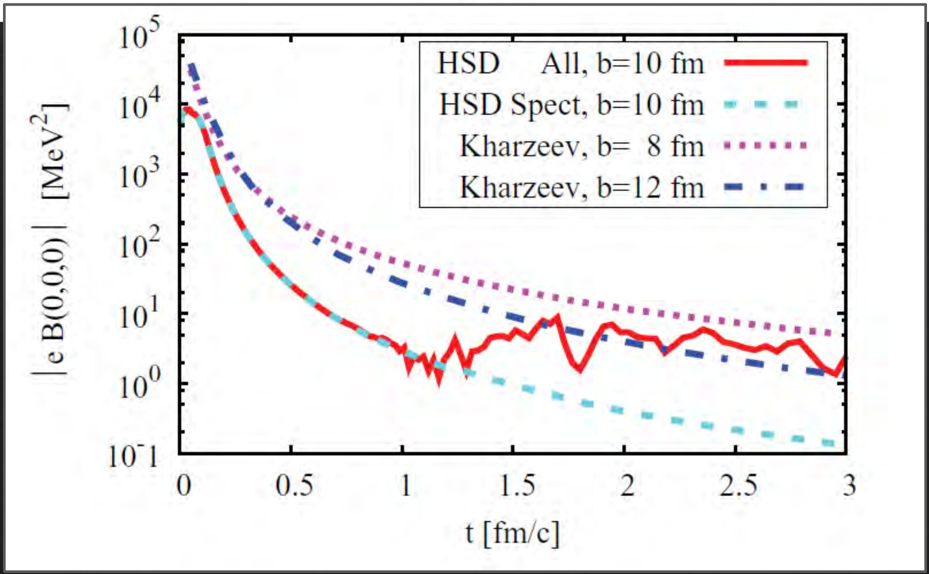

Voronyuk *et al*. (HSD), PRC 83 (2011) 054911

Electromagnetic fields: A+A vs p+A

Au+Au @ RHIC 200 GeV b=7 fm

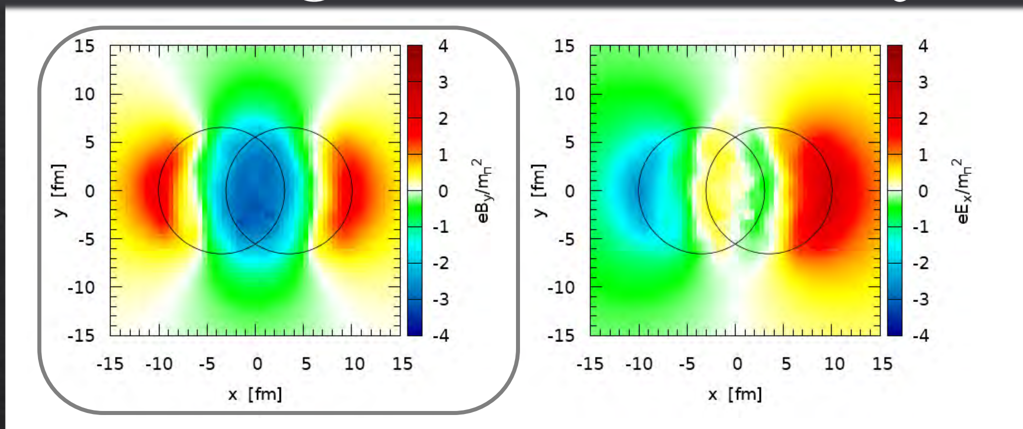

B_y E_x

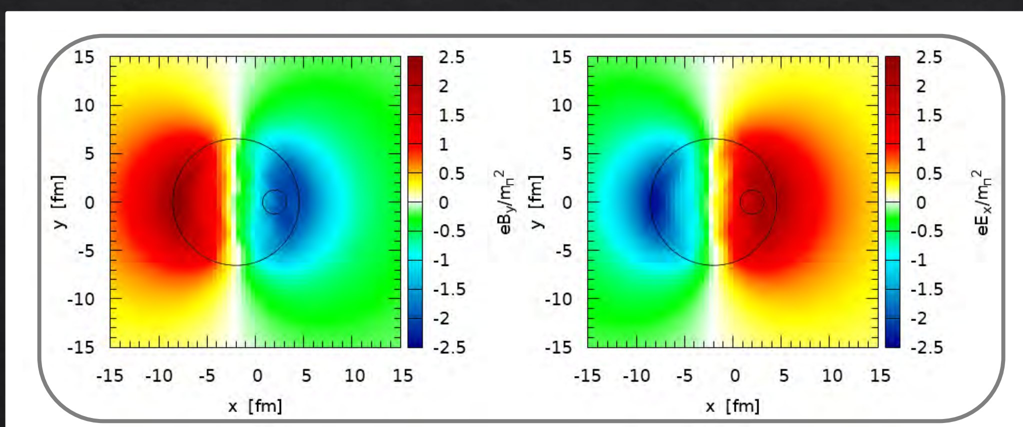

p+Au @ RHIC 200 GeV b=4 fm

SYMMETRIC SYSTEMS

transverse momentum increments due to electric and magnetic fields compensate each other

ASYMMETRIC SYSTEMS

an intense electric fields directed from the heavy nuclei to light one appears in the overlap region

LO, Moreau, Voronyuk and Bratkovskaya, PRC 101 (2020) 014917

Centrality determination : A+A vs p+A

A+A

centrality characterizes the amount of overlap in the interaction area

p+A

multiplicity fluctuation mixes events from different impact parameters

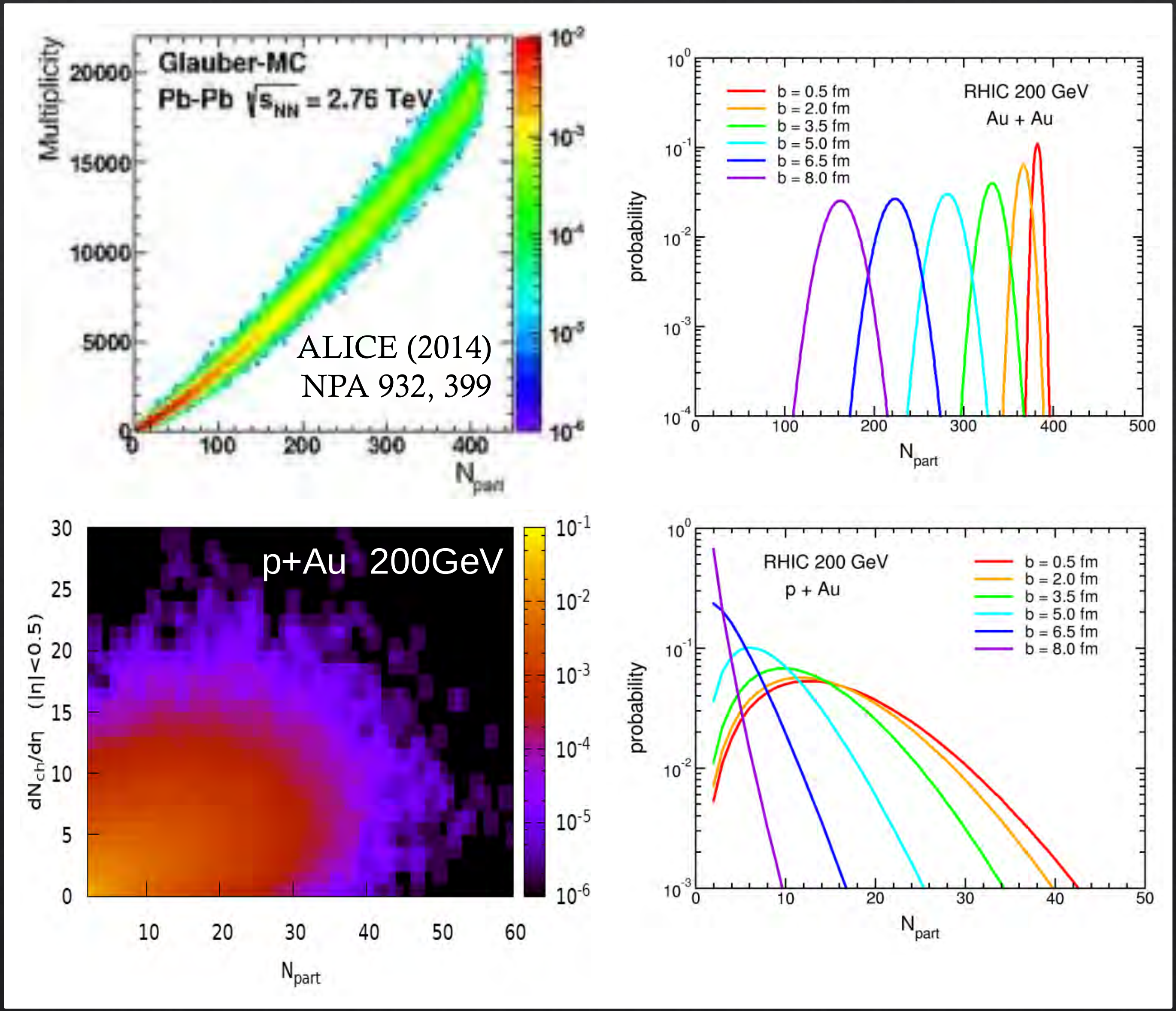

LO, Moreau, Voronyuk and Bratkovskaya, PRC 101 (2020) 014917

p+Au: rapidity distributions

PSEUDORAPIDITY DISTRIBUTION OF CHARGED PARTICLES

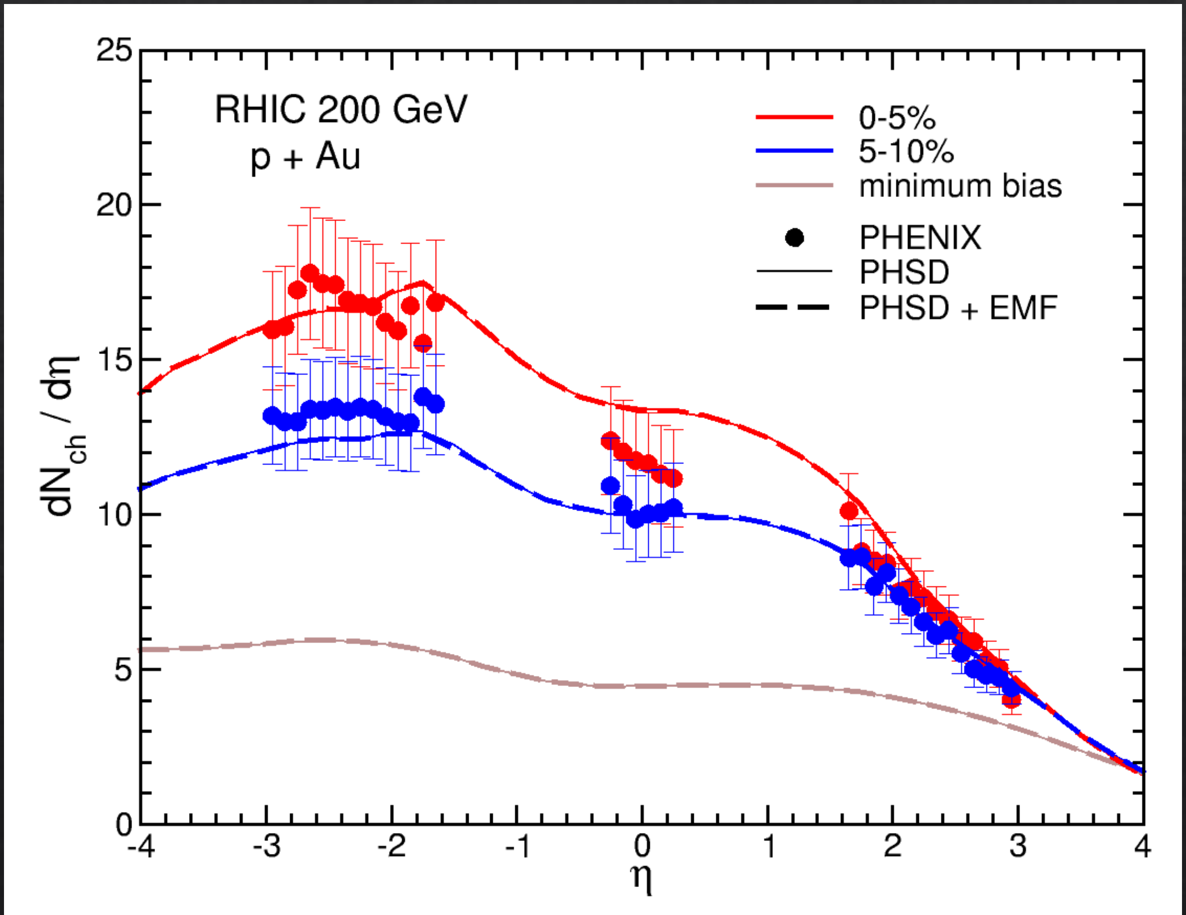

$$\eta = -\ln\left(\tan\frac{\theta}{2}\right)$$

pseudorapidity
(θ: polar angle of the particle)

- enhanced particle production in the Au-going directions
- asymmetry increases with centrality of the collision

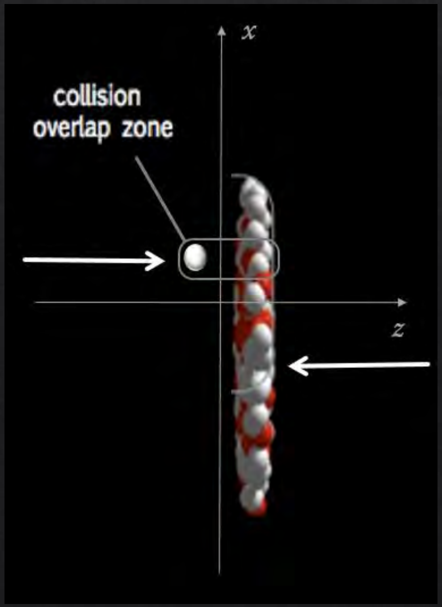

LO, Moreau, Voronyuk and Bratkovskaya, PRC 101 (2020) 014917
Exp. Data: PHENIX Collaboration, PRL 121 (2018) 222301

p+Au: rapidity distributions

RAPIDITY DISTRIBUTION OF IDENTIFIED PARTICLES
channel decomposition

large amount of particles escapes from the medium just after production from QGP hadronization without further rescattering

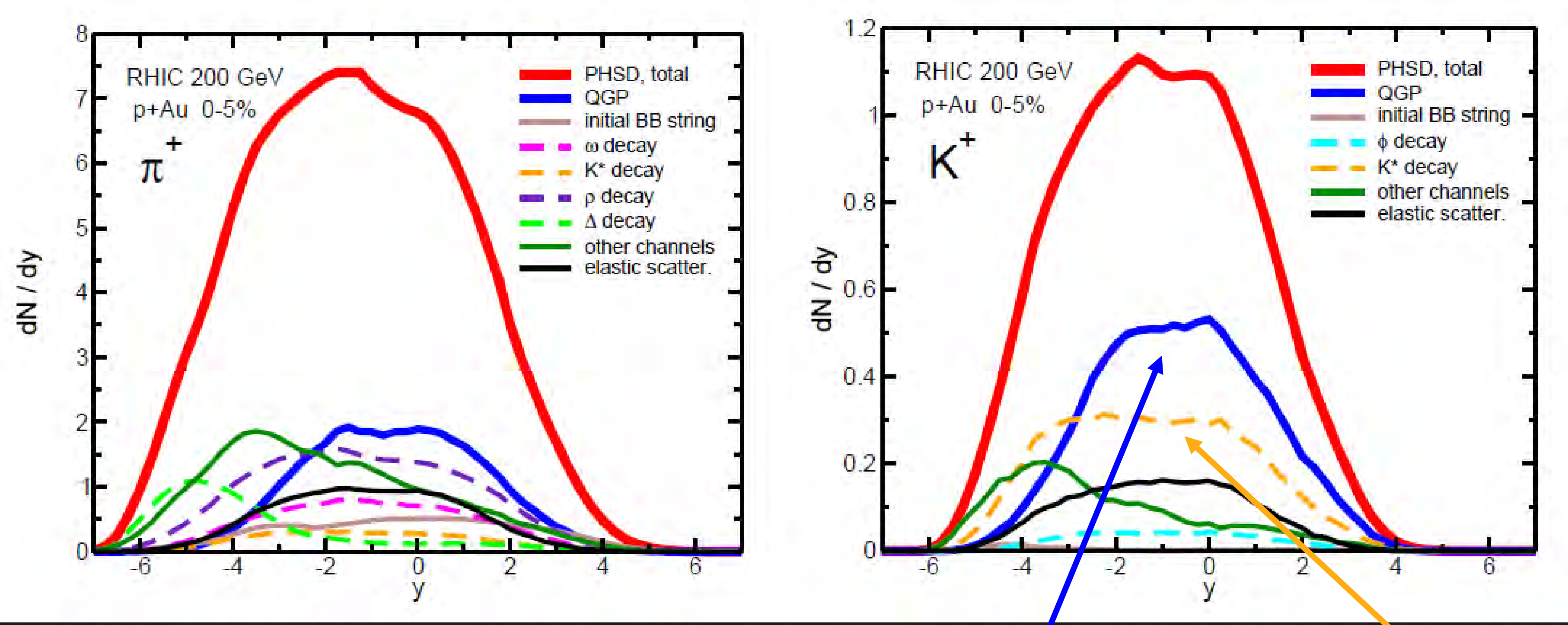

- p+A: production of kaons directly from QGP hadronization larger than from K* decay
- A+A: kaons created by K* decay are about twice those generated directly from QGP

Anisotropic radial flow v_n

Quark-Gluon Plasma

hydrodynamical behavior with very low specific viscosity η/s and formation of collective flows

azimuthal particle distributions w.r.t. the reaction plane

$$\frac{dN}{d\varphi} \propto 1 + \sum_n 2\, v_n(p_T) \cos[n(\varphi - \Psi_n)]$$

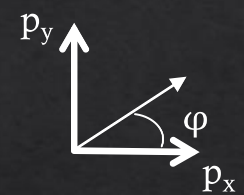

flow coefficients

event-plane angle

$$v_n = \frac{\langle \cos[n(\varphi - \Psi_n)] \rangle}{Res(\Psi_n)}$$

event-plane angle resolution

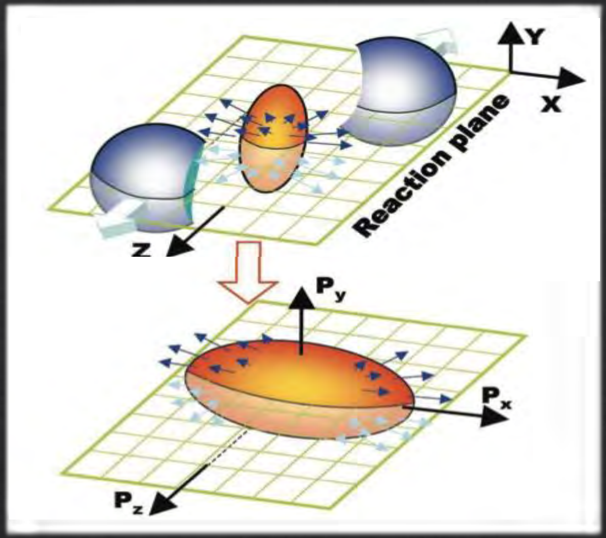

not a simple **almond shape** but a **"lumpy" profile** due to fluctuations of nucleon position in the overlap region

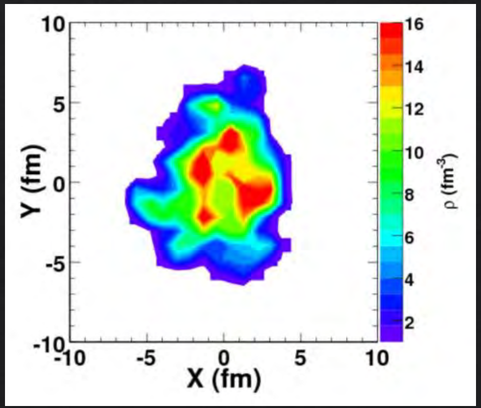

Plumari *et al.*, PRC 92 (2015) 054902

The DIRECTED FLOW v_1 is a collective sidewards deflection of particles

- initial-state fluctuations
- orbital angular momentum
- ELECTROMAGNETIC FIELDS

p+Au: directed flow

rapidity dependence of the DIRECTED FLOW OF IDENTIFIED PARTICLES

$$v_1(y) = \frac{\langle \cos[\varphi(y) - \Psi_1] \rangle}{Res(\Psi_1)}$$

$$y = \tanh^{-1}\frac{v}{c}$$

rapidity
(v: velocity of the particle)

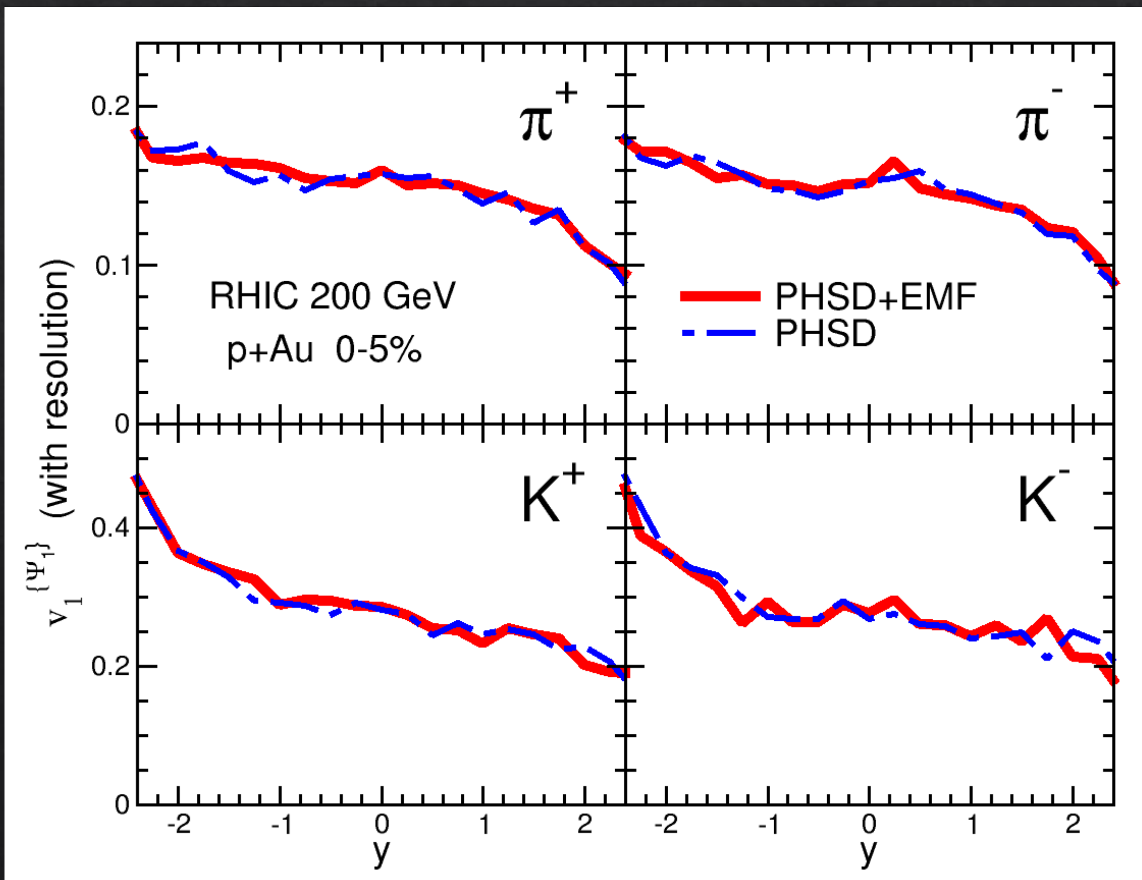

SPLITTING of positively and negatively charged particles INDUCED BY THE EMF?

5% central collisions

no visible changes
with and without
electromagnetic fields

BUT…

LO, Moreau, Voronyuk and Bratkovskaya, PRC 101 (2020) 014917

p+Au: directed flow

rapidity dependence of the
DIRECTED FLOW OF PIONS

$$v_1(y) = \langle \cos[\varphi(y)] \rangle$$

fixed impact parameter *b*

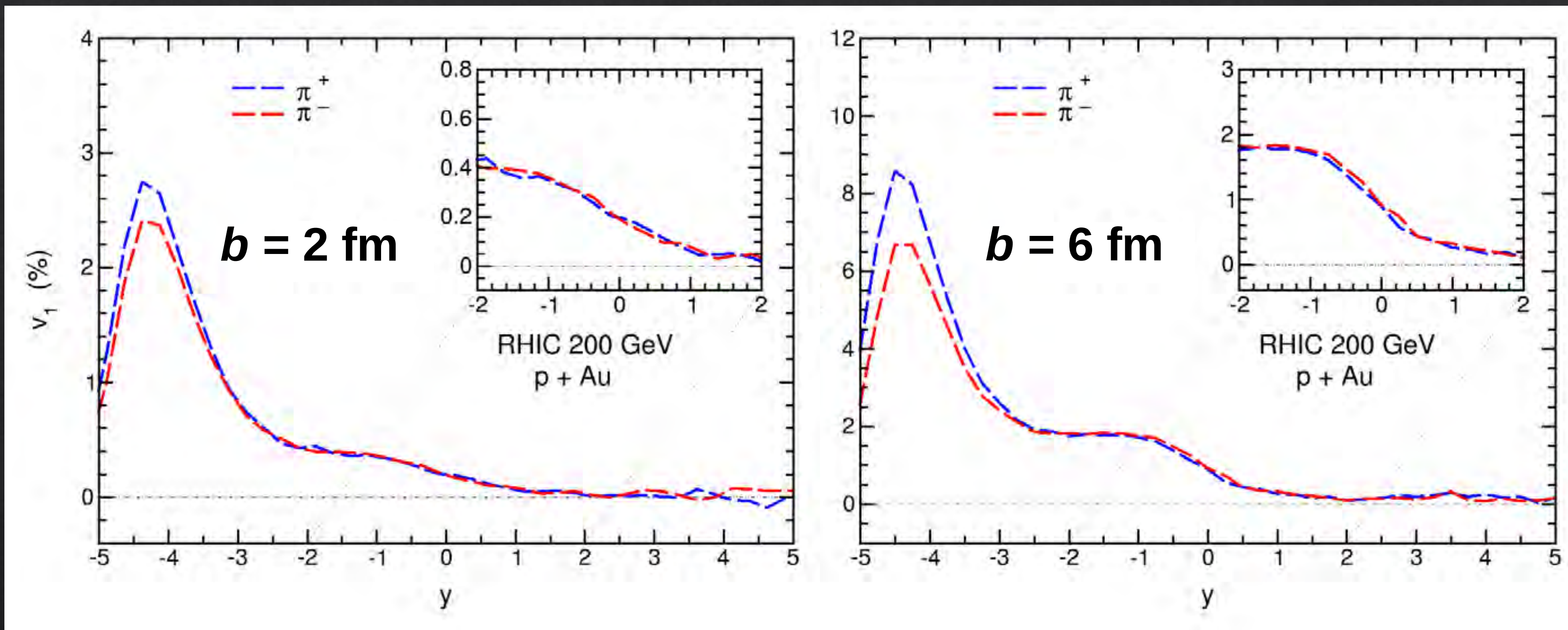

LO, Moreau, Voronyuk and Bratkovskaya, PRC 101 (2020) 014917

SPLITTING INDUCED BY THE EM FIELD?

p+Au: directed flow

rapidity dependence of the
DIRECTED FLOW OF PIONS

$$v_1(y) = \langle \cos[\varphi(y)] \rangle$$

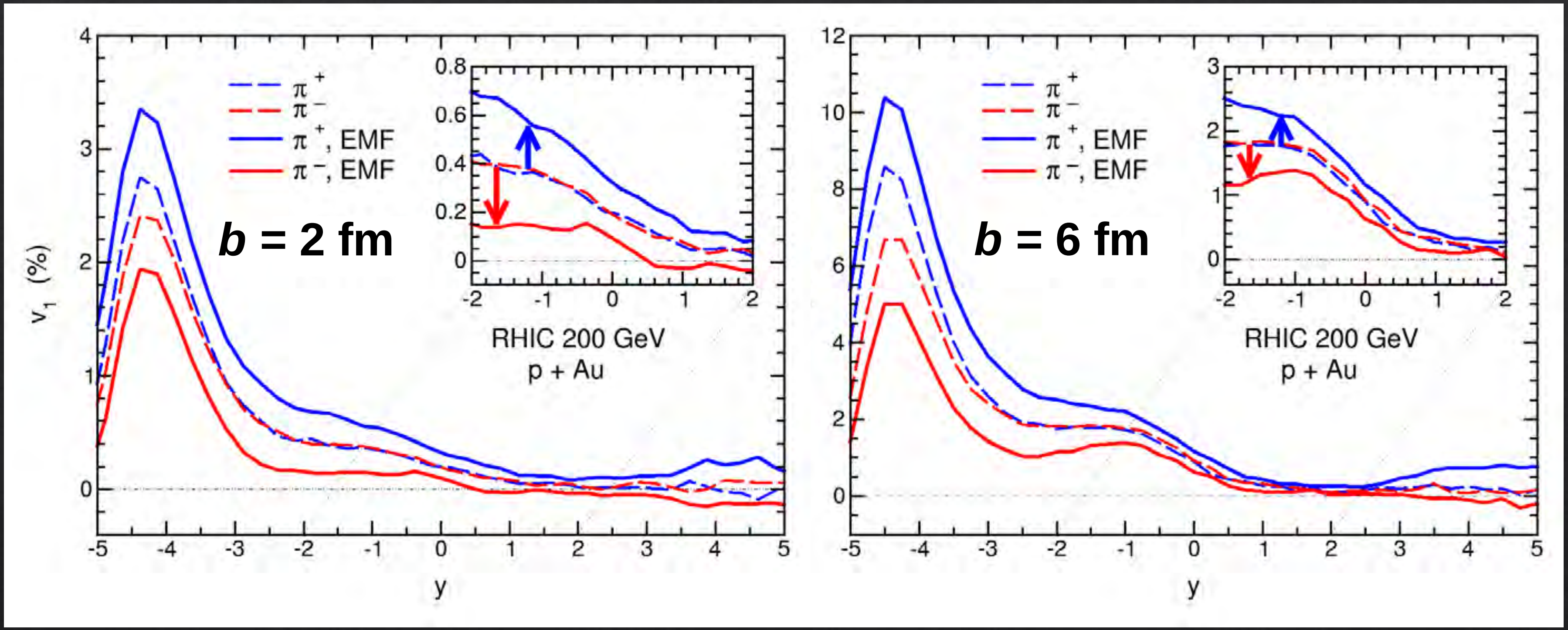

LO, Moreau, Voronyuk and Bratkovskaya, PRC 101 (2020) 014917

Splitting of π^+ and π^- induced by the electromagnetic field

p+Au: directed flow

rapidity dependence of the
DIRECTED FLOW OF PIONS

collective sidewards deflection of particles

$$v_1 = \langle \cos\varphi \rangle = \langle p_x / p_T \rangle$$

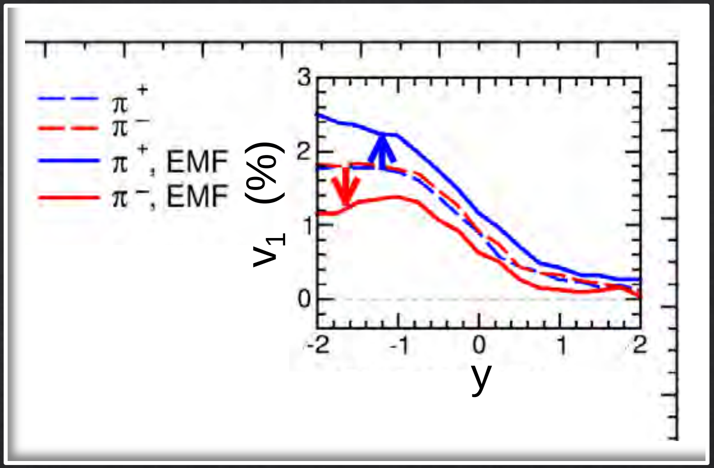

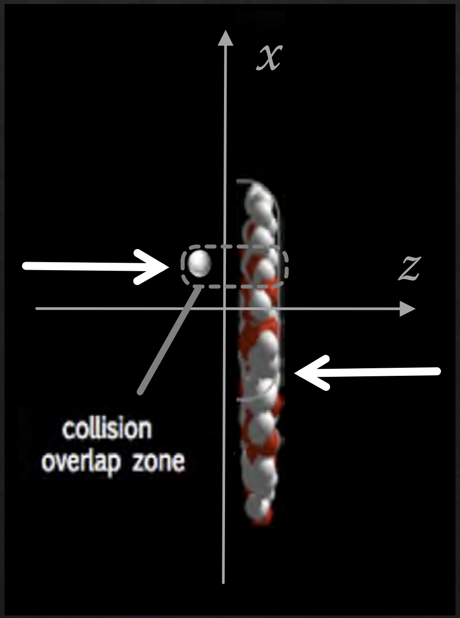

p+Au: directed flow

rapidity dependence of the
DIRECTED FLOW OF PIONS

collective sidewards deflection of particles

$$v_1 = \langle \cos\varphi \rangle = \langle p_x / p_T \rangle$$

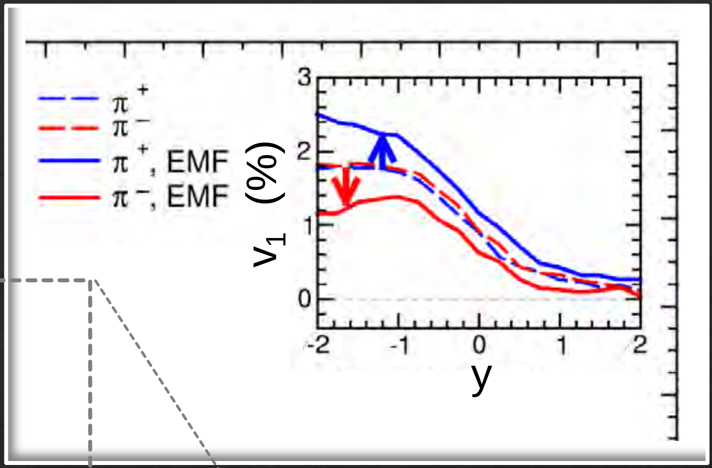

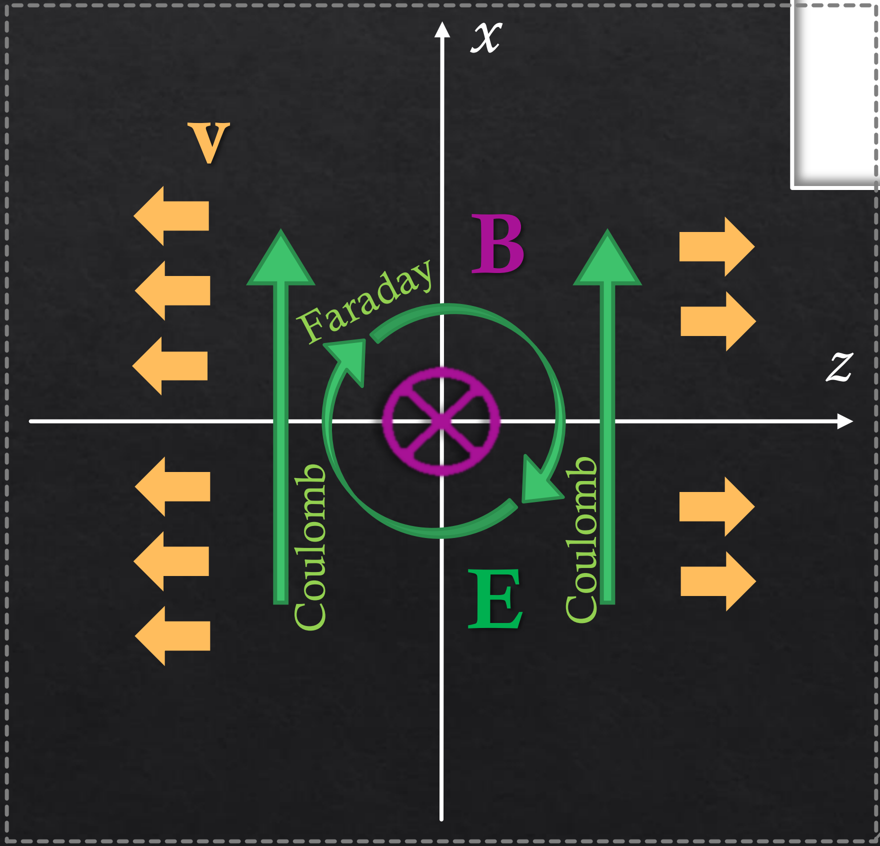

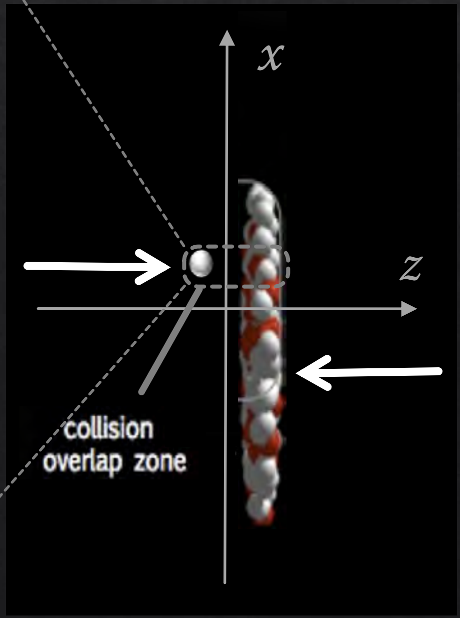

p+Au: directed flow

rapidity dependence of the
DIRECTED FLOW OF PIONS

collective sidewards deflection of particles

$$v_1 = \langle \cos\varphi \rangle = \langle p_x/p_T \rangle$$

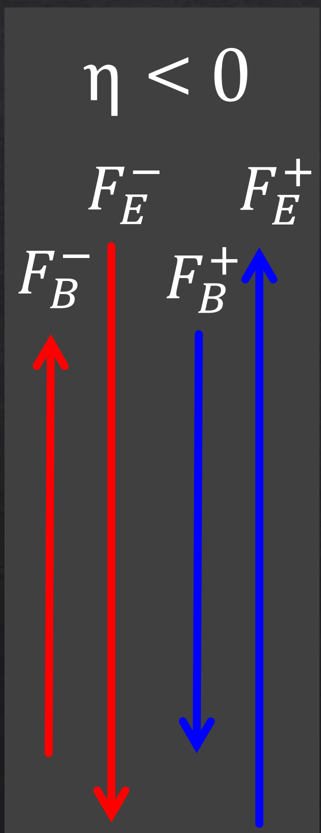

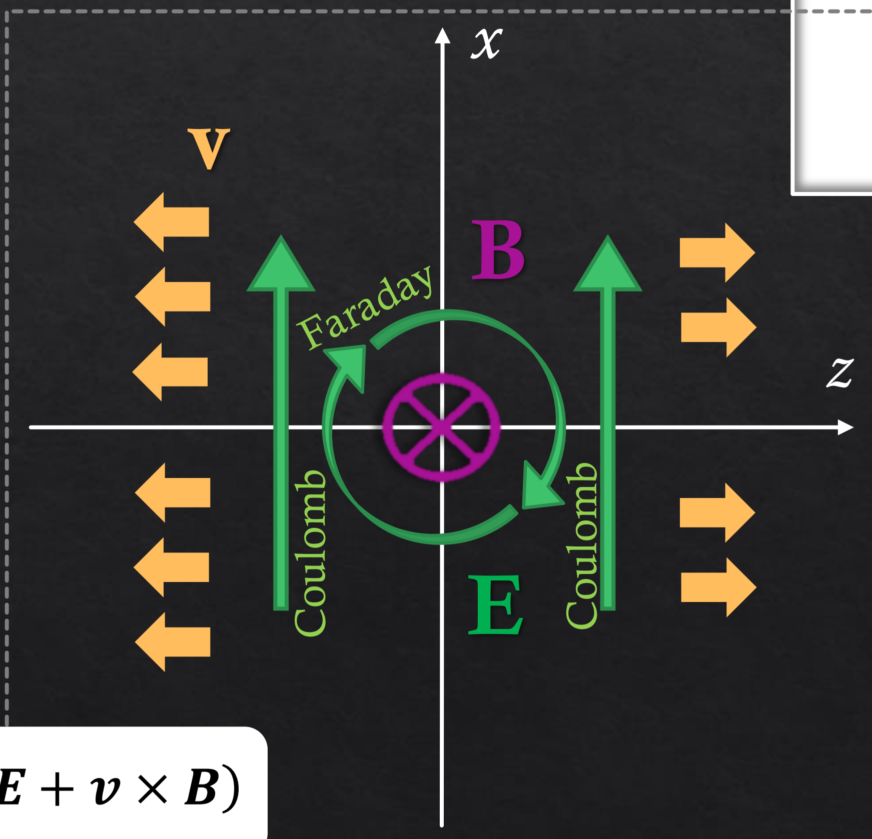

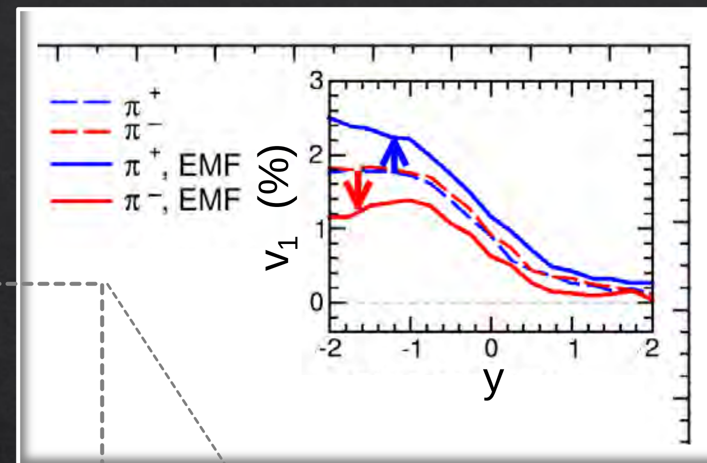

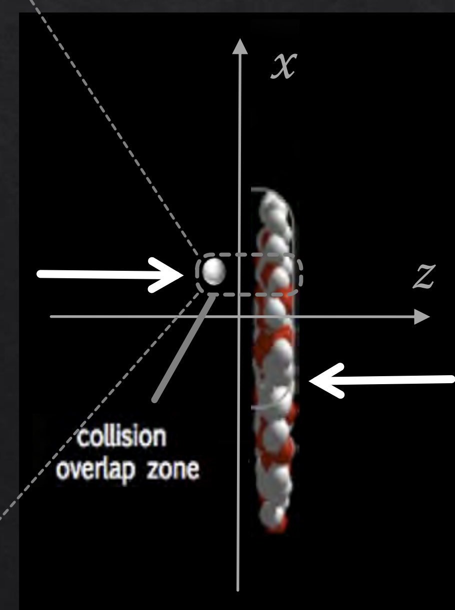

$$\boldsymbol{F}_{\boldsymbol{Lorentz}} = q(\boldsymbol{E} + \boldsymbol{v} \times \boldsymbol{B})$$

p+Au: directed flow

rapidity dependence of the DIRECTED FLOW OF PIONS

$$v_1(y) = \langle \cos[\varphi(y)] \rangle$$

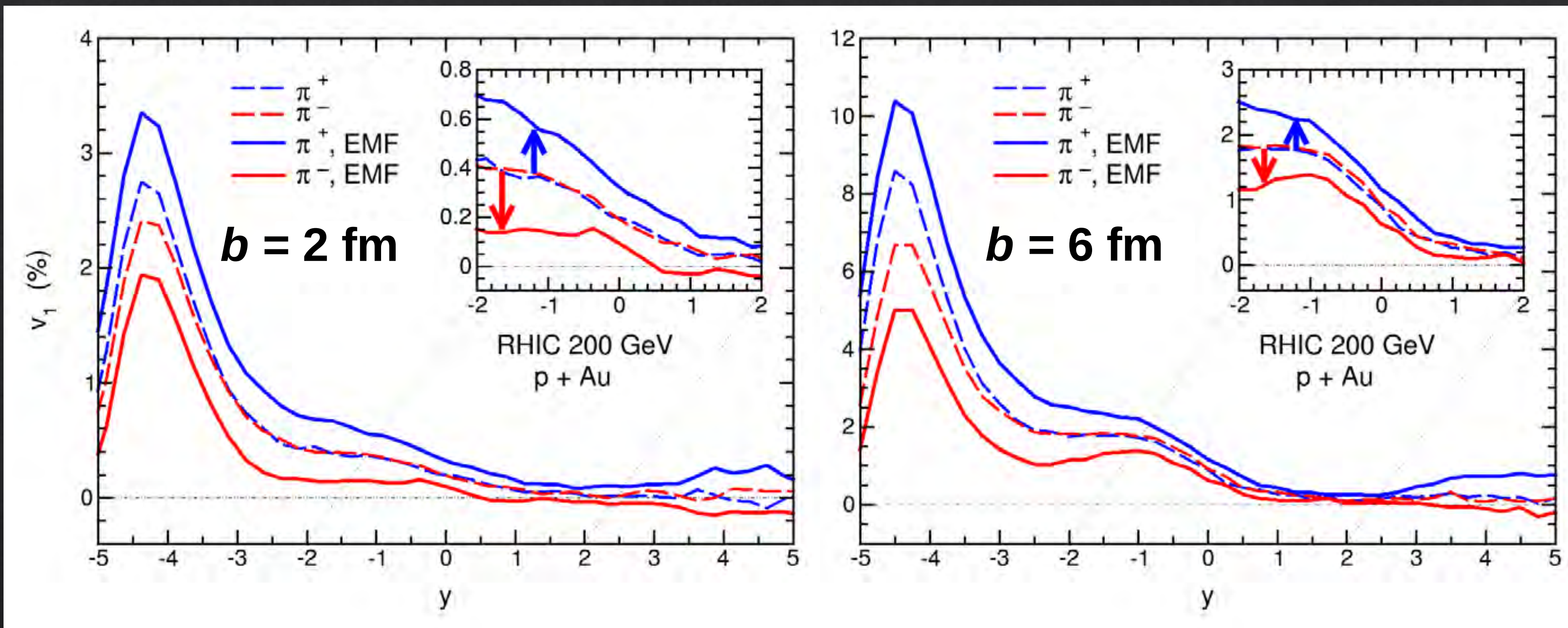

LO, Moreau, Voronyuk and Bratkovskaya

Splitting of π^+ and π^- induced by the electromagnetic field

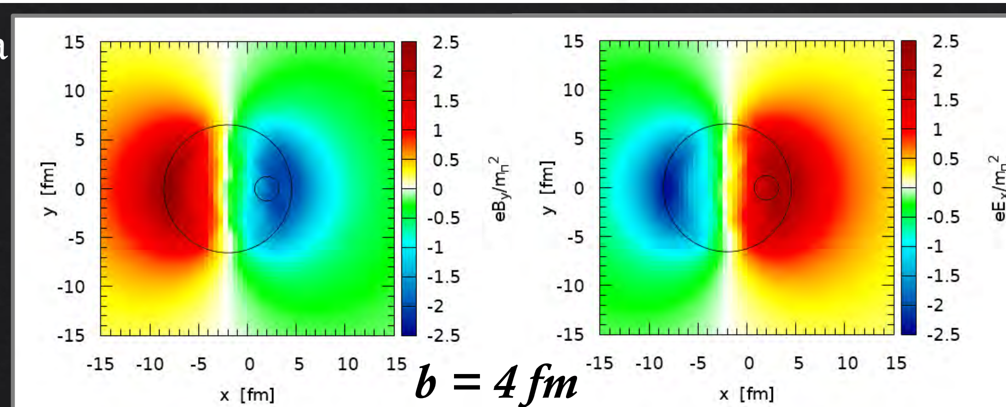

p+Au: directed flow

rapidity dependence of the
DIRECTED FLOW OF KAONS

$$v_1(y) = \langle \cos[\varphi(y)] \rangle$$

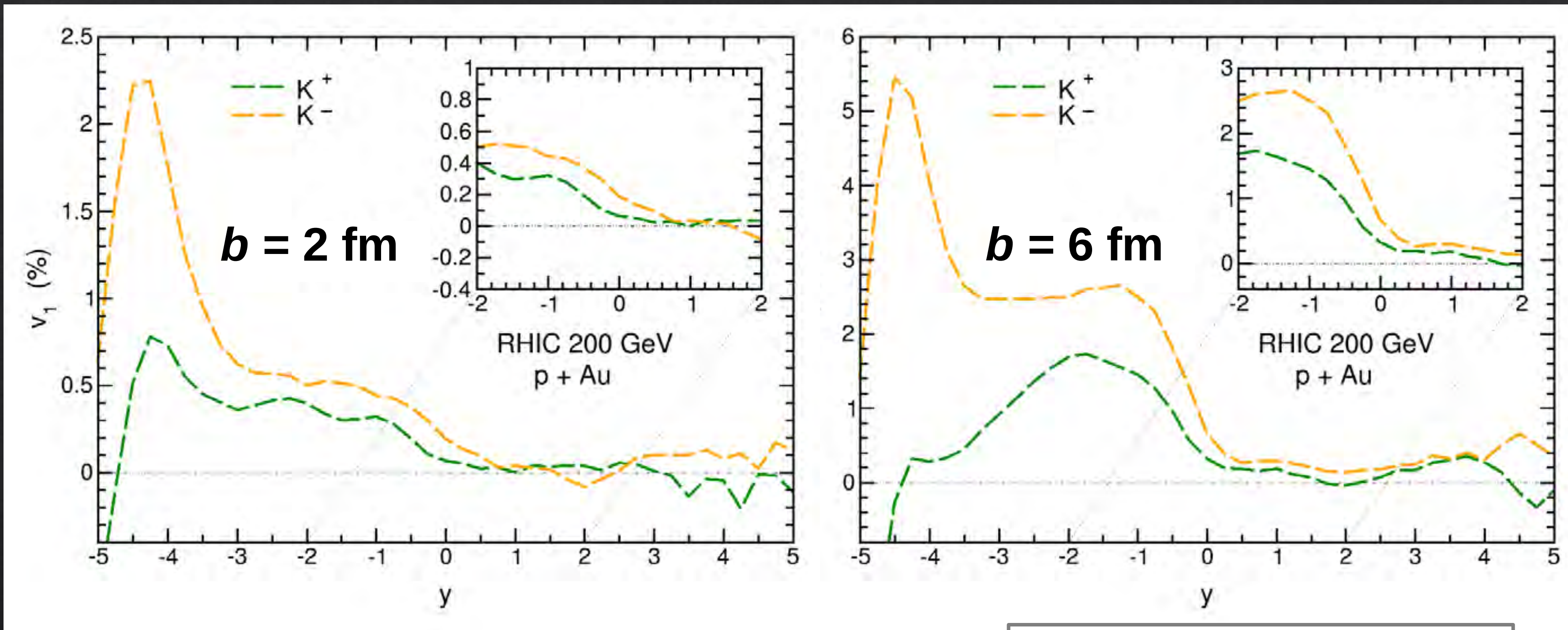

LO, Moreau, Voronyuk and Bratkovskaya, PRC 101 (2020) 0149

different v_1 also in simulations without EMF

more contributions to K^+ $(\bar{s}u)$ with respect to K^- $(s\bar{u})$
from quarks of the initial colliding nuclei

STAR Coll., PRL 120 (2018) 062301

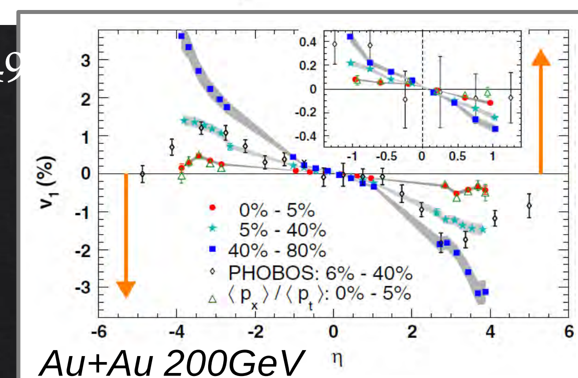

STAR Coll., PRL 101 (2008) 252301

p+Au: directed flow

rapidity dependence of the
DIRECTED FLOW OF KAONS

$$v_1(y) = \langle \cos[\varphi(y)] \rangle$$

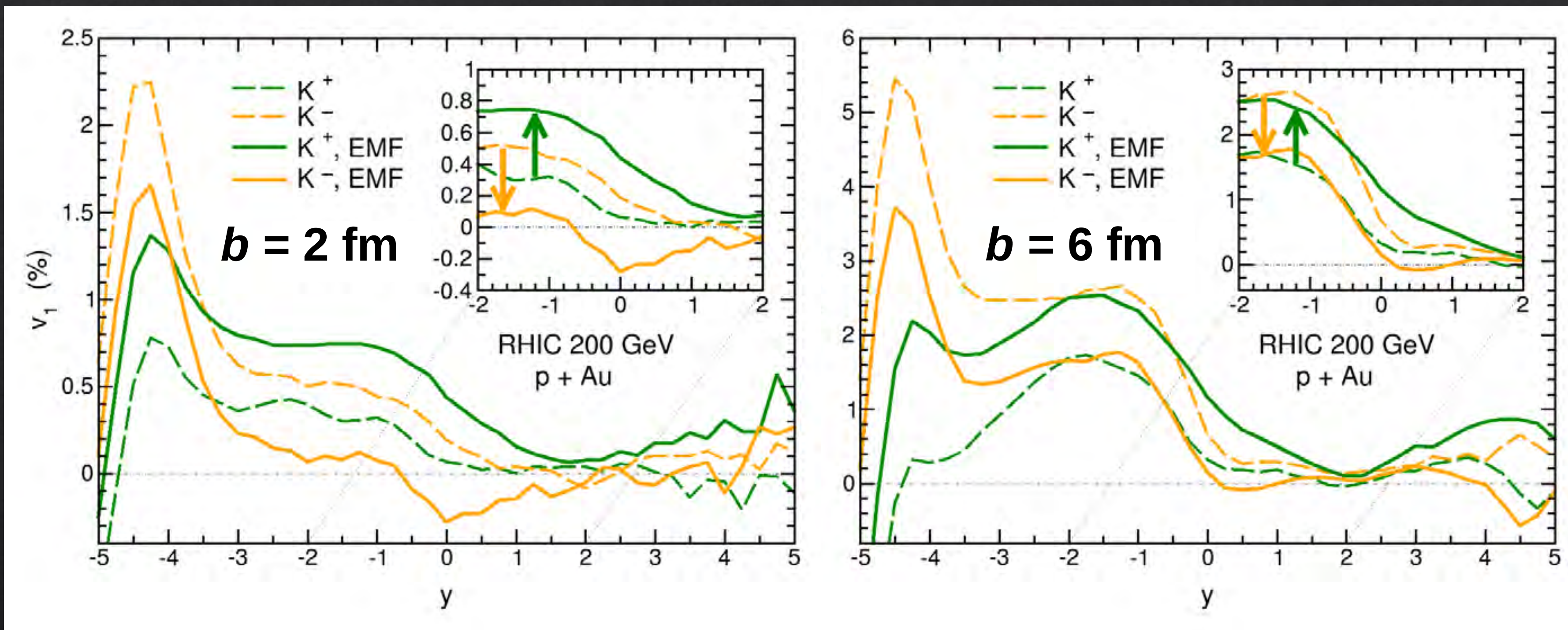

LO, Moreau, Voronyuk and Bratkovskaya, 101 (2020) 0149

Splitting of K⁺ and K⁻ induced by the electromagnetic field

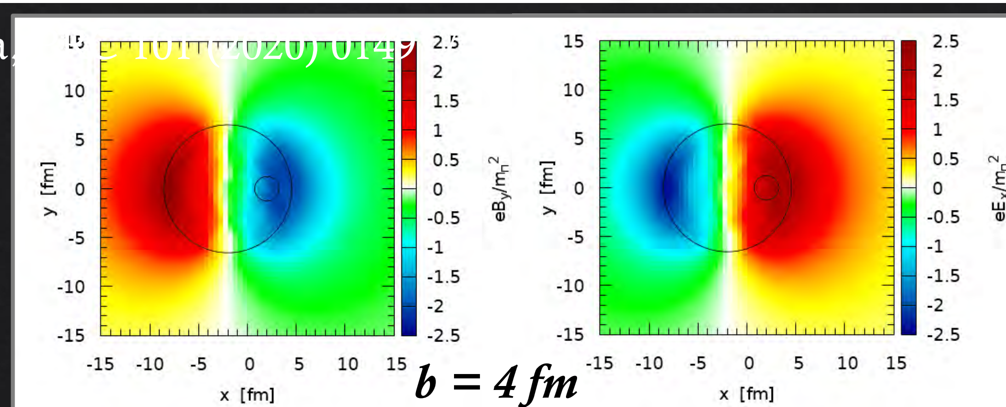

p+Au: directed flow

ELECTROMAGNETICALLY-INDUCED SPLITTING in the directed flow of hadrons with same mass and opposite charge

$$\Delta v_1{}^{emf} \equiv \Delta v_1{}^{(PHSD+EMF)} - \Delta v_1{}^{(PHSD)}$$

$$\Delta v_1 \equiv v_1^+ - v_1^-$$

LO, Moreau, Voronyuk and Bratkovskaya, PRC 101 (2020) 014917

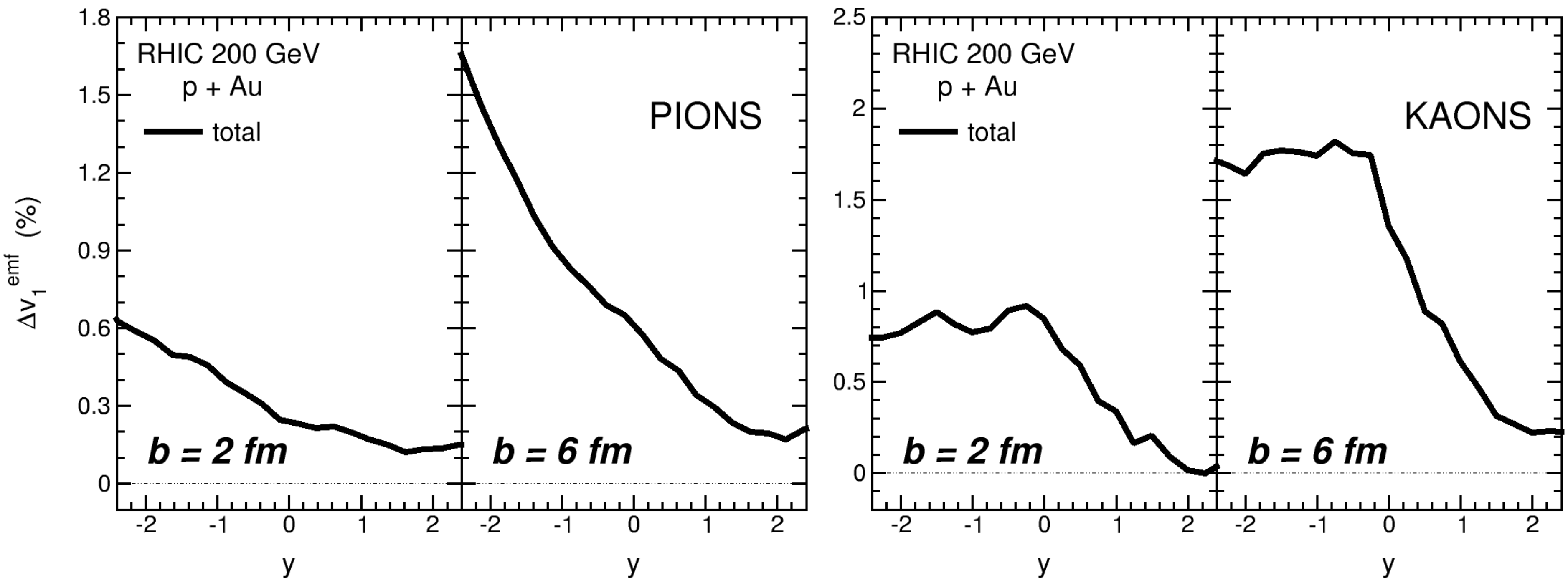

- **magnitude increasing with impact parameter**
- **larger splitting for kaons than for pions**

$$\boldsymbol{F}_{\boldsymbol{Lorentz}} = q(\boldsymbol{E} + \boldsymbol{v} \times \boldsymbol{B})$$

p+Au: directed flow

ELECTROMAGNETICALLY-INDUCED SPLITTING in the directed flow of hadrons with same mass and opposite charge

$$\Delta v_1{}^{emf} \equiv \Delta v_1{}^{(PHSD+EMF)} - \Delta v_1{}^{(PHSD)}$$

$$\Delta v_1 \equiv v_1^+ - v_1^-$$

LO, Moreau, Voronyuk and Bratkovskaya, PRC 101 (2020) 014917

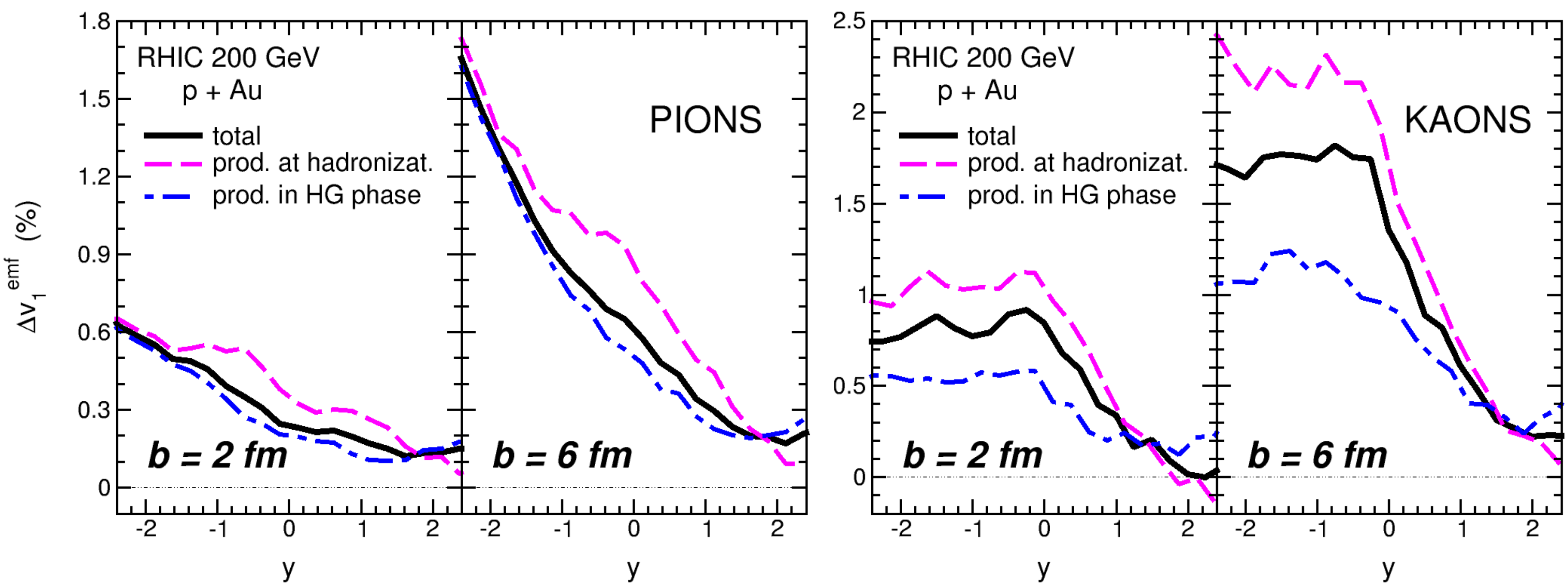

- **splitting generated at partonic level higher than that induced in the hadronic phase, especially for kaons**

CONCLUDING….

The Parton-Hadron-String-Dynamics (PHSD) approach describes the entire dynamical evolution of large and small colliding systems

PHSD includes consistently and dynamically the electromagnetic fields produced since the very early stage of the collision

Study of p+Au collisions at top RHIC energy

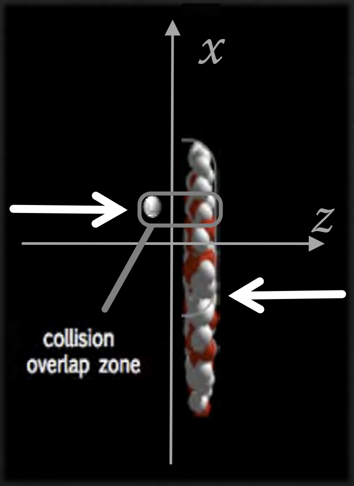

- ✓ asymmetry of charged-particle rapidity distributions increasing with centrality
- ✓ the electric field is strongly asymmetric inside the overlap region
- ✓ effect of electromagnetic fields in directed flow of mesons: splitting between positively and negatively charged particle
- ✓ electromagnetically-induced splitting generated in the deconfined phase larger than that produced in the hadronic phase

CONCLUDING….

The Parton-Hadron-String-Dynamics (PHSD) approach describes the entire dynamical evolution of large and small colliding systems

PHSD includes consistently and dynamically the electromagnetic fields produced since the very early stage of the collision

Study of p+Au collisions at top RHIC energy

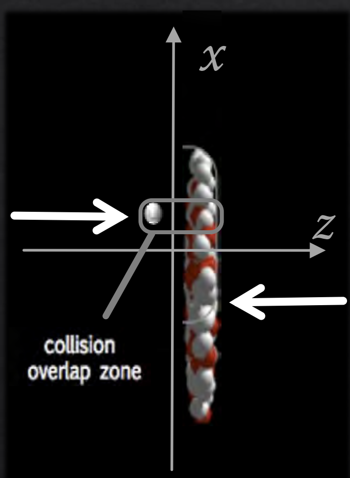

- ✓ asymmetry of charged-particle rapidity distributions increasing with centrality
- ✓ the electric field is strongly asymmetric inside the overlap region
- ✓ effect of electromagnetic fields in directed flow of mesons: splitting between positively and negatively charged particle
- ✓ electromagnetically-induced splitting generated in the deconfined phase larger than that produced in the hadronic phase

Generalized Transport Equations (GTE)

After the first order gradient expansion of the Wigner transformed Kadanoff-Baym equations and separation into the real and imaginary parts one obtain GTE which describes the dynamics of broad strongly interacting quantum states

drift term **Vlasov term** **backflow term** **collision term = ‚gain‘ - ‚loss‘ term**

$$\diamond\{P^2 - M_0^2 - Re\Sigma^{ret}_{XP}\}\{S^<_{XP}\} - \boxed{\diamond\{\Sigma^<_{XP}\}\{ReS^{ret}_{XP}\}} = \frac{i}{2}\left[\Sigma^>_{XP}\,S^<_{XP} - \Sigma^<_{XP}\,S^>_{XP}\right]$$

$$\diamond\{F_1\}\{F_2\} := \frac{1}{2}\left(\frac{\partial F_1}{\partial X_\mu}\frac{\partial F_2}{\partial P^\mu} - \frac{\partial F_1}{\partial P_\mu}\frac{\partial F_2}{\partial X^\mu}\right)$$

off-shell behavior

GTE govern the propagation of the Green functions $i\,S^<_{XP} = A_{XP}\,N_{XP}$

number of particles

particle spectral function

Dressed propagators (S_q, Δ_g)

$$S = (P^2 - \Sigma^2)^{-1}$$

with complex self-energies (Σ_q, Π_g):

$$\Sigma = m^2 - i2\gamma\omega$$

- the real part describes a dynamically generated mass (m_q, m_g)
- the imaginary part describes the interaction width (γ_q, γ_g)

Cassing and Juchem, NPA 665 (2000) 377; 672 (2000) 417; 677 (2000) 445

Dynamical QuasiParticel Model (DQPM)

The DQPM describes QGP in terms of interacting quasiparticle: massive quarks and gluons with Lorentzian spectral functions

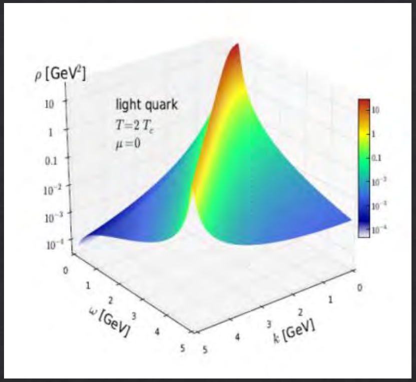

$$A_j(\omega,\mathbf{p}) = \frac{\gamma_j}{\tilde{E}_j}\left(\frac{1}{(\omega-\tilde{E}_j)^2+\gamma_j^2} - \frac{1}{(\omega+\tilde{E}_j)^2+\gamma_j^2}\right)$$

$$\tilde{E}_j = p^2 + m^2 - \gamma^{\ 2}$$

GLUONS QUARKS

MASSES

$$m_g^2 = \frac{g^2}{6}\left(N_c + \frac{1}{2}N_f\right)T^2\,, \qquad m_q^2 = g^2\frac{N_c^2-1}{8N_c}T^2$$

WIDTHS

$$\gamma_g = \frac{1}{3}N_c\frac{g^2 T}{8\pi}\ln\left(\frac{2c}{g^2}+1\right)\,, \quad \gamma_q = \frac{1}{3}\frac{N_c^2-1}{2N_c}\frac{g^2 T}{8\pi}\ln\left(\frac{2c}{g^2}+1\right)$$

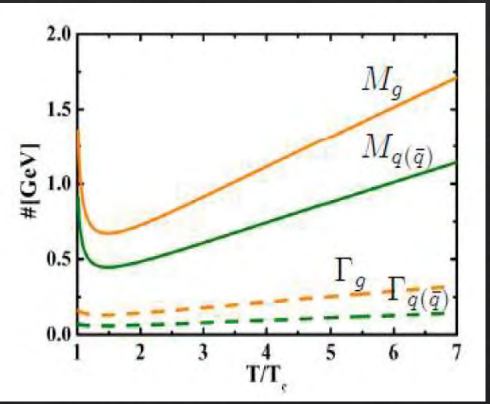

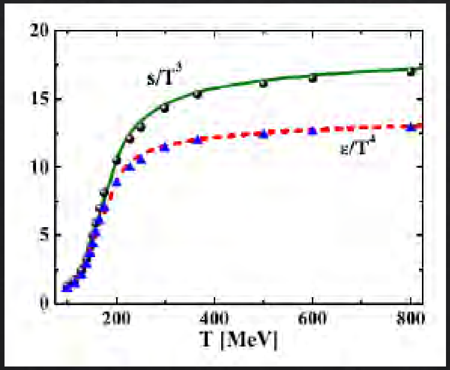

$$g^2(T/T_c) = \frac{48\pi^2}{(11N_c - 2N_f)\ln(\lambda^2(T/T_c - T_s/T_c)^2}$$

RUNNING COUPLING

parameters from fit of lattice QCD thermodinamics

Peshier, PRD 70 (2004) 034016
Peshier and Cassing, PRL 94 (2005) 172301
Cassing, NPA 791 (2007) 365; NPA 793 (2007)

PHSD extended to include chemical potential dependence of scattering cross sections
Moreau, Soloveva, LO, Song, Cassing and Bratkovskaya, PRC 100 (2019) 014911

retarded electromagnetic fields

$$\mathbf{B} = \nabla \times \mathbf{A}, \qquad \mathbf{E} = -\nabla\Phi - \frac{\partial \mathbf{A}}{\partial t}$$

General solution of the wave equation for the electromagnetic potentials

$$\mathbf{A}(\mathbf{r},t) = \frac{1}{4\pi}\int \frac{\mathbf{j}(\mathbf{r}',t')\ \delta(t-t'-|\mathbf{r}-\mathbf{r}'|/c)}{|\mathbf{r}-\mathbf{r}'|}\ d^3r'\,dt'$$

$$\Phi(\mathbf{r},t) = \frac{1}{4\pi}\int \frac{\rho(\mathbf{r}',t')\ \delta(t-t'-|\mathbf{r}-\mathbf{r}'|/c)}{|\mathbf{r}-\mathbf{r}'|}\ d^3r'\,dt'$$

$$\mathbf{r}' \equiv \mathbf{r}(t')$$

$$t' = t - \frac{\mathbf{r}-\mathbf{r}'}{c}$$

Liénard-Wiechert potentials for a moving point-like charge

$$\Phi(\mathbf{r},t) = \frac{e}{4\pi}\left[\frac{1}{R(1-\mathbf{n}\cdot\boldsymbol{\beta})}\right]_{\mathrm{ret}} \qquad \mathbf{A}(\mathbf{r},t) = \frac{e}{4\pi}\left[\frac{\boldsymbol{\beta}}{R(1-\mathbf{n}\cdot\boldsymbol{\beta})}\right]_{\mathrm{ret}}$$

ret: evaluated at the times t'

$$\mathbf{R} = \mathbf{r} - \mathbf{r}'$$

$$\mathbf{n} = \frac{\mathbf{R}}{R}$$

$$\boldsymbol{\beta} = \frac{\mathbf{v}}{c}$$

retarded electromagnetic fields

Retarded electric and magnetic fields for a moving point-like charge

$$\mathbf{E}(\mathbf{r},t) = \frac{e}{4\pi}\left[\frac{\mathbf{n}-\boldsymbol{\beta}}{(1-\mathbf{n}\cdot\boldsymbol{\beta})^3\gamma^2R^2} + \frac{\mathbf{n}\times\left((\mathbf{n}-\boldsymbol{\beta})\times\dot{\boldsymbol{\beta}}\right)}{(1-\mathbf{n}\cdot\boldsymbol{\beta})^3 cR}\right]_{\mathrm{ret}} \qquad \mathbf{B}(\mathbf{r},t) = [\mathbf{n}\times\mathbf{E}(\mathbf{r},t)]_{\mathrm{ret}}$$

elastic Coulomb scatterings

inelastic bremsstrahlung processes

$$\mathbf{R} = \mathbf{r} - \mathbf{r}' \qquad \mathbf{n} = \frac{\mathbf{R}}{R} \qquad \boldsymbol{\beta} = \frac{\mathbf{v}}{c}$$

Neglecting the acceleration

$$e\mathbf{E}(t,\mathbf{r}) = \alpha_{em}\frac{1-\beta^2}{\left[(\mathbf{R}\cdot\boldsymbol{\beta})^2 + R^2(1-\beta^2)\right]^{3/2}}\mathbf{R}$$

$$e\mathbf{B}(t,\mathbf{r}) = \alpha_{em}\frac{1-\beta^2}{\left[(\mathbf{R}\cdot\boldsymbol{\beta})^2 + R^2(1-\beta^2)\right]^{3/2}}\boldsymbol{\beta}\times\mathbf{R}$$

magnetic field created by a single freely moving charge

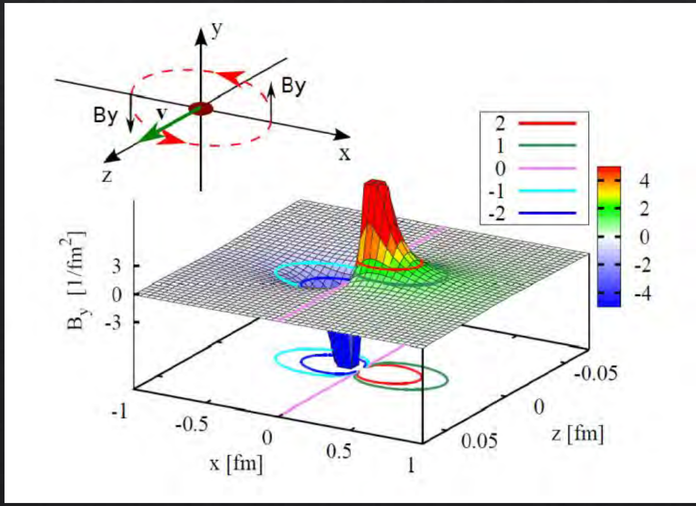

Voronyuk *et al*. (HSD), PRC 83 (2011) 054911

Electromagnetic fields in asymmetric systems

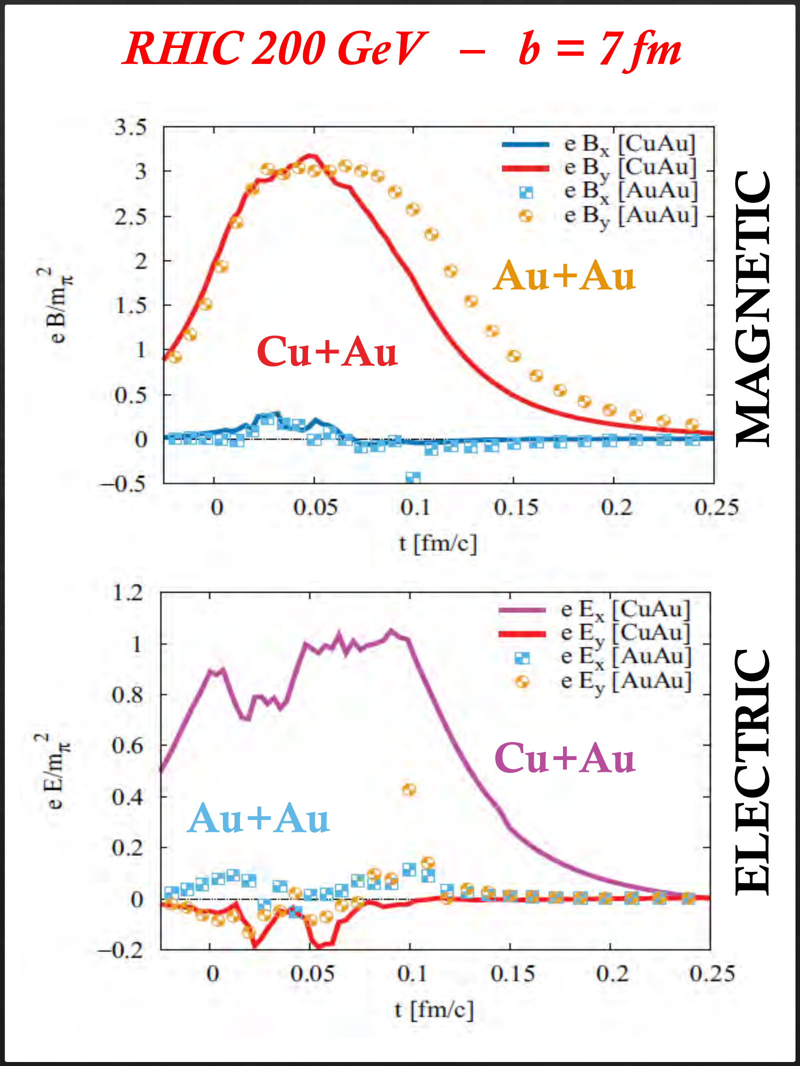

Voronyuk *et al.* (PHSD), PRC 90 (2014) 064903
Toneev *et al.* (PHSD), PRC 95 (2017) 034911

✓ SYMMETRIC SYSTEMS (e.g. Au+Au)
transverse momentum increments due to electric and magnetic fields compensate each other

✓ ASYMMETRIC SYSTEMS (e.g. Cu+Au)
an intense electric fields directed from the heavy nuclei to light one appears in the overlap region

SMALL SYSTEMS (e.g. p+Au)?

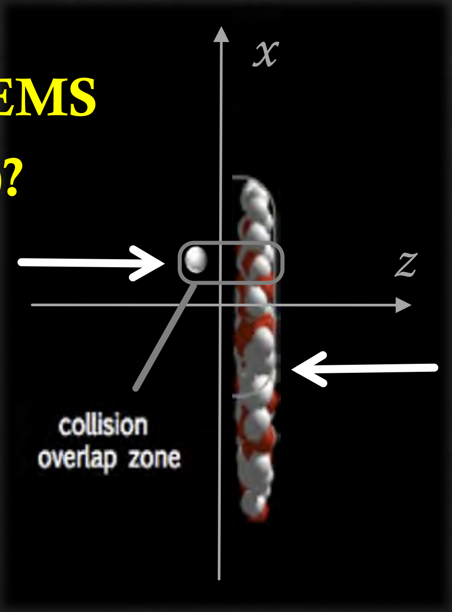

p+Au: electromagnetic fields

p+Au @ RHIC 200 GeV b=4 fm

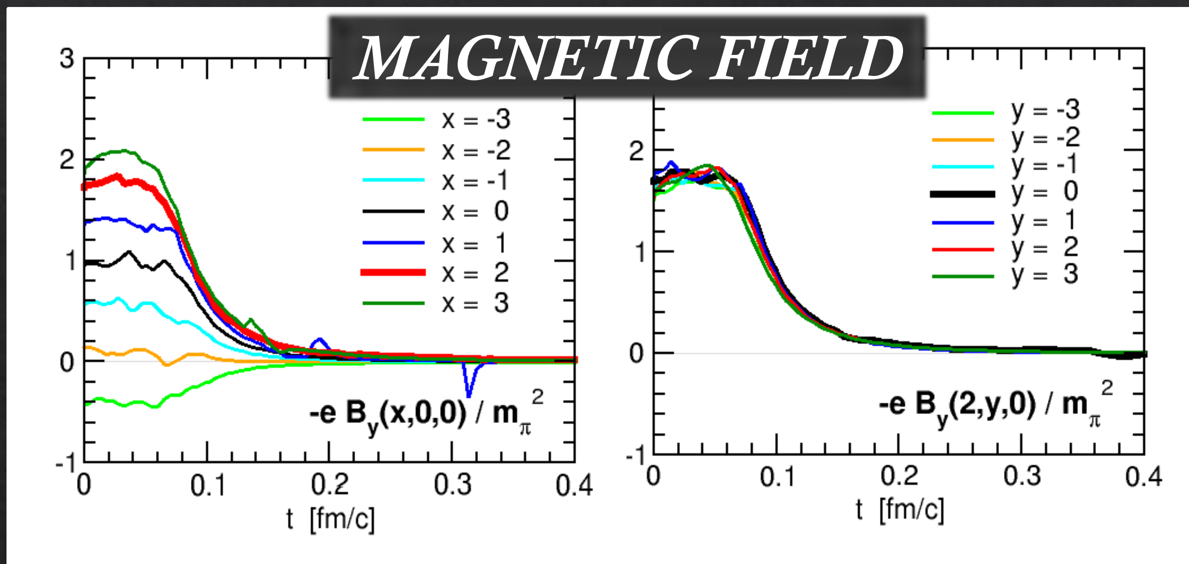

B_y

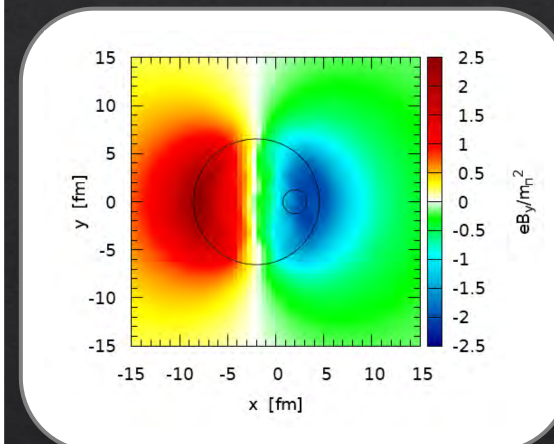

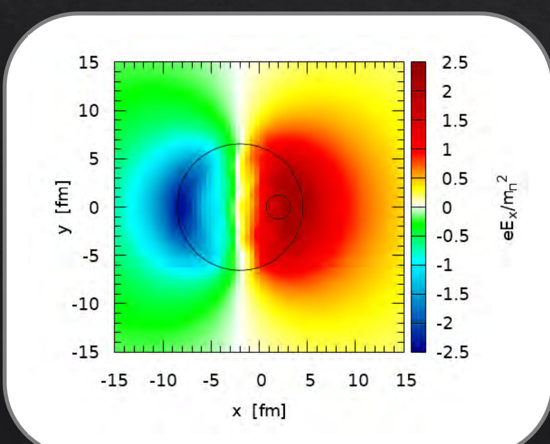

E_x

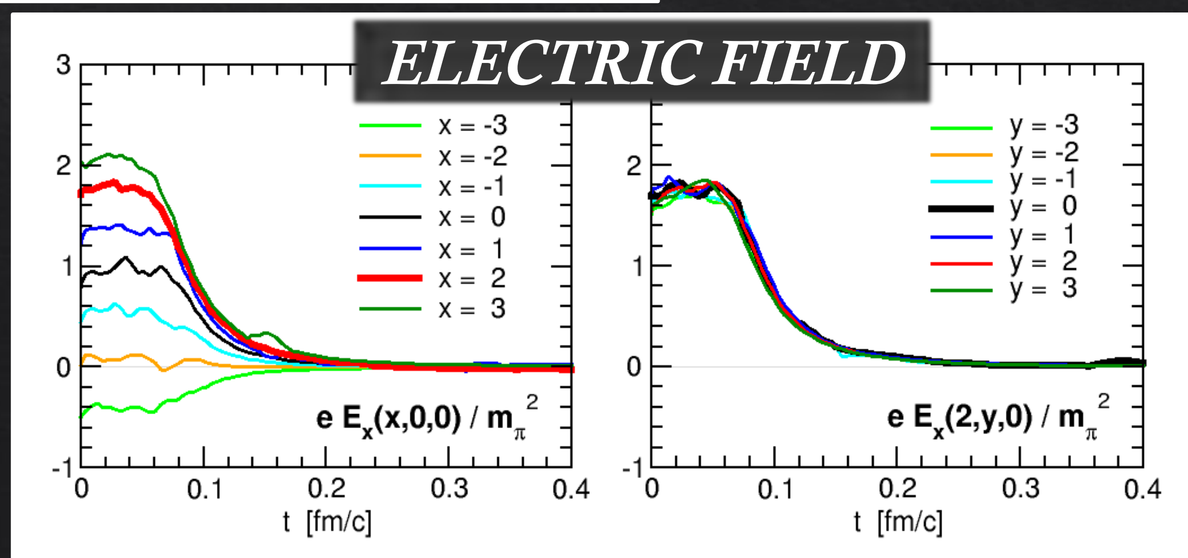

Centrality determination : A+A vs p+A

LO, Moreau, Voronyuk and Bratkovskaya, 1909.06770

Miller *et al.*, ARNPS 57 (2007) 205

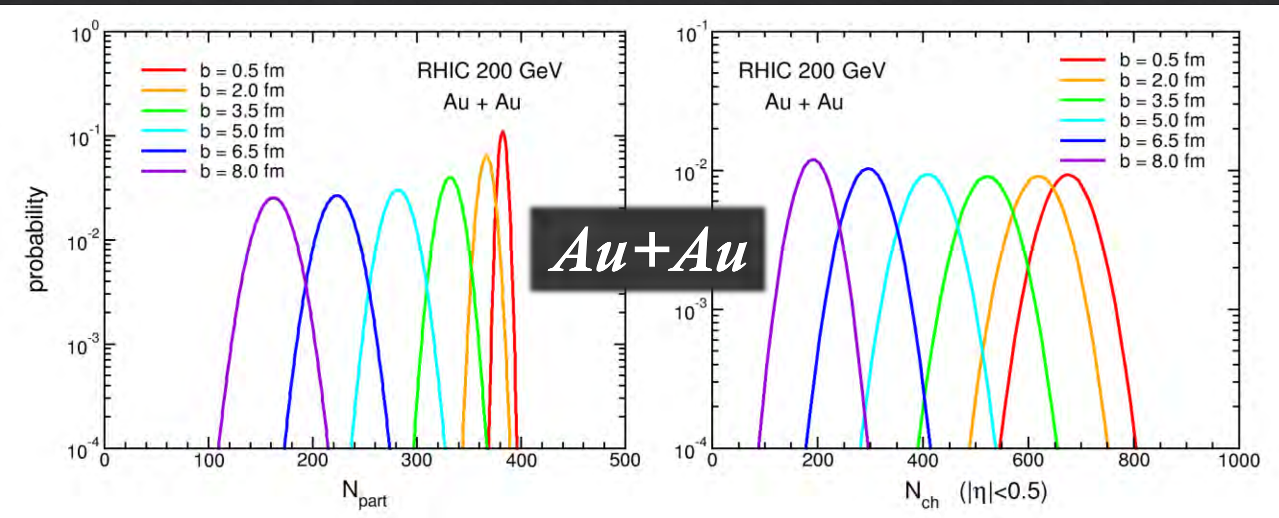

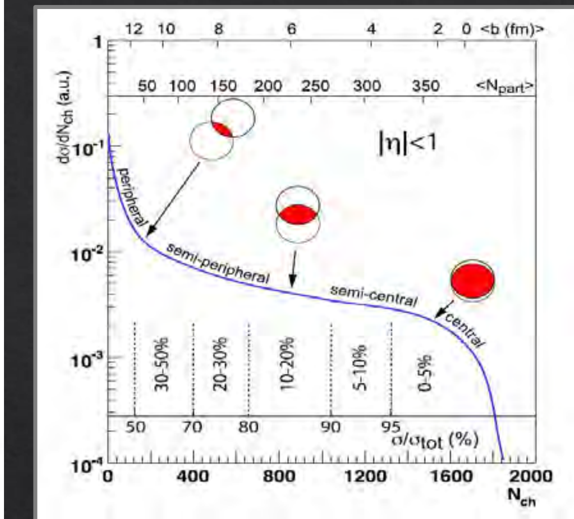

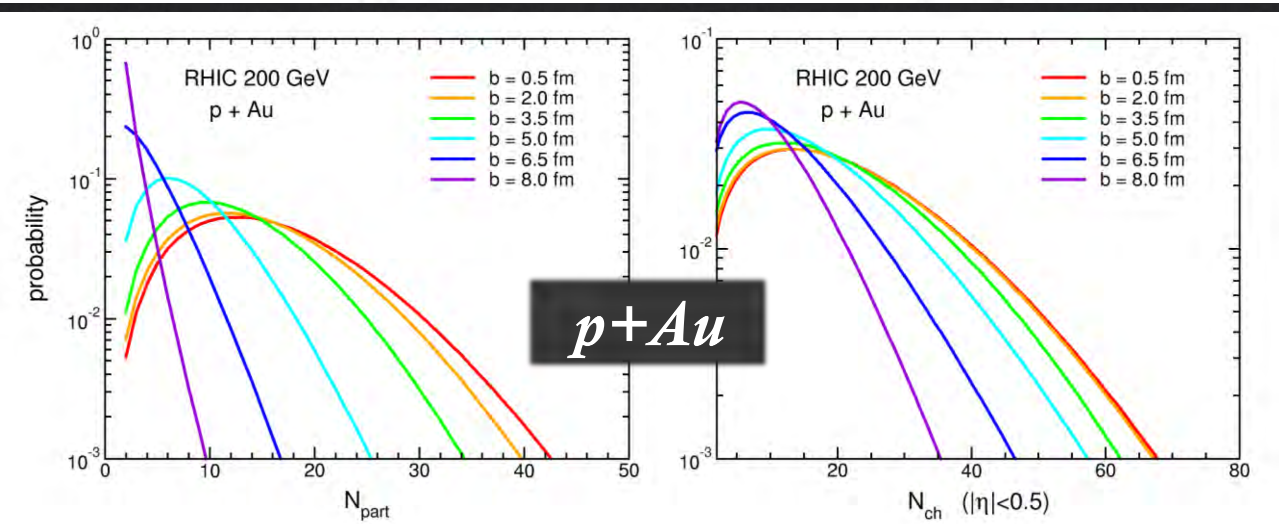

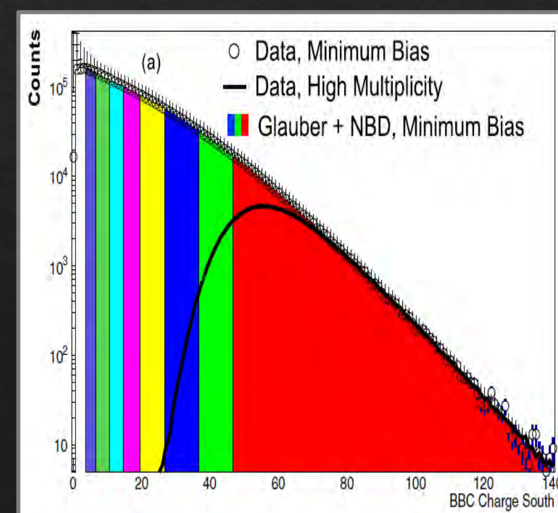

PHENIX, PRC 95 (2017) 034910

In p+A multiplicity fluctuation in the final state mixes events from different impact parameters!

p+Au: rapidity distributions

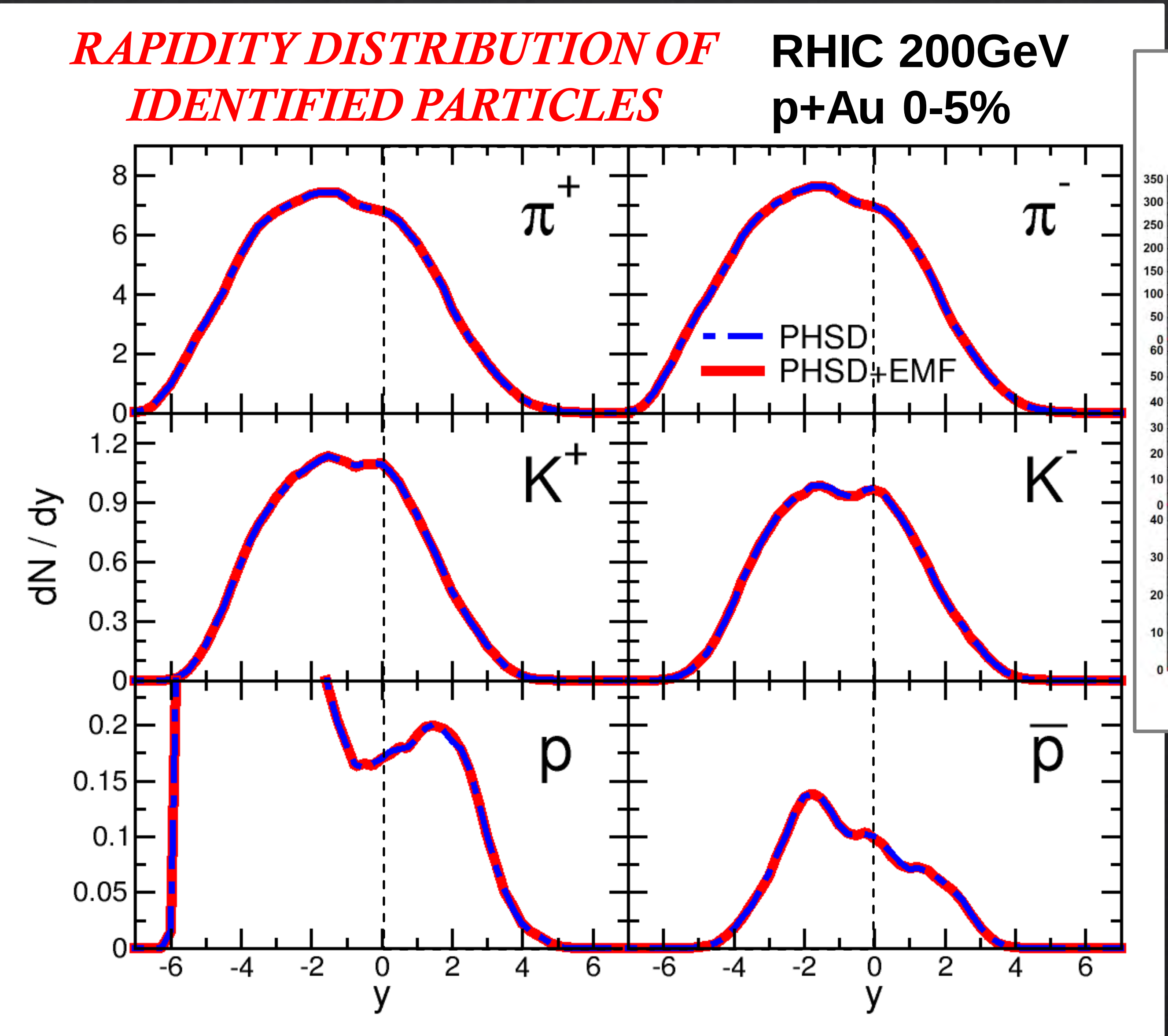

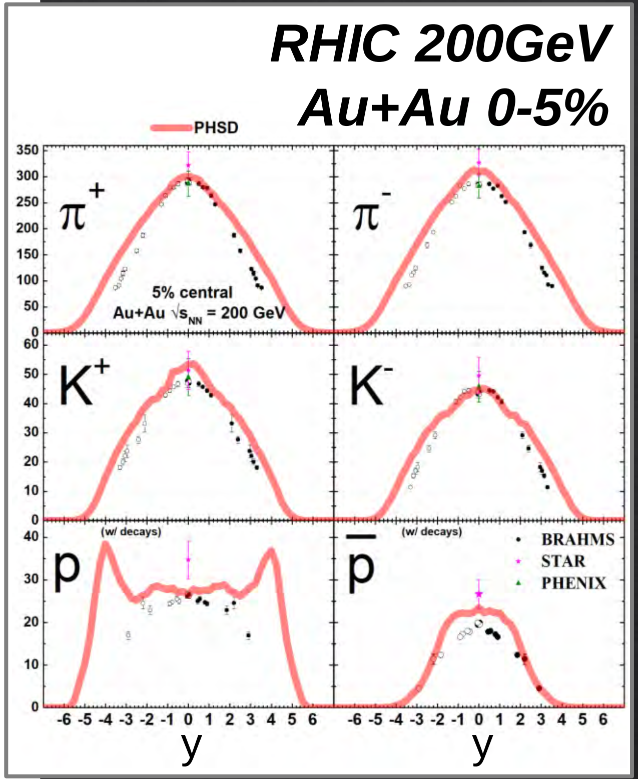

symmetric
colliding system

LO, Moreau, Voronyuk and Bratkovskaya, 1909.06770

Anisotropic radial flow

A DEEPER INSIGHT… INITIAL-STATE FLUCTUATIONS AND FINITE EVENT MULTIPLICITY

azimuthal particle distributions
w.r.t. the reaction plane

$$\frac{dN}{d\varphi} \propto 1 + \sum_n 2 v_n(p_T) \cos[n(\varphi - \Psi_n)]$$

n-th order
flow harmonics

$$v_n = \frac{\langle \cos[n(\varphi - \Psi_n)] \rangle}{Res(\Psi_n)}$$

event-plane angle resolution
(three-subevent method)

Important especially for small colliding system, e.g. p+A

n-th order
event-plane angle

$$\Psi_n = \frac{1}{n} \mathrm{atan2}(Q_n^y, Q_n^x)$$

$$Q_n^x = \sum_i \cos[n\varphi_i]$$

$$Q_n^y = \sum_i \sin[n\varphi_i]$$

Since the finite number of particles produces limited resolution in the determination of Ψ_n, the v_n must be corrected up to what they would be relative to the real reaction plane

Poskanzer and Voloshin, PRC 58 (1998) 1671

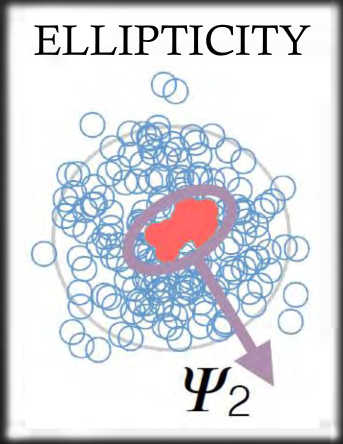

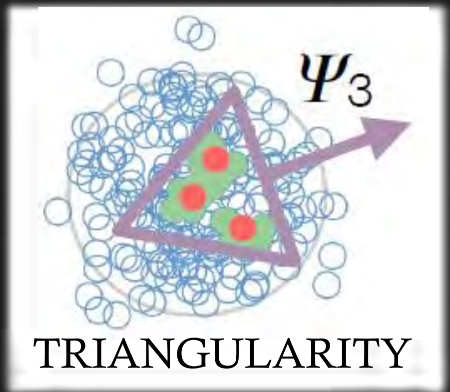

p+Au: elliptic flow

ELLIPTIC FLOW OF CHARGED PARTICLES

$$v_2(p_T) = \frac{\langle \cos[2(\varphi(p_T) - \Psi_2)] \rangle}{Res(\Psi_2)}$$

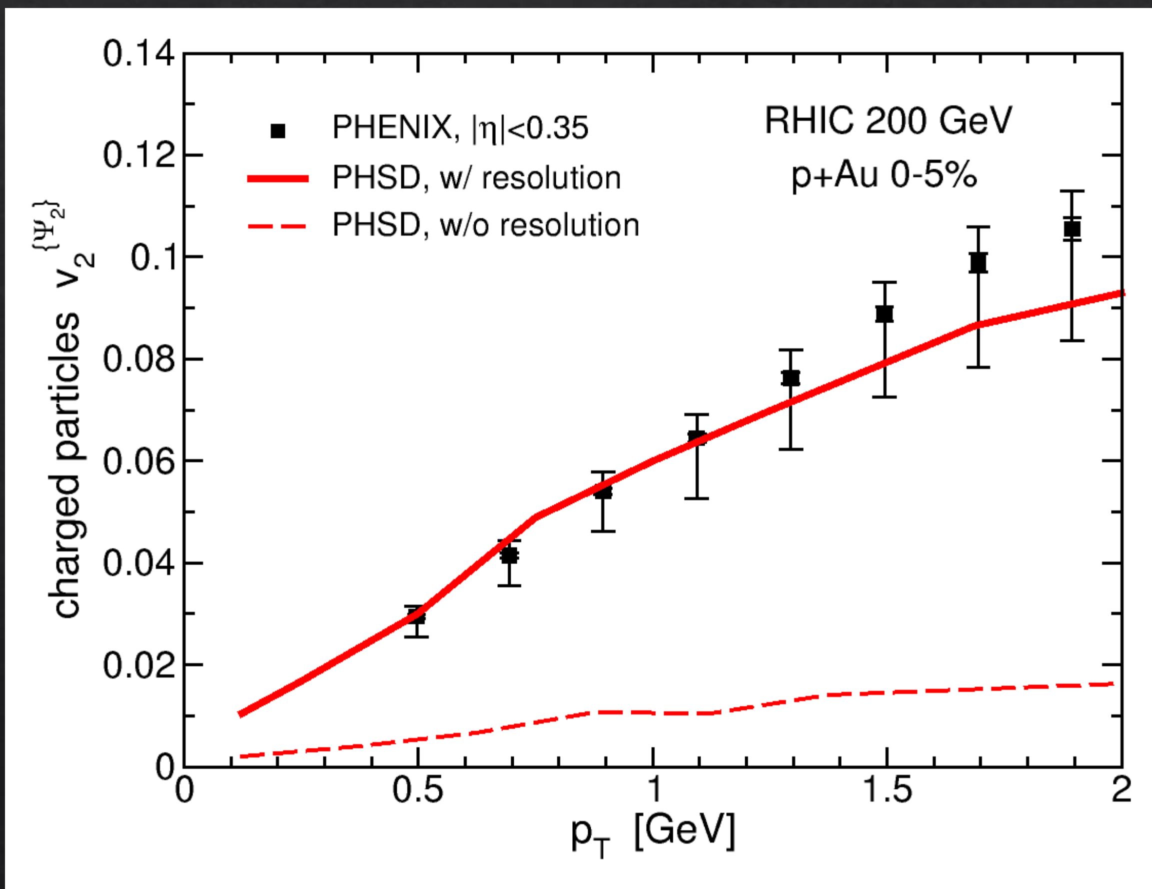

LO, Moreau, Voronyuk and Bratkovskaya, PRC 101 (2020) 014917

Exp. data: Aidala et al. (PHENIX Collaboration), PRC 95 (2017) 034910

- magnitude correlated with the determination of the reaction plane
- comparable to that found in large colliding systems

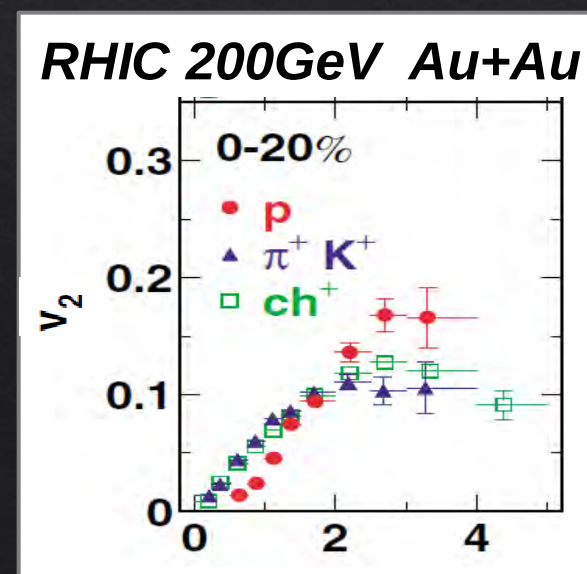

PHENIX, PRL 91 (2003) 182301

p+Au: directed flow

pseudorapidity dependence of the
DIRECTED FLOW OF CHARGED PARTICLES

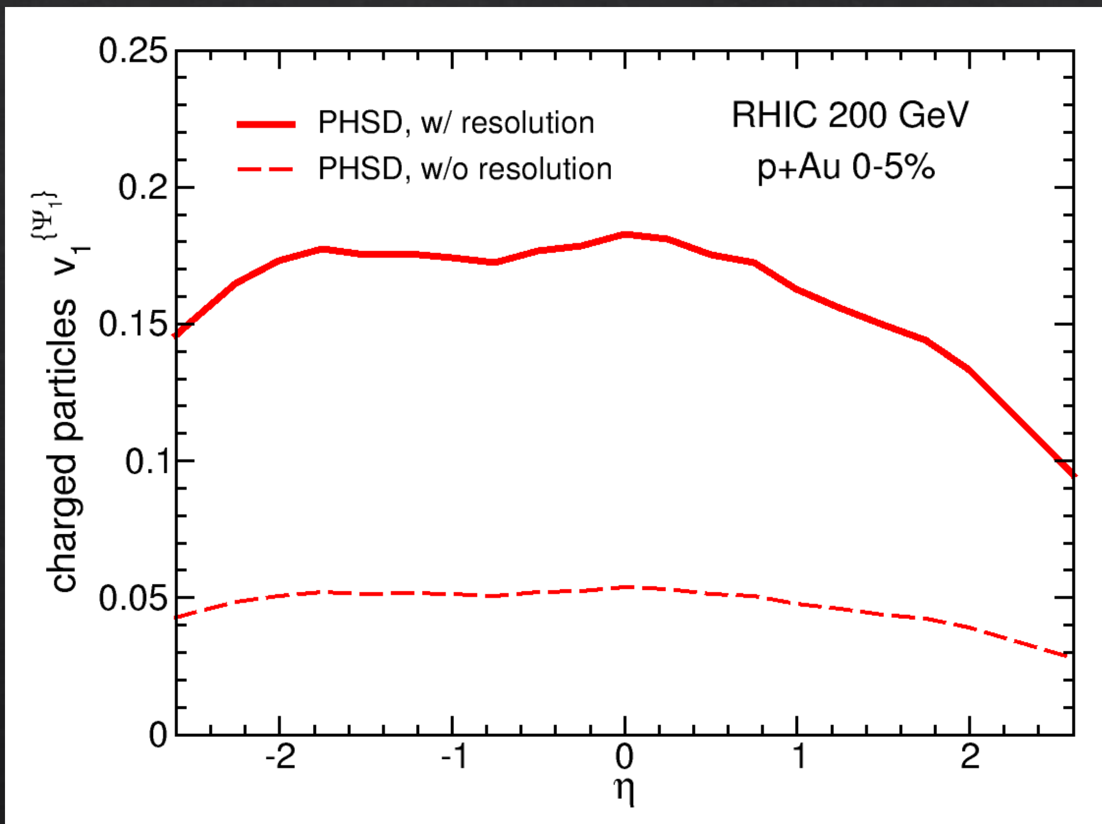

LO, Moreau, Voronyuk and Bratkovskaya, 1909.06770

$$v_1(\eta) = \frac{\langle \cos[\varphi(\eta) - \Psi_1] \rangle}{Res(\Psi_1)}$$

Event-plane angle in $-4 < \eta < -3$: $Res(\Psi_1^{PHSD}) = 0.397$

magnitude correlated with the determination of the reaction plane

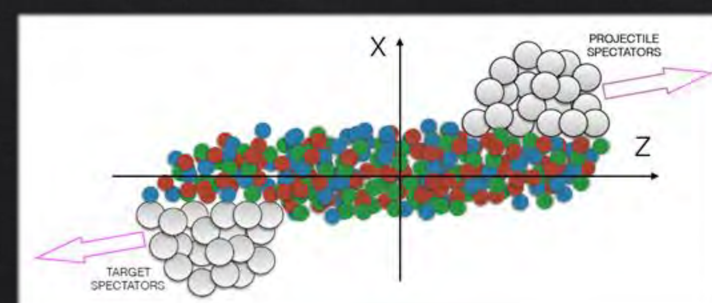

Voloshin and Niida, PRC 94 (2016) 021901

p+Au: directed flow

STAR Collaboration, PRL 101 (2008) 252301

pseudorapidity dependence of the
DIRECTED FLOW OF CHARGED PART

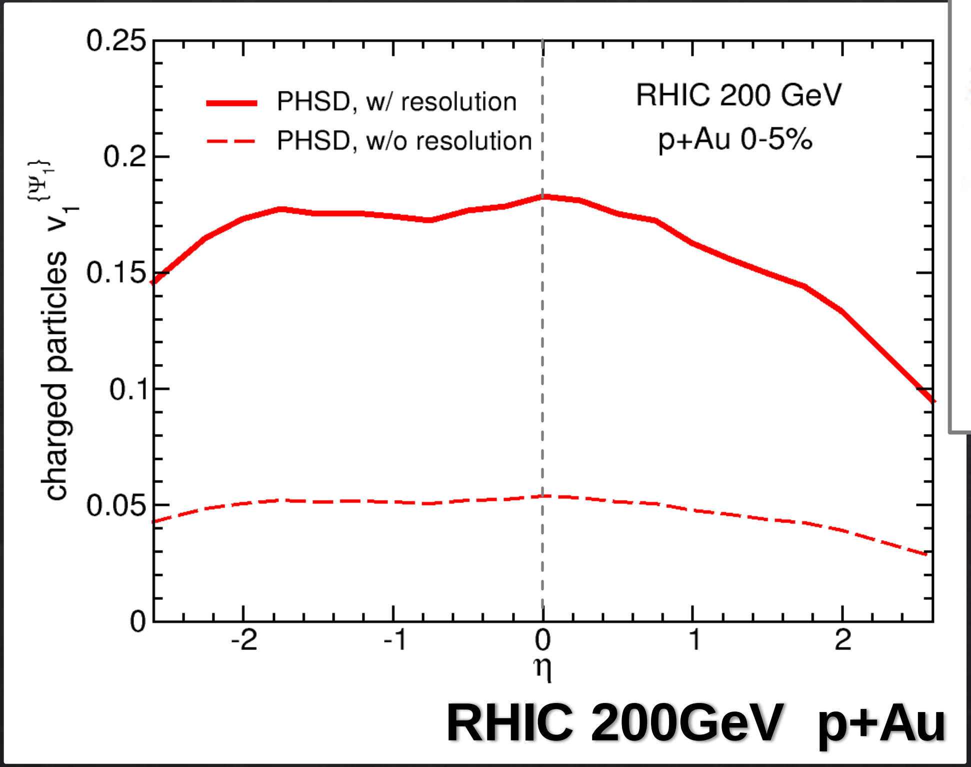

LO, Moreau, Voronyuk and Bratkovskaya, 1909.06770

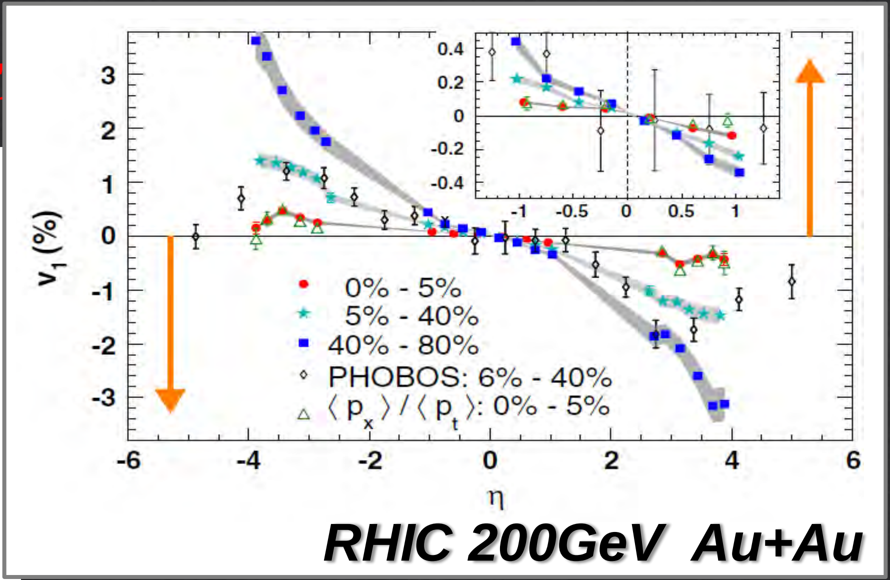

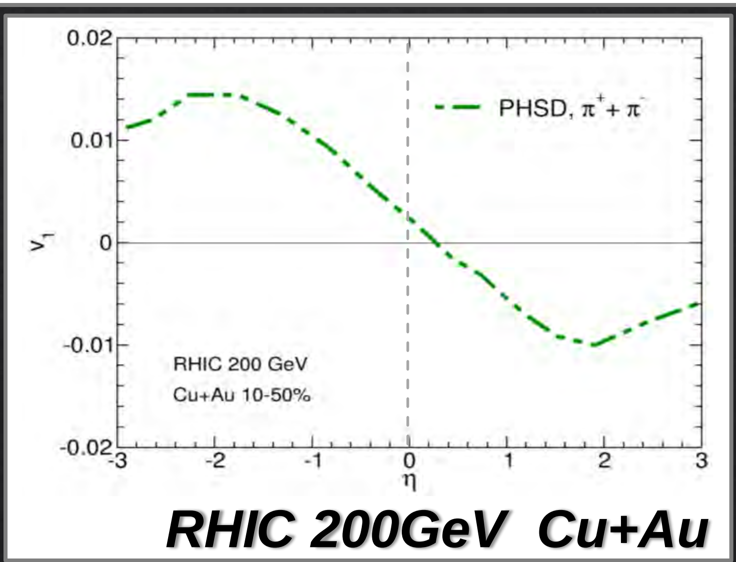

Voronyuk *et al.*, PRC 90 (2014) 064903
Toneev *et al.*, PRC 95 (2017) 034911

Quark charm process scattering in Quark-Gluon Plasma medium : extension to off-shell dynamics

Maria Lucia Sambataro

University of Catania
INFN - Laboratori Nazionali del Sud
sambataro@lns.infn.it

GGI School 'Frontiers in Nuclear and Hadronic Physics 2020'
Feb.24-Mar.06 2020

Outline

- Hard probes in Quark-Gluon Plasma
- Quasi-particle model(QPM) and Dynamical quasi-particle model(DQPM)
- Transport coefficients for quark charm $\rightarrow$ on-shell vs off-shell mode
- Momentum evolution of quark charm: Fokker-Planck approach, Boltzmann approach and off-shell extension.
- Conclusions

Heavy quarks in QGP medium

$M_C \sim 1.3\ GeV/c^2$ e $M_B \sim 4.2\ GeV/c^2$

Plasma physics $M_{HQ} >> T_{QGP}$

- negligible thermal production
- $\tau_C \gtrsim \tau_{QGP}$, $\tau_B > \tau_{QGP}$

with $\tau_{QGP} \approx 5 - 10 fm/c$

Particle physics $M_{HQ} >> \Lambda_{QCD}$

- pQCD initial production

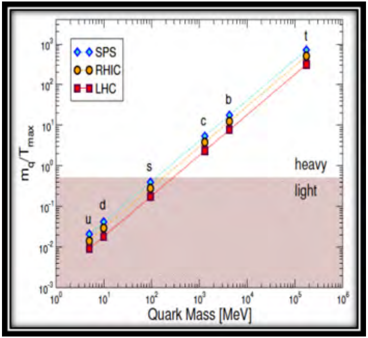

Nonperturbative effects in HQ scattering:
QPM vs. DQPM

Quasi Particle Model (QPM)

The interaction is encoded in the quasi-particle masses:

$$m_g^2 = \frac{1}{6} g(T)^2 \left[\left(N_c + \frac{1}{2} N_f \right) T^2 + \frac{N_c}{2\pi^2} \sum_q \mu_q^2 \right],$$

$$m_{u,d,s}^2 = \frac{N_c^2 - 1}{8 N_c} g(T)^2 \left[T^2 + \frac{\mu_{u,d}^2}{\pi^2} \right]$$

Coupling constant $g(T)$ fitted to the energy density of lQCD:

$$g^2(T) = \frac{48\pi^2}{[(11N_c - 2N_f) ln[\lambda(\frac{T}{T_c} - \frac{T_s}{T_c})]]^2}$$

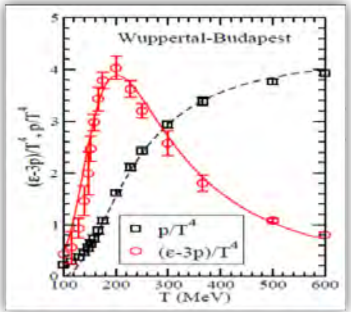

Salvatore Plumari et. al. Phys. Rev. D84, 094004 (2011).

Nonperturbative effects in HQ scattering:
QPM vs. DQPM

Dynamical Quasi Particle Model (DQPM)

Partons are dressed by non perturbative spectral function $A(q^0)$.
In N.R. approximation:

$$A_i^{BW}(m_i) = \frac{2}{\pi} \frac{m_i^2 \gamma_i^*}{(m_i^2 - M_i^2)^2 + (m_i \gamma_i^*)^2}$$

with

$$\int_0^\infty dm_i A_i(m_i, T) = 1.$$

Fitting lQCD thermodynamics:

$$\gamma_g(T) = \frac{1}{3} N_C \frac{g^2(T/T_C)T}{8\pi} ln\left[\frac{2c}{g^2(T/T_C)} + 1\right]$$

$$\gamma_q(T) = \frac{1}{3} \frac{N_C^2 - 1}{2N_C} \frac{g^2(T/T_C)T}{8\pi} ln\left[\frac{2c}{g^2(T/T_C)} + 1\right]$$

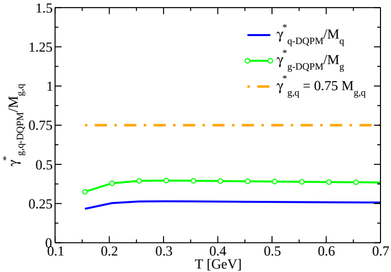

i.e T=200 MeV
DQPM widths
$\gamma_g^* \approx 260$ MeV, $\gamma_q^* \approx 110$ MeV

Artif.widths ($\gamma^*/M = 0.75$)
$\gamma_g^* \approx 520$ MeV, $\gamma_q^* \approx 330$ MeV,
$2 - 3$ times larger than DQPM widths.

H.Berrehrah et al., Phys. Rev. C89, 054901 (2014).

Transport coefficients: Drag and Diffusion coefficients

Soft scattering approx.
Fokker Planck approach:

$$\frac{df_c}{dt} = \gamma\frac{\partial(pf_c)}{\partial p} + D\frac{\partial^2 f_c}{\partial p^2}.$$

$$\langle p\rangle = p_0 e^{-\gamma t}$$

$$\langle \Delta p^2\rangle = \frac{3D}{\gamma(1-e^{-2\gamma t})}$$

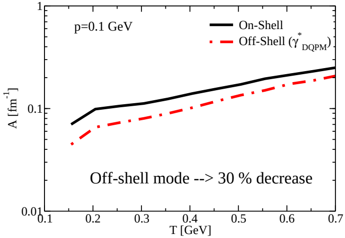

Drag and diffusion coefficients:

$$\gamma = \int d^3k|M_{g(q)+C\to g(q)+C}(k,p)|^2 p$$

$$D = \frac{1}{2}\int d^3k|M_{g(q)+C\to g(q)+C}(k,p)|^2 p^2$$

$D = TE\gamma \rightarrow$ Fluctuation dissipation theorem

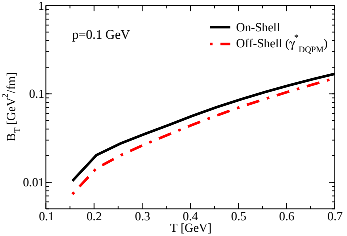

$\gamma \rightarrow A(p)$ and $D \rightarrow B_{i,j}(p)$

$$B_{i,j}(\mathbf{p},T) = B_L(p,T)P^{||}_{i,j}(\mathbf{p}) + B_T(p,T)P^{\perp}_{i,j}(\mathbf{p})$$

Transport coefficients: Drag and Diffusion coefficients

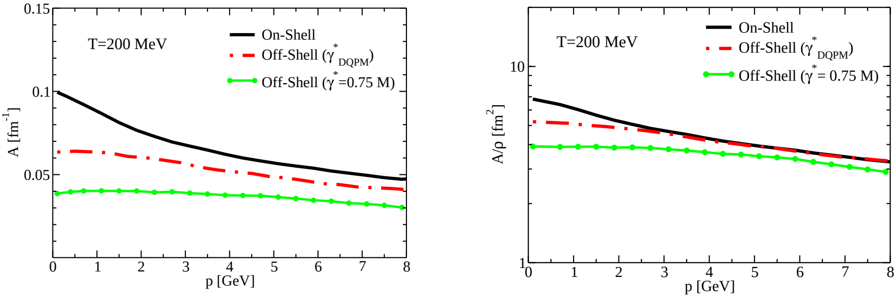

High momentum p region:
DQPM widths $\rightarrow \sim 30\%$ decrease
Larger widths $(\gamma^*/M = 0.75) \rightarrow \sim 40\%$ decrease

- Transport coefficient scales with density of the system ρ
- Larger breaking of the scaling for larger widths, especially for low p region $(p \lesssim 2 - 3 GeV)$.

Charm dynamics in QGP: Energy loss

Boltzmann vs.Langevin vs.Off-shell extension DQPM widths

Boltzmann equation and off-shell extension

$p^\mu \partial_\mu f_Q = C[f_Q, f_{g,q}]$

Plasma uniform $\rightarrow$ $p^0 \partial_0 f_Q = C[f_Q, f_{g,q}]$

$\frac{\partial f_Q}{\partial t} = \frac{1}{E_Q} C[f_q, f_g, f_Q]$

$f(t + \Delta t, p) = f(t, p) + \frac{1}{E_Q} C[f]$

$C[f_q, f_g, f_Q]$ Collision integral calculated both in on-shell and off-shell mode

Langevin equation

Soft scattering approx.

$dx_i = \frac{p_i}{E} dt$

$dp_i = -A p_i dt + C_{i,j} \rho_j \sqrt{dt}$

A drag force, $C_{i,j}$ stochastic force

Fluc.Diss.Theorem (FDT) $\rightarrow$ $D = TEA$

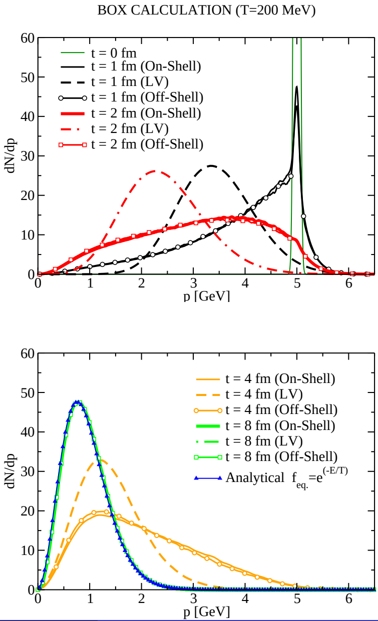

Charm dynamics in QGP: Energy loss

Boltzmann vs.Langevin vs.Off-shell extension $\gamma^*/M = 0.75$

Boltzmann equation and off-shell extension

$p^\mu \partial_\mu f_Q = C[f_Q, f_{g,q}]$

Plasma uniform $\rightarrow$ $p^0 \partial_0 f_Q = C[f_Q, f_{g,q}]$

$\frac{\partial f_Q}{\partial t} = \frac{1}{E_Q} C[f_q, f_g, f_Q]$

$f(t+\Delta t, p) = f(t,p) + \frac{1}{E_Q} C[f]$

$C[f_q, f_g, f_Q]$ Collision integral calc. both in on-shell and off-shell mode

Langevin equation

Soft scattering approx.

$dx_i = \frac{p_i}{E} dt$

$dp_i = -Ap_i dt + C_{i,j} \rho_j \sqrt{dt}$

A drag force, $C_{i,j}$ stochastic force

Fluc.Diss.Theorem (FDT) $\rightarrow$ $D = TEA$

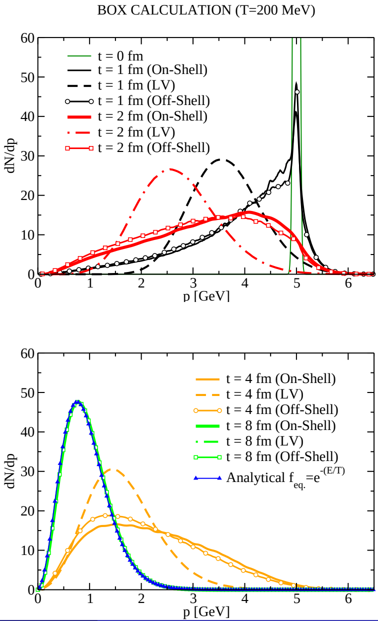

Charm dynamics in QGP: Energy loss

Boltzmann vs. Off-shell extension $\boxed{\gamma^*/M = 0.75}$ $\rightarrow$ Drag scaled with ρ !

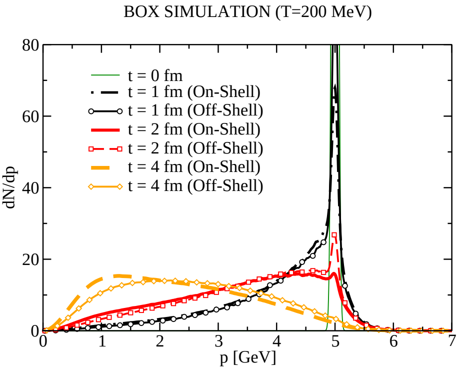

- Off-shell effects sizeable especially at low p region
- Off-shell evolution $\sim$ On-shell evolution

The difference between on-shell and off-shell mode can be adsorbed by multiplying scattering matrix for a k factor!

Conclusions

- The off-shell effect can be sizeable at low momentum of quark charm ($\sim$ 15%).
- The decrease of transport coefficients in the high momentum region can be seen mostly as a mere effects of the equilibrium bulk density ρ.
- Breaking of scaling for $\gamma^* = 0.75M$, but momentum evolution does not show significant difference with respect to on-shell one.
- Boltzmann approach seems to be a better approximation than Langevin equation for momentum evolution of quark charm at fixed T.

Thank you for your attention!

FDT validity

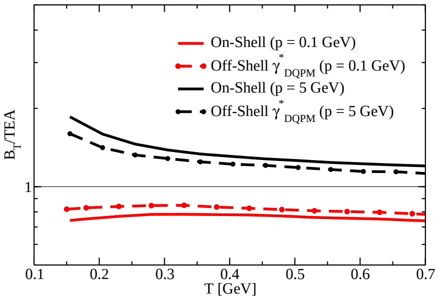

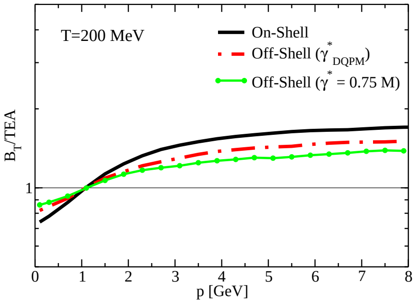

- (DQPM widths) $\rightarrow$ Improvement for FDT validity of about 10%.
- (Larger widths) $\rightarrow$ Improvement for FDT validity of about 17%

for different values of momentum p and T of the system.

QGP observable: Nuclear modification factor

$R_{A,A}$

It expresses the effective energy loss of high p_T partons experimentally visible in A-A collision with respect to production in p-p collisions

$$R_{AA} = \frac{f_C(p, t_f)}{f_C(p, t_0)}$$

No interaction means $R_{AA} = 1$.

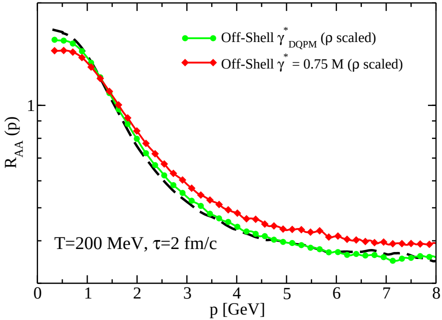

- Off-shell dynamics (γ^*_{DQPM}) $\sim$ On-shell dynamics in high p region, sizeable difference $\sim$ 10% in low p region.
- Off-shell dynamics ($\gamma^* = 0.75M$) $\rightarrow$ difference of about 15% respect to on-shell evolution.

As for momentum evolution, the difference between on-shell and off-shell mode can be adsorbed by multiplying scattering matrix for a k factor!

IFT - UNESP
INSTITUTO DE FÍSICA TEÓRICA

SPRACE

Femtoscopy of the D meson and nucleon interaction

Isabela Maietto*, Gastao Krein, Sandra Padula

Institute of Theoretical Physics - IFT - UNESP

Outline

- Motivation
- Femtoscopy and Correlations
- $\bar{D}N$ observables
- Results
- Summary

Motivation

- Femtoscopy: correlation function of two particles as a function of relative momentum
  - Obtain the source size
  - Sensitive to the effects of the final-state interaction
    - Coulomb interaction
    - Strong Interaction
    - Isospin

Motivation

- Femtoscopy: correlation function of two particles as a function of relative momentum
  - Obtain the source size
  - Sensitive to the effects of the final-state interaction
    - Coulomb interaction
    - Strong Interaction
    - Isospin

- Here, discuss **DN interaction**, no experimental data available yet
  - Important for the quest of possible existence of D-mesic nuclei (an exotic nuclear state)
  - Through D-mesic nuclei, one can possibly access chiral symmetry restoration effects
    - Because, properties of light quarks in D mesons are sensitive to temperature and density

Correlation Function

Two-particle correlation function:

$$C(\mathbf{p_1}, \mathbf{p_2}) = \frac{P(\mathbf{p_1}, \mathbf{p_2})}{P(\mathbf{p_1})P(\mathbf{p_2})} \tag{1}$$

Experimentally can be obtained as:

$$C(q) \propto \frac{N_{\mathrm{same}}(q)}{N_{\mathrm{mixed}}(q)} \tag{2}$$

Correlation Function

Two-particle correlation function:

$$C(\mathbf{p_1}, \mathbf{p_2}) = \frac{P(\mathbf{p_1}, \mathbf{p_2})}{P(\mathbf{p_1})P(\mathbf{p_2})} \tag{1}$$

Experimentally can be obtained as:

$$C(q) \propto \frac{N_{\text{same}}(q)}{N_{\text{mixed}}(q)} \tag{2}$$

$$\text{If } C(\mathbf{p_1}, \mathbf{p_2}) \to 1 \text{ no particle correlation}$$

$$\text{If } C(\mathbf{p_1}, \mathbf{p_2}) \neq 1 \text{ particles are correlated}$$

Correlation Function

The Correlation Function can be written with an equal-time approximation, e.g., the particles states are emitted simultaneously in the pair rest frame $t_1 = t_2$ and $P = p_1 + p_2 = 0$:

$$C(\mathbf{p_1}, \mathbf{p_2}) = \frac{N(\mathbf{p_1}, \mathbf{p_2})}{N(\mathbf{p_1})N(\mathbf{p_2})} \approx \int d\mathbf{r} S_{12}(\mathbf{r}) |\Psi(\mathbf{r}, \mathbf{q})|^2 \tag{3}$$

Correlation Function

The Correlation Function can be written with an equal-time approximation, e.g., the particles states are emitted simultaneously in the pair rest frame $t_1 = t_2$ and $P = p_1 + p_2 = 0$:

$$C(\mathbf{p_1}, \mathbf{p_2}) = \frac{N(\mathbf{p_1}, \mathbf{p_2})}{N(\mathbf{p_1})N(\mathbf{p_2})} \approx \int d\mathbf{r} S_{12}(\mathbf{r}) |\Psi(\mathbf{r}, \mathbf{q})|^2 \tag{3}$$

where,

- $S(\mathbf{r})$ is the source function. Tipically, this can be represented with a spherical Gaussian source:

$$S_{12}(\mathbf{r}) = \frac{1}{(4\pi R^2)^{\frac{3}{2}}} \exp\left\{\left[-\frac{r^2}{4R^2}\right]\right\} \tag{4}$$

  - R is the width of the source.
- $\Psi(\mathbf{r}, \mathbf{q})$ is the wave function, where $\mathbf{q}$ is the relative momentum: $q = |p_1 - p_2|$

Correlation Function

Partial Wave Decomposition:

$$\Psi(r,q) = \sum_{l=0}^{\infty} (2l+1) i^l \psi_l(r) P_l(cos\theta) \qquad (5)$$

Correlation Function

Partial Wave Decomposition:

$$\Psi(r,q) = \sum_{l=0}^{\infty} (2l+1) i^l \psi_l(r) P_l(cos\theta) \tag{5}$$

Supose now, that only the s-wave is affected by the interaction:

$$\Psi(r,q) \quad = \quad \psi_0(r,q) + \sum_{l=1}^{\infty} (2l+1) i^l \psi_l^{free}(r,q) P_l(\cos\theta)$$

Correlation Function

Partial Wave Decomposition:

$$\Psi(r,q) = \sum_{l=0}^{\infty} (2l+1) i^l \psi_l(r) P_l(cos\theta) \tag{5}$$

Supose now, that only the s-wave is affected by the interaction:

$$\begin{aligned}\Psi(r,q) &= \psi_0(r,q) + \sum_{l=1}^{\infty} (2l+1) i^l \psi_l^{free}(r,q) P_l(\cos\theta) \\ &= \psi_0(r,q) + \sum_{l=0}^{\infty} (2l+1) i^l \psi_l^{free}(r,q) P_l(\cos\theta) - \psi_0^{free}\end{aligned} \tag{6}$$

- ψ_0 is the wave function for $l = 0$;
- $\psi_0^{free} = j_0(qr) = \dfrac{\sin(qr)}{qr}$; $\sum_l \psi_l^{free}(r,q) P_l(\cos\theta) = e^{iqr}$

Then,

$$\Psi(r,q) = \psi_0(r,q) + e^{iqr} - j_0(qr) \tag{7}$$

Replacing this expression in (2):

Correlation Function

Then,

$$\Psi(r,q) = \psi_0(r,q) + e^{iqr} - j_0(qr) \tag{7}$$

Replacing this expression in (2):

$$\boxed{C(q) = 1 + 4\pi \int drr^2 S(r) \left[|\psi_0(q,r)|^2 - j_0^2(qr) \right]} \tag{8}$$

Then,

$$\Psi(r,q) = \psi_0(r,q) + e^{iqr} - j_0(qr) \tag{7}$$

Replacing this expression in (2):

$$\boxed{C(q) = 1 + 4\pi \int drr^2 S(r) \left[|\psi_0(q,r)|^2 - j_0^2(qr)\right]} \tag{8}$$

Expressing ψ_0 in the assymptotic form:

$$\begin{aligned} \psi_0(r,q) &= \frac{1}{qr}\sin\left(qr + \delta(q)\right) = \frac{1}{2iqr}\left(e^{ikr+i\delta_0} - e^{-ikr-i\delta_0}\right) \\ &= \frac{e^{-i\delta_0}}{qr}\left(sin(qr) + qe^{iqr} f_0(q)\right) \end{aligned} \tag{9}$$

Correlation Function - Lednicky Model

Finally, one can obtain the Lednicky Model for the Correlation Function [Lednicky, 1982]:

Correlation Function - Lednicky Model

Finally, one can obtain the Lednicky Model for the Correlation Function [Lednicky, 1982]:

$$\boxed{C(q) = 1 + \frac{|f(q)|^2}{2R^2} + \frac{2\,\mathrm{Re}\,[f(q)]}{\sqrt{\pi}R}F_1(2qR) - \frac{\mathrm{Im}\,[f(q)]}{R}F_2(2qR)} \tag{10}$$

- $F_1(z) = \int_0^z \frac{e^{t^2-z^2}}{z}dt$, with $z = 2qR$;
- $F_2(z) = \frac{(1-e^{-z^2})}{z}$

Correlation Function - Lednicky Model

Finally, one can obtain the Lednicky Model for the Correlation Function [Lednicky, 1982]:

$$\boxed{C(q) = 1 + \frac{|f(q)|^2}{2R^2} + \frac{2\,\mathrm{Re}\,[f(q)]}{\sqrt{\pi}R} F_1(2qR) - \frac{\mathrm{Im}\,[f(q)]}{R} F_2(2qR)} \tag{10}$$

- $F_1(z) = \int_0^z \frac{e^{t^2 - z^2}}{z} dt$, with $z = 2qR$;
- $F_2(z) = \frac{(1 - e^{-z^2})}{z}$

An additional commonly used aporoximation is to use the effective range expansion for the scattering amplitude:

- $f(q) \approx \left[-\frac{1}{a_l^I} + \frac{1}{2} r_l^I q^2 + iq \right]^{-1}$, for $q \to 0$

  a_l^I is the scattering lenght and r_l^I is the effective range

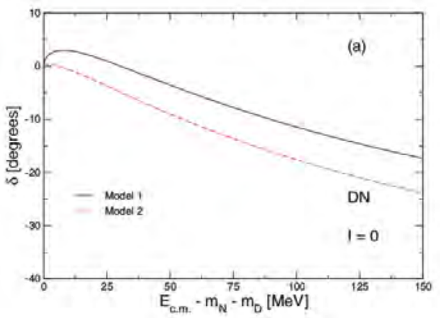

C. E. Fontoura, G. Krein, and V. E. Vizcarra, 2013

- Models:
  - Short distance: quark-interchange (Model 1 and Model 2)
  - Long distance: meson-exchange
- Model 1 (MELTT):
  - Lattice Simulation of QCD in Coulomb gauge
- Model 2 (MESS2):
  - Szczepaniak and Swanson

Extract the observables (for I=0):

$$q \cot \delta_0^I(q) \approx -\frac{1}{a_0^I} + \frac{1}{2} r_0^I q^2$$

Results

MELTT_model1: $a_0^0 = -0.16$ fm and $r_0^0 = 21$ fm

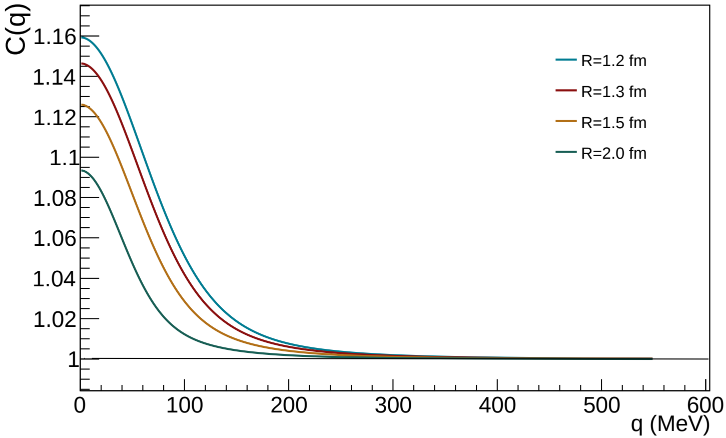

MELTT_model1 and MESS2_model2

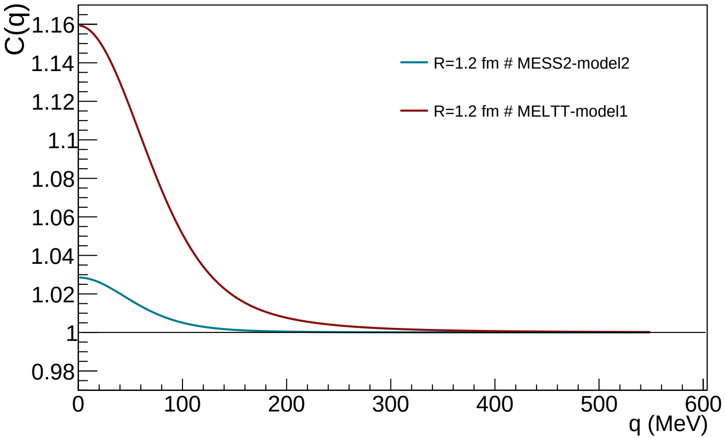

Summary

Summary

- Correlation function of the D meson and Nucleon
  - Contains information on the DN interaction, unknown so far

- Important for quest D-mesic nuclei [1,2]

- D-mesic nuclei, possibly access chiral symmetry restoration in medium

- Explore other models for the DN interaction

[1] K. Tsushima, D. H. Lu, A. W. Thomas, K. Saito, and R. H. Landau, 1999
[2] G. Krein, A. W. Thomas, K. Tsushima, 2018

Thanks!

Grazie mille!

Acknowledgment

CAPES

The Galileo Galilei Institute
For Theoretical Physics
Centro Nazionale di Studi Avanzati dell'Istituto Nazionale di Fisica Nucleare

Backup

Microscopic Hamiltonian

$$H = H_0 + H_{int} \tag{11}$$

with,

$$\begin{aligned} H_{int} &= -\frac{1}{2}\int dxdy\rho^a(x)V_C(|x-y|)\rho^a(y) \\ &+ \frac{1}{2}\int dxdyJ_i^a(x)D^{ij}(|x-y|)J_j^a(y) \end{aligned} \tag{12}$$

Models

- Model 1:

$$V_C(k) = \frac{8\pi}{k^4}\sigma_{Coul} + \frac{4\pi}{k^2}C \tag{13}$$

with $\sigma_{Coul} = (552\ \mathrm{MeV})^2$ and $C = 6.0$

- Model 2:

$$V_C(k) = \frac{8\pi}{k^4}\sigma + \frac{4\pi}{k^2}\alpha(k) \tag{14}$$

with,

$$\alpha(k) = \frac{4\pi Z}{\beta^{\frac{3}{2}} \ln\left(C + \frac{k^2}{\Lambda_{\mathrm{QCD}}}\right)^{\frac{3}{2}}}$$

and $\Lambda_{\mathrm{QCD}} = 250\ \mathrm{MeV}$, $Z = 5.94$, $C = 40.68$, $\beta = \dfrac{121}{12}$

MELTT_model1: $a_0^1 = 0.25$ fm and $r_0^1 = 2.2$ fm

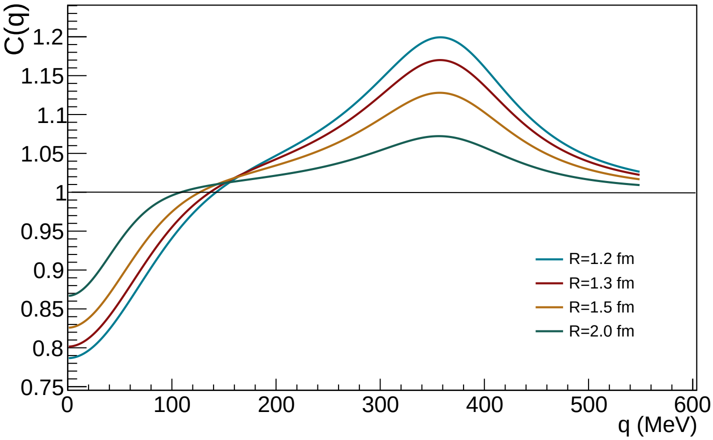

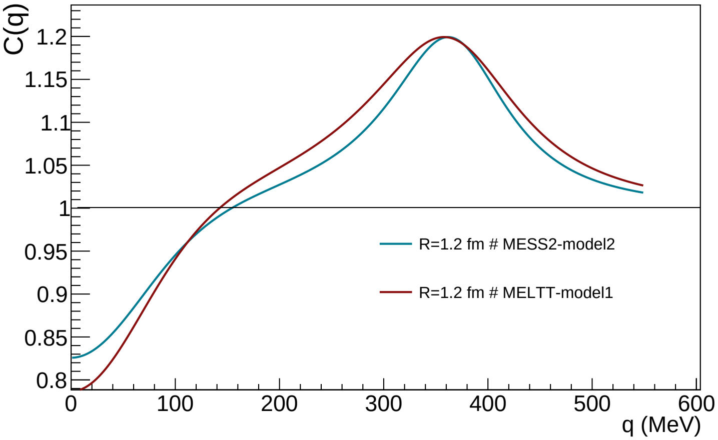
C(q)
1.2
1.15
1.1
1.05
1
0.95
0.9
0.85
0.8
0
100
200
300
400
500
600
q (MeV)
R=1.2 fm # MESS2-model2
R=1.2 fm # MELTT-model1

MESS2_I0_Model2 - (Lednicky Model) - $a_0 = 0.03$ fm and $r_0 = 350$ fm